Self-Adaptive Model-Based Control for VAV Systems

Cristobal Guerrero Lopez

A Thesis in the Department of Building,
Civil and Environmental Engineering

Presented in the Partial Fulfillment of the Requirements for the Degree of Master of Applied Science (Building Engineering) at

Concordia University

Montreal, Quebec, Canada

March 2020

CONCORDIA UNIVERSITY

School of Graduate Studies

This is to certify that the thesis prepared by

By: Cristóbal Guerrero López

Entitled: Self-Adaptive Model-Based Control for VAV Systems

and submitted in partial fulfillment of the requirements for the degree of

Master of Applied Science (Building Engineering)

complies with the regulations of the University and meets the accepted standards with respect to originality and quality.

Signed by the final examining committee:

_____ Chair
Dr. R. Zmeureanu

_____ Co-Supervisor
Dr. A. Athienitis

_____ Co-Supervisor
Dr. B. Lee

_____ Examiner
Dr. C. Lai External (to program)

_____ Examiner
Dr. M. Ouf

_____ Examiner
Dr. R. Zmeureanu

Approved by _____
Dr. M. Nokken, GPD
Department of Building, Civil and Environmental Engineering

_____
Dr. Amir Asif, Dean
Gina Cody School of Engineering and Computer Science

Date _____

Abstract

Self-Adaptive Model Based Control for VAV Systems

Cristobal Guerrero Lopez

In North America one of the main users of primary energy are buildings, where HVAC equipment operation is the largest consumer of total energy by end use. This has triggered the need to develop better active strategies and building technologies for the enhancement of HVAC equipment performance. Great examples of solutions that large commercial and institutional buildings adopted, were the widespread use of Building Automation Systems (BAS), and approaches like Variable Air Volume (VAV) systems for ventilation, which allow for better part load regulation, reduction of energy consumption and building operation costs, without compromising occupant comfort or safety. But despite all these improvements, most BAS still rely on conventional control methods like rule based on-off control paired with Proportional Integral Derivative (PID) loops, which are single input single output (SISO) models that are not suitable for the complexities of the multivariable requirements of building systems. These outdated strategies have been estimated to annually waste up to 30% of building's energy. To mitigate these issues the research community has strongly endorsed the use of more advanced and proven effective control methods such as Model-Based Control (MBC), in which abundant work has been done for the supervisory level control like optimal start/stop, setpoint reset scheduling, etc. However, little attention has been given to local level control where PID control remains the chief workhorse of HVAC systems. Mainly because of the difficulties of creating models, as well as the lack of research regarding the implementation of mechanisms required for continuous calibration (also known as adaptability) of model parameters as they start to drift away from their initial values due to system changes or deterioration, which challenges the reliability of any MBC approach. For such reasons the present body of work was conceived to design a practical methodology for a self-adaptive MBC and field data driven approach to improve VAV systems energy efficiency, based on the Total Air Volume (TAV) control method by modifying the shortcomings of its modeling, adaptability and control strategy procedures. Using a regular VAV system inside a high-rise institutional building as an experimental testbed for the proof of concept of this methodology. The results of the test demonstrated that the self adaptive field calibrated TAV method can match and exceed the capabilities of PID control, by improving response time, offset, and above all energy efficiency, were an average 56% of energy consumption was achieved in contrast to the conventional duct static pressure PID control.

Acknowledgements

First, I would like to extend my immense gratitude towards my two supervisors, Professor Bruno Lee and Professor Andreas Athienitis for their immense support and guidance towards developing this project. For giving insightful and great advice and allowing me to work in projects that gave me pivotal lessons for both my professional and personal life.

I would also like to acknowledge the great support of the Concordia University building facilities staff, for granting me permission to use their equipment freely, in particular to Daniel Gauthier who help me overcome and troubleshoot all of the immense technical challenges the project was faced with, also providing the opportunity for hands on experience with lots of patience, which in my opinion is an integral part of becoming a real engineer.

To all the people who work in the lab, but particularly to Vasken Dermardiros, for his opinions a general guidance regarding the application and development of model-based controls.

Another very special thanks is for somebody who this project would have never been finished without, and that is my colleague and friend Charalampos Vallianos, who had no obligation to help me, but there he was holding heavy testing equipment for hours without end, meeting me at late and early hours of the day to troubleshoot issues, and run experiments, as well as helping me with my technical, scientific and general questions, and who also help me draft the general calibration methodology listed on section 6 of the present document.

To my friends who encouraged me along the way Camilo Palma, Clarissa Romero, Madeline Saylor, Sunera and Vinura Paranagama, especially to Natalye Abigail Guzman whose softness, love and kindness made me feel better after those long days of work. Other persons who were essential for me while seeing this project through, were my friends and second family, Jesus Simon Rubi Lamas and Felipe Aguirre Delgado, who have been taking care of my family on my absence, and have always proven to be the bests friends a person could ask for.

But above all I would like to thank my brother Nicolas Guerrero for being and admirable person, my father Jorge Luis Guerrero for always supporting me and guiding me through the hardships life, and my mother Martha Silvia Lopez for always believing in me and taking care of me, for waking up early to take me to school and putting food on the table, I love you and I would have never achieved anything in my life if it was not for you, muchas gracias del corazón papá y mamá.

Table of Contents

List of Figures

List of Tables

Nomenclature

Scripts

abs	Absolute
b	Barometric
c	Operating condition
D	Derivative
I	Integral
$inlet$	Fan inlet
L	Lower bound
$outlet$	Fan outlet
P	Proportional
R	Return air
s	Static
S	Supply Air
SEF	System effect factor
sp	Setpoint
U	Upper bound
v	Velocity

Variables

ΔP_{Tloss}	Total pressure loss, *in. WC*
A	Area, ft^2
D	Diameter, *ft*
dp	Damper position
e	Error
f	Friction factor
fs	Fan speed
H	Fan power input, *kW*
HR	Humidity ratio, lb_m/lb_a
J	Cost function
K	Gain coefficient
k	Damper drag coefficient
L	Length, *ft*
MV	Measured Value
N	Fan speed, *RPM*
P	Pressure*, in. WC ; or in. HG*
Q	Volumetric flow rate*, ft^3/min (l/s)*
q	Branch airflow ratio
R	Airflow resistance
SP	Setpoint
t	Time, s

T	Temperature, $°F\ (°C)$
u	Control input
w	State disturbances
x	State variables
y	System output
τ	Time step
λ	Branch airflow ratio coefficient
ρ	Density of fluid, lb/ft^3

1 Introduction

1.1 Motivation

Globally 78% of Green House Gases (GHG) emissions are a direct consequence of generating and consuming energy by humans. During the year 2015 in Canada, 20% of the primary energy consumption was attributed to buildings (12% and 8% to the residential and commercial sectors respectively). In commercial and institutional buildings, space heating and cooling constitute 60% of the total energy consumption by end use [1]. Meanwhile in the U. S. it was estimated that the commercial sector made up for 18% of all primary energy consumption, where HVAC systems embody around 44% of energy consumption by end use [2].

For these reasons in North America, decreasing the required energy consumption for Heating, Ventilation and Air Conditioning (HVAC) systems, continues to be a key component in the energy efficiency improvement and flexibility of buildings. One widely implemented approach for enhancing building performance since the early 80s has been the use of Building Automation Systems (BAS), which are not only a powerful tool for diagnostics, security and maintenance of buildings, but also encompass as a main goal to operate HVAC systems at optimum energy efficiency, whilst maintaining the desired indoor environmental conditions which uphold the comfort and health of the building occupants, by regulating parameters like indoor air temperature, humidity, pressure and ventilation rates, among others [3].

But even with the deployment of BAS within commercial and institutional buildings, inadequate sensing, monitoring, and inefficient control operations of building systems can lead up to a 30% of annual energy waste. Although building diagnostics, detailed operation strategies and improved system maintenance can aid in reducing faults and improving performance, more sophisticated control engineering methods coupled with new building technologies like data acquisition systems and open communication protocols for diagnostics and interoperability, have been shown to enable additional savings beyond those of the benchmark of the original projected behaviour of a building [4]. It is estimated that edifices with BASs that incorporate these state-of-the-art methods can achieve an annual energy consumption reduction between 10% and 30% of building equipment [5].

Currently the vast majority of BASs implemented, rely on conventional control engineering methods like the standard Rule-Based Controllers (RBC) with hysteresis, paired with Cascade Proportional Integrative Derivative (PID) control algorithms, which are not ideal for the complex multi-variable control nature of HVAC systems [6]. A survey conducted for the current trends, development and application of advanced control methods across several industries by five major control engineering companies, recorded that out of all their clients who are using these types of control systems less than 5% are those related to building applications, and as for the industries that are main

users of advanced control engineering methods, like oil refineries and petrochemical plants, Model Predictive Control (MPC) is the more widely utilized approach [7].

Model-Based Control (MBC) strategies like MPC are based on the idea, that a system's future state or outputs, can be simulated over a finite time horizon, by the interaction between its present state or inputs, and its disturbances, allowing the controller to solve and optimize the performance of the system based in pre-set constrains to meet the desired objectives of the process. In building systems MPC has been used primarily for whole building control, at the supervisory level of BAS with favorable results when weighted against conventional control strategies, where the MBC algorithm seeks the best energy and/or cost efficient control settings by modifying the building's operation modes and zones setpoints, to minimize the energy input or operation cost, with the constrain of keeping the controlled variables within the desired limits, to sustain satisfactory levels of comfort and safety [8]. However, MPC has not gained wide adoption due to several reasons like, the significant effort and the deep knowledge required to model accurately whole building systems; the uncertainty in simulating major building disturbances, like weather prediction, occupancy, infiltration; and the lack of development of self-adaptive mechanisms, for both building response and optimization, to guarantee robustness and reliability of the control system [9].

Local level components of HVAC systems have a wide array of modeling techniques available which have been successfully validated for both control and simulation purposes. These local level component models do not deal with the same degree of uncertainty a whole building model would, yet local level MBC experiences a lag in implementation of advanced control methods, relying overwhelmingly on conventional control approaches as well. [10].

Scalability, standardization, and a simple methodology as well as tools that ease the design of modeling are essential in order to help introduce advanced control strategies to the current market of building technologies applications [11].

The present work is geared to the application of a practical and simple self-adaptive MBC based on the Total Air Volume (TAV) approach for Variable Air Volume (VAV) multizone ventilation systems. Modifying the original modeling and calibration process of the TAV control method by relying only in field measured data and the main characteristics of the installed equipment. Changing as well the TAV control method strategy with the intention of developing a robust control engineering methodology that can be applied to new or existing buildings local level control components, not by replacing but by complimenting the supervisory capabilities of BAS for diagnosis, fault detection, performance, energy efficiency and maintenance.

1.2 Background

VAV systems were introduced during the 1970s energy crisis as a more efficient alternative for multizone ventilation applications to Constant Air Volume (CAV) systems. The reason behind this was that CAV systems conditioned large volumes of air and removed humidity, thus the discharge air was supplied at a very cold temperature, since in multizone applications individual temperature control was required, reheating for great volumes of conditioned air had to be provided, which wasted lots of energy.

To mitigate this issue VAV systems modulated the volume of air according to the required necessities of each zone, while maintaining the supply air temperature constant, unlike CAV systems which can only modulate their supply air temperature and operate continuously at their full airflow capacity. VAV systems reduced operational cost and energy consumption, thus they became the most common system for commercial and institutional buildings [12, 13].

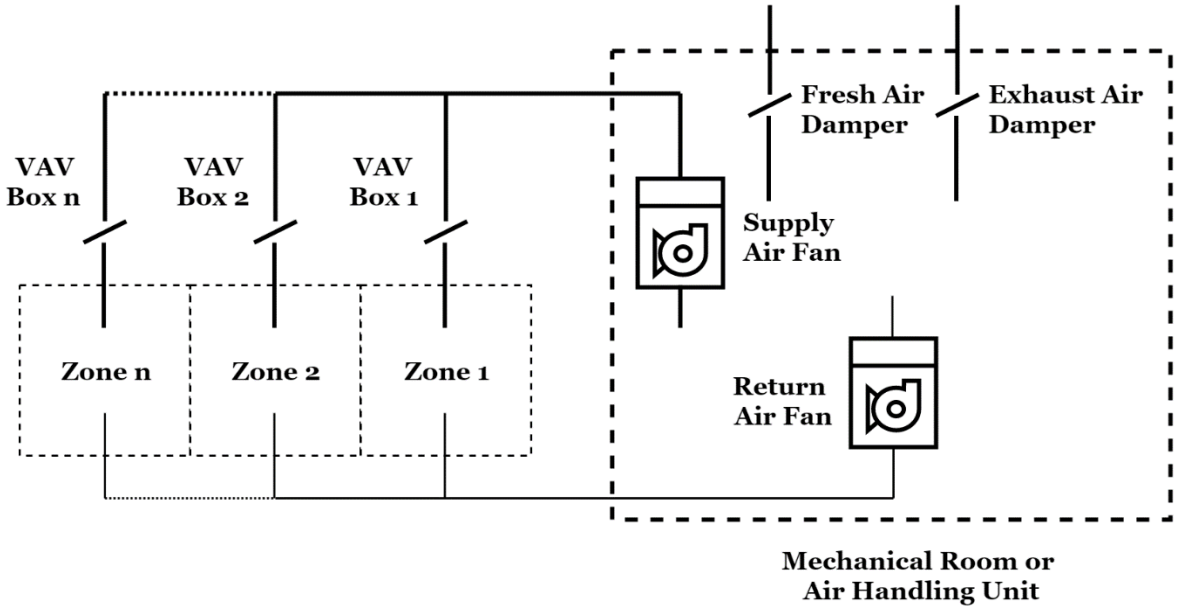

Figure 1.1 Typical commercial multizone VAV system configuration.

BAS for commercial and institutional buildings rely on conventional PID control as the main method used to regulate VAV systems, because it is easy to implement as no deep knowledge of HVAC is required, but this approach is not the most energy or cost efficient on the long run, which will be demonstrated later in this document.

1.3 Objectives

To partially fulfil the requirements of Master of Applied Science in Building Engineering degree the present research provides a methodology for creating a self-adaptive Model-Based Control approach that can be applied to any kind of commercial VAV system, to save energy and improve equipment performance. To complement the study, procedures for model calibration and adaptability will be provided, as well as a comparison of the TAV controller versus the current Ruled-Based (RB) PID control strategy to illustrate the advantages, challenges and drawbacks of implementing a Model-Based Control approach. To accomplish this goal the ensuing tasks will be performed:

- Classify the key components of VAV systems and their functionality.
- Model the primary components of VAV systems.
- Establish the framework and structure of the Model-Based Control approach.
- Design a calibration method for the model based on field measured data, and the characteristics of the on-site equipment.
- Provide a self adaptability mechanism (automatic calibration) for ensuring reliability and optimal performance over operational life of the system.
- Test the TAV approach and collect the data to review the performance of the control system in contrast to the current RB PID control in rubrics such as response time, overshoot, offset, and energy efficiency improvement.
- Offer conclusions and recommendations based on the obtained results.

1.4 Outline

The thesis can be structured into the following sections:

- **Section 1:** States the motivation of the project, gives a brief overview of the experimental setup, and places the main goals of this thesis.

- **Section 2:** Provides and overview of what are VAV systems, what are their main components and configurations. It offers a summary of the current modeling techniques for air systems and the need for adaptability for MBC methods. It also dives into conventional and advanced operation and control strategies presently available for VAV systems, with an emphasis on what is the scope of supervisory control versus local level control.

- **Section 3:** Gives a brief introduction to the TAV control method. It offers general approaches for modeling air system and fans, which are the two main categories of components of VAV systems. It also details the interactions between the air system and the fan.

- **Section 4:** Explains and goes into detail to describe the experimental setup and offers the model design and structure for the VAV system that was used as a proof of concept.

- **Section 5:** Details the necessary steps and required measurements for calibration of the control model. It delivers a generalized procedure to create and field calibrate any VAV system model. This section includes a method for providing adaptability to the air system model, necessary to maintain reliable control of the system.

- **Section 6:** Supplies the sequence of operation for the TAV control strategy, the detailed formulation of the controller's operation and lays out the overall TAV control methodology for implementation in a real VAV system.

- **Section 7:** Describes in detail the test results for both TAV control and PID control using the same control routine for both methods. It compares their performance for four key metrics response time, overshoot, offset and energy efficiency.

- **Section 8:** Summarizes the thesis and clearly states the benefits of using an advanced self-adaptive TAV control method over the conventional PID control, currently used for the vast majority of commercial and institutional VAV ventilation systems.

2 Literature Review

The following section gives a brief overview of VAV systems, what are the current modeling techniques available, their applicability in model-based controls, and a comprehensive review for the most recent developments regarding control strategies of these systems.

2.1 VAV Systems

A ventilation system that supplies air at a fixed temperature and varies its air flow rate to meet the cooling or heating demand of a conditioned zone is called a VAV system, this in contrast to Constant Air Volume (CAV) systems that supply air at fixed flow rate and modulate supply air temperature. VAV systems for multiple zones are comprised of a centralized Air Handling Unit (AHU) that typically contains variable speed fans, coils for heating and cooling, controls, sensors, filters, dampers, mixing plenum, and a main discharge duct that branches of to VAV boxes that supply air to each ventilated zone (Figure 2.1). VAV boxes are equipped with an adjustable damper or valve (usually round) that regulates the amount of air flow delivered into every conditioned space. VAV boxes can contain supplementary coils or heat exchangers if additional heating or cooling is requested by the zone [14].

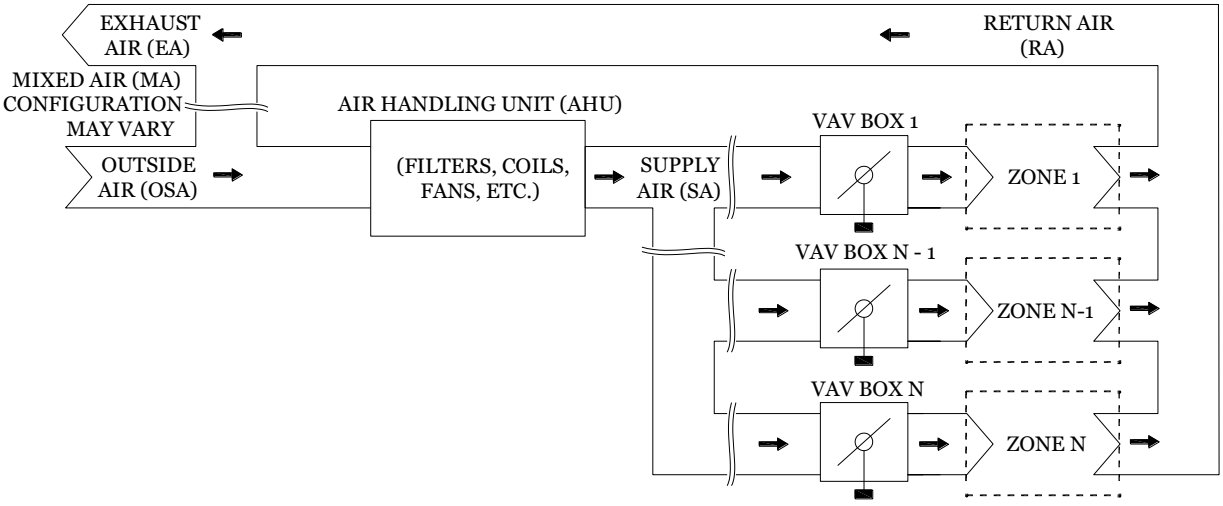

Figure 2.1 VAV system arrangement.

In commercial building applications VAV systems are favored over CAV systems, due to the high energy use that stems from the fact that fans are always operated at maximum design air flow rate even at part-load conditions in CAV systems. Since CAV systems supply air cooled at a low enough temperature to match the maximum cooling load, their use in multizone reheat systems is also restricted, because extra heat is always needed to avoid overcooling the zones that are at part-load conditions. VAV systems in general have greater energy efficiency thanks to the trimming of fan energy as a result of lowering supply air flow rates to better match the zone's oscillating heating and cooling load

conditions, which in turn provides improved control over the temperature and relative humidity of individual zones [15].

2.1.1 Air Distribution of VAV Systems

Air-conditioned spaces in buildings are divided into two categories, perimeter zones in which their loads are mainly driven by the external conditions of the building, and interior zones that are characterized primarily by the loads inside the space. VAV systems are ideal candidates for conditioning the perimeter zones in a building, since a key factor of these types of zones is their orientation, as load variations are mainly managed by solar irradiance and outdoor temperature, this allows for energy saving by varying the air quantity as needed to each of these zones regardless of their individual load requirements [15].

2.1.1.1 *Single-Zone VAV Systems*

Single-zone configurations vary the supply and return airflow rate to a conditioned space to satisfy the zone's air temperature setpoint, to achieve this they regulate their fans speed according to the conditioned zone demands. They are mainly used for large clear places like arenas, indoor stadiums, assembly halls, and factories [16].

2.1.1.2 *VAV Cooling, VAV Reheat, and Perimeter Heating VAV Systems*

For cooling in multizone arrangements VAV systems are coupled with VAV boxes that adjust the air quantity as needed by each conditioned zone, in order to maintain the expected air temperature setpoint of the conditioned space. Plain VAV boxes are usually used in interior zones, whilst VAV boxes with reheat coils are provided in the perimeter zones of the edifice to avoid overcooling in VAV Reheat systems. Perimeter heating VAV systems instead of installing reheating coils inside the VAV boxes, use heating devices mounted directly on the parameter zones of the building. VAV Reheat systems are a simple solution for perimeter zones of commercial buildings in mild climates, but become infective in locations that experience long and cold winters, where Perimeter Heating is preferred [16].

2.1.1.3 *Dual-Duct VAV Systems*

Dual-Duct VAV systems are used in multizone applications. They consist of two supply air ducts; one is heated and the other one cooled. For perimeter zones they use a VAV mixing box with two inlets, one is supplied by cool air, and the second one by the hot air, they mix the air in relation to the need for cooling or heating of the zone. In interior zones they use single inlet VAV boxes connected to the cooling duct, the purpose of this configuration is to offset the amount of cooling delivered by the central AHU.

The Dual-Duct array can be achieved in several different arrangements, the most common is having a single AHU unit with a dual-deck array, one for the cool air, and the other one the hot air (called cold deck and hot deck respectively). AHUs that feature a cold and hot deck, can have single fan array to supply air to both of the decks, or dual independent fan arrays, one for each deck, the later allows for major flexibility and energy savings, thus it is the predominant configuration for building applications. One less

common configuration is using two AHUs, but this is not typical as it increases the complexity of the installation and the control system.

Dual-Duct VAV systems are regarded as being more flexible when compared to VAV Reheat systems, as they can not only synchronize the airflow rates to match every zone load, but they can also control better the delivery of outdoor air in each ventilated space. Since Dual-Duct VAV systems can transfer the heat gains from the interior zones to the perimeter zones by using the recirculated air, and can also manage the outside air mixing ratio to offset both the heating or cooling load, they are considered to have greater energy efficiency than other VAV systems. Dual-Duct VAV systems are popular in high-rise building applications, due to their flexible operating profile [16].

2.1.1.4 *Fan-Powered VAV Systems*

Another option for multizone arrays is Fan-Powered VAV systems. These systems use VAV boxes that include fans in series or parallel, for parameter zones, with the goal of mixing the zone's air with the primary incoming supply air from the VAV box. In this system both the Fan-Powered and VAV boxes can provide cooling for interior and perimeter zones. Fan-Powered VAV boxes in cooling mode will recirculate the perimeter and internal zones return air at a fixed rated while metering the incoming primary cold supply air, reducing it when the need for cooling is low, and raising it when the zone demand is high. When the temperature is low enough for the system to demand heating in either the perimeter or internal zones, reheat coils (or other heating devices) that are installed inside the Fan-Powered VAV Boxes are enabled to provide additional heating. Because this system mixes the cold incoming air of the central AHU with the warm air from the zone it can prevent cold air jets and surface condensation problems, but the inclusion of fans in the VAV boxes can increase the energy consumption of the ventilation system, as well as the operating noise level, and can have greater cost both for initial installation and maintenance. Office buildings and schools are common places where Fan-Powered VAV systems are applied, attributed to their good cold air distribution performance [16].

2.1.2 VAV Boxes

Regarding pressure, there are two types of VAV boxes (also called terminal units), pressure dependent and pressure independent units. Dual-Duct VAV Systems use a special kind of terminal unit called Mixing VAV Box that has two inlets that can be adjusted individually to regulate the temperature of the supply air by mixing the incoming hot and cold streams as required by the zone's temperature setpoint. Furthermore, VAV systems that mix the central primary supply air with return air from the zone to offset cooling capacity such as Fan-Powered VAV Systems or Induction VAV systems, involve the use of terminal units that are either in series or parallel, in regards to the position of the fan or induction cavity to the main supply air discharge. Parallel Fan-Powered Boxes need smaller fans since their airflow rate is less than Series Fan-Powered Boxes, but they have more complicated control specifications in order to properly balance out the flows

of the supply and recirculation air. Induction units are rarely used anymore because of their high inlet static pressure requirement to achieve the necessary velocity for induction, thus raising the fan energy consumption of the central AHU of the system [15].

2.1.2.1 *Pressure Dependent VAV Boxes*

In pressure dependent units and variable diffusers, the zone temperature measurement directly dictates the regulation of the actuator position. Since these kinds of units do not monitor the system pressure when multiple dampers are closing to restrict air flow, the overall system airflow tends to be reduced, relying completely on the capacity of the central fan to be able to adjust to the fluctuations of the system. As a consequence, pressure dependent boxes starve zones from air that are located far away in the ductwork from the fan under high load demands [3].

2.1.2.2 *Pressure Independent VAV Boxes*

Pressure independent units have two cascading control loops, the first one controls the zone temperature, and the second its airflow rate. This master and sub-master array works by modulating the unit damper position based on an airflow rate setpoint which is reset by the zone temperature controller and its measurement of space temperature. The advantage of measuring the airflow being delivered is that the unit can quickly adjust to system pressure changes, in turn regulating the zone's temperature in a more steady pace [17].

2.2 Modeling Techniques for VAV Systems Control

VAV Systems can be modeled as steady state (static) or transient (dynamic) models. For control applications steady state models are not useful as their parameters remain unchanged over time and are unable to portray the dynamic characteristics needed to regulate a real system, thus transient models that do reflect the time varying parameters of a VAV system, are the techniques useful to develop control methods [18]. Transient models can be classified into white box (physics-based) models, black box and grey box (hybrid) models [19].

2.2.1 Physics Based

This modeling technique relies on the fundamental laws of energy. Crucial factors to develop a white box model are in depth knowledge of the system and its governing physical principals. For VAV systems the main characteristics that are used for creating a model are derived from heat transfer and fluid dynamics. To simplify physics-based techniques assumptions are stated, for what are deemed non-crucial parameters of a system. They are typically represented as time-domain differential equations, but for practical applications they are converted to frequency domain transfer functions or time-domain state-space models [19]. White box models offer the advantage of portraying the behaviour of a system in a logical and hierarchical manner according to the system's parametric features, making them easy to understand, but also robust in the presence of unexpected system disturbances. The disadvantages of physics-based approaches are that they require large amounts of field measured data of the system to calibrate the model accurately. Systems with a large number of parameters become cumbersome and take more time to iterate output values (the computational effort grows), making them inadequate to control whole building or higher-level components of VAV systems [11]. Physics based approaches are mainly used for modeling lower level components of VAV systems like, chillers, boilers, AHU, fans, coils, mixing plenums, actuators, sensors, etc. They are also widely applied to size and select components in the design stage of a VAV system [20].

2.2.2 Black Box Models

To create black box models existing historical data from the performance of the actual system to be modeled must be gathered, afterwards with this information links are established between the input and output variables through the use of mathematical techniques, for example, statistical regression or Artificial Neural Networks (ANN) [21]. Below is a summary of the main approaches that have been developed using black box models for VAV systems, as well as their pros and cons.

2.2.2.1 *Machine Learning Algorithms*

Popular approaches in this category are ANNs and support vector machine (SVM). These approaches function well for modeling complex and non-linear system dynamics. Algorithms use training data sets managed by a learning algorithm, where the expected response outcome is known before hand. ANNs have been successfully used to predict estimates of the performance of HVAC components, whilst SVM algorithms have been used for whole building load calculation [8].

These approaches have several shortcomings for implementing them on control systems, they require large amounts of data from the actual system to test and validate the model; if the model is subjected to unexpected conditions that vary from those of the original training data set, there is no way to be able to discern what parameters of the model are degrading its performance since there is no clear physical relationship to the actual system; and finally these algorithms are difficult to implement online with the system [19].

2.2.2.2 *Fuzzy-Logic (FL) Models*

Fuzzy-logic models are based in the knowledge of experts, which are programmed in the form of if-then-else statements, these instructions are stated in tables or datasets. They are regarded as being robust because their structure and logic are clearly organized in to a set of rules, that can be easily understood and modified to change the model if needed [20]. FL models are typically paired in HVAC systems with other modeling and control approaches to improve their overall performance this includes PID controllers, and ANNs [19]. In VAV systems applications they have been implemented for regulating zone temperature and indoor conditions [22].

The issue of this approach in regards to HVAC control is their need of a large quantity of data required for training and testing a model of a component which might not have a lot of info readily available, coupled with their necessity of employing personnel with in depth knowledge of the system's different operating states [8].

2.2.2.3 *Statistical Models*

For HVAC control applications the main approaches used under this rubric are autoregressive exogenous (ARX), autoregressive moving average exogenous (ARMAX), ARIMA, Box-Jenkins (BJ), and output error (OE). The reason that these methods are useful in control applications can be attributed to their structure which contemplates both inputs and outputs of the modeled system which enables them to work under a closed loop system [19].

Statistical models are great for modeling VAV system components when manufacturer or measured data is available. Curve fitting system data into polynomials has been used to reliably create a relationship between fan power consumption and fan speed for VAV systems [23]. The setbacks of this methodology are that they may not be able to capture the non-linear dynamics of the airflow of a VAV systems, and they require online retuning of the model parameters if the system is modified [20].

2.2.3 Grey Box (Hybrid Models)

Hybrid models are derived from the merging of physical and black box models, they are created with the structural and hierarchical characteristics of physics-based techniques, whereas their parameters can be estimated using machine learning, statistical approaches, etc. This is flexible as it can be generalized to create models for systems with similar architectures, and parameters can be chosen to display accurately the effects of typical patterns of the system, rather than be modeled explicitly in the physical equations. Grey boxes are usually defined as transfer functions or state space models, and are ideal candidates for control applications since they overcome the issues of accuracy, generalization capability, complexity and low computational cost that their white and black box modeling counterparts have [24]. They have been deployed successfully for the control of higher and lower-class components in HVAC systems, in applications like zone temperature regulation, and regulation of cooling coils [20]. The main problem that hybrid models face to successfully be applied in control systems, is their adaptability, parameters need to be tuned and updated online in real time when they have strayed away from those originally specified by the training data, otherwise the controlled system could be subjected to lower performance or malfunction [8].

2.3 Operation and Control Strategies of VAV Systems

The basic elements of a VAV system control are, sensors, controller, control devices (actuators), and a power source. In commercial buildings VAV systems must be regulated to maintain the necessary indoor conditions required for the comfort, health and safety of occupants, consuming the minimum possible energy to accomplish this. To achieve this the main controlled parameters are fan speed, static pressure, zone air temperature, humidity, ventilation rates, supply air flow rate, in addition to heating and cooling output. Although control systems can be of open loop (feedforward) or closed loop (feedback) type, in Air Conditioning (AC) applications closed loop is the preferred approach. Feedback control in AC allows for operational efficiency by measuring the oscillatory behaviour of the controlled variables through the system's sensors (as a consequence of changes in ambient temperature, occupancy and lighting, among others), these measurements are computed and weighted against the setpoints by the controller, which in turn calculates the most effective response the system should have to draw the least amount of energy in order to adjust the actuators to attain the desired system conditions, this can not be achieved in an open control loop control configuration [25]. The following section is a comprehensive classification of control engineering methods and their recent developments in regards to VAV systems [25, 26]. Furthermore, a review of VAV systems Sequences of Operation (SOO) including strengths and weaknesses will be provided [3].

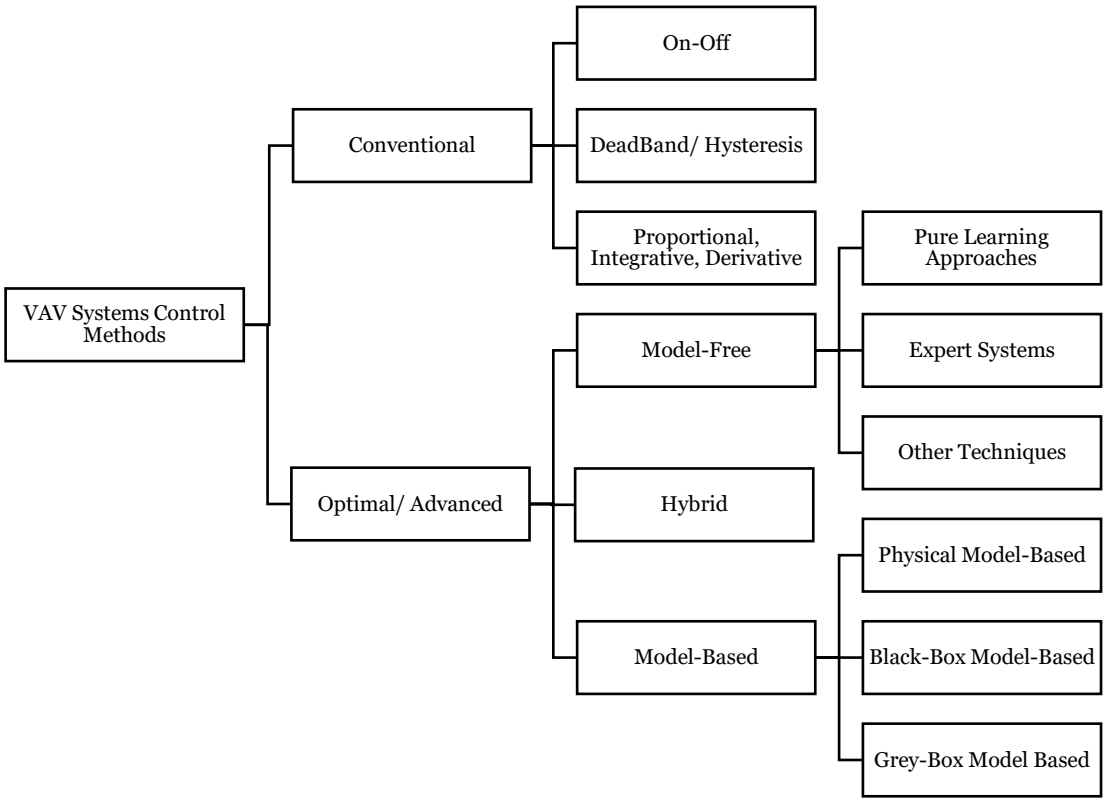

Figure 2.2 Classification of control engineering methods for VAV Systems [25].

2.3.1 Conventional Control Methods

In HVAC systems the earliest control devices employed to start and stop equipment automatically were thermostats [25]. These devices operated in an On-Off scheme, engaging/disengaging the equipment when the zone temperature setpoint had been reached, since the periods the AC system could maintain the zone temperature in the exact value of the setpoint where short, this caused the equipment to cycle constantly, raising the peak energy consumption. To combat this issue thermostats were manufactured with a dead-band (hysteresis) control feature, in which the HVAC equipment could remain off while the zone was within a determined temperature range (this approach is also called bang-bang control). The problem with dead-band control is that since no modulation of the HVAC equipment is possible overcooling and heating are always present at part-load conditions, wasting a considerable amount of energy, this is commonly called "system overshoot" [27]. To overcome "system overshoot" in buildings, HVAC control systems implemented the use of Proportional-Integrative-Derivative (PID) controllers, which allows the regulation of actuators in direct response from the deviation of a zone's established setpoint [28].

2.3.1.1 *Proportional-Integrative-Derivative (PID) Control*

PIDs controllers are comprised of three parts: a proportional part (P) which adjust the output signal in direct measure to the instantaneous error (deviation from the setpoint), an integral part (I), which regulates the output signal in proportion to the accumulated error, and a derivative part (D), which drives the output signal in proportion to the slope or rate of instantaneous change of the error. The total of the output signal is the weighted sum of each of the three PID component values. The values of these weights are determined from a procedure called tuning in which the goal is to reach and maintain the setpoint as quickly as possible with as little "system overshoot". PID algorithms measure the error value of a system and use it as an input parameter to calculate the output signal, based on the summed contributions from the "P", "I", and "D" control components. To calculate the present value of a system's error the difference between the setpoint and the measured value is used:

$$e(t) = SP(t) - MV(t) \qquad (2\text{-}1)$$

Where:

$e(t)$ = Error at present time

$SP(t)$ = Setpoint

$MV(t)$ = Measured Value of the process variable

The contributions from each of the PID elements are as follows:

$$P = u_P(t) = e(t)$$

$$I = u_I(t) = \int_0^t e(\tau)\, d\tau$$

$$D = u_D(t) = \frac{de(t)}{dt}$$

The timeframe of the integral part is calculated from the initial run until the present time (denoted by the time constant τ). The weighted sum of all the PID values determine the magnitude of the signal output:

$$u(t) = K_P u_P(t) + K_I u_I(t) + K_D u_D(t) \qquad (2\text{-}2)$$

Where K_P, K_I, and K_D are the gain coefficients, and the subscripts, P, I, and D represent their contribution [29].

2.3.1.1.1 PID control of VAV systems

In VAV systems PIDs loops, are mainly set to regulate air flow, air temperature, duct static pressure, and damper position. In a VAV system, the supply air temperature will be constant or have a reset schedule set by the supervisory control, while the airflow is modified to meet the conditioned space heating or cooling demand. The total airflow delivered by the central fan to the system is regulated according to the change of airflow demand of every VAV box [3].

To illustrate how PID controllers work in single duct VAV systems refer to the control schematic below (Figure 2.3). In this example the system is furnished with supply and return air fans that have variable speed control. The supply air (SA) temperature setpoint is provided to the Temperature Control (TC-PID) by a thermostat in the zone, or by a supervisory controller, the TC-PID uses the measurement provided by the SA temperature sensor (T1) to calculate the error value and output a signal for the positions of the heating valve (HV) when the system is in heating, or cooling valve (CV) when the system is in cooling, the TC-PID also relays the zone temperature setpoint to the Damper Control (DC-PID), to regulate the intake of outside air (also called fresh air). The DC-PID compares the enthalpy of the return air (RA) measured by the RA temperature and humidity sensors (T3 & H3) and the enthalpy of the outside air (OSA) measured by the OSA temperature and humidity sensors (T4 & H4), in cooling mode it will maintain the position of the OSA damper at its minimum if the enthalpy from the OSA air is larger than that of the RA. If the enthalpy from the OSA air drops below the enthalpy of the RA, and the TC-PID is still in cooling demand, the CV will be disabled, to save energy and the OSA and RA dampers will be modulated to mix their air streams to meet the air temperature setpoint this is known as economizer mode. Once the OSA damper reaches its fully open position and cooling is still requested by the TC-PID, the cooling coil valve (CV) is enabled again. The Pressure Control PID (PC-PID) maintains the supply air static pressure,

according to the duct static pressure setpoint provided by the supervisory system, or is set as constant value, the PC-PID oscillates the speed of the supply fan motor (M1) according to the error measured by the supply duct static pressure sensor (P1), as fan speed changes both the supply air static pressure and airflow volume do it as well. Finally, the RA flow rate control PID (FC-PID), keeps the airflow difference based in a pre-set airflow ratio setpoint between the SA and RA, the air volumes for the SA and RA are measured through flow sensors (F1 & F2 correspondingly), the output of the FC-PID regulate the speed of RA fan motor (M2) to meet the required airflow ratio [30].

Airflows	**PID Controllers**	**Actuators**	**Sensors**
EA: Exhaust Air	TC-PID: Temperature Control	D: Damper	H: Humidity
OA: Outside Air	DC-PID: Damper Control	CV/CC: Cooling - Valve / Coil	F: Flow
RA: Return Air	PC-PID: SA Static Pressure Control	HV/HC: Heating - Valve/ Coil	P: Static Pressure
SA: Supply Air	FC-PID: RA Flow Rate Control	M: Motor	T: Temperature

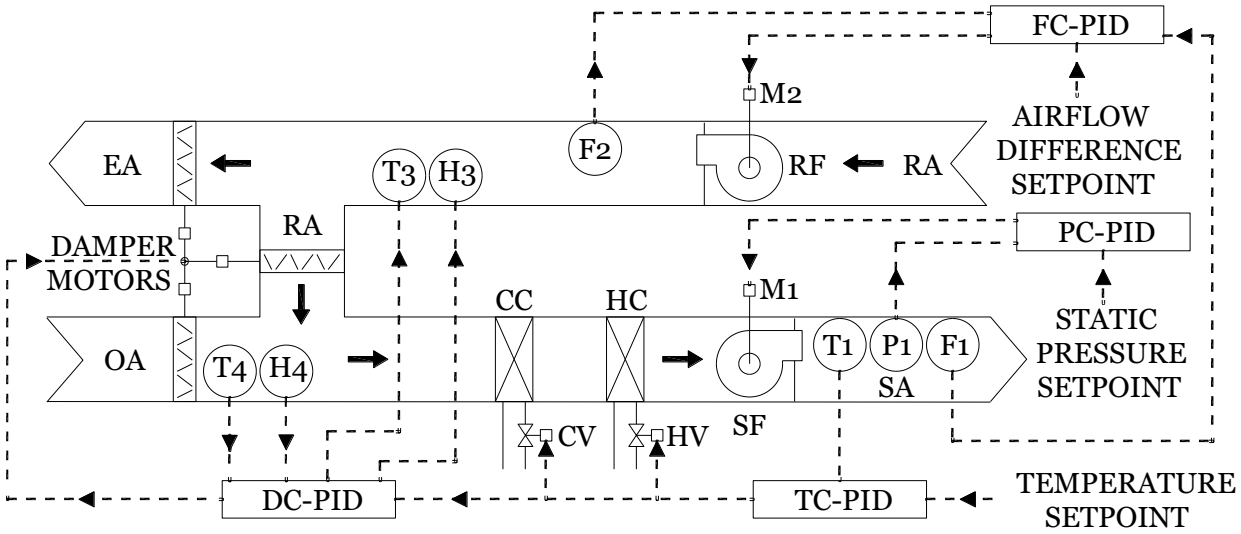

Figure 2.3 Control schematic of a single-duct VAV system [3].

2.3.1.1.2 Tuning of PID control loops

Although, the vast majority of controllers for VAV applications are furnished with PID capability, usually the "Derivate" gain value is set to zero in the tuning process, because the PI contributions alone are regarded as being adequate enough to avoid large system overshoots, and adding the "Derivate" gain to the PID controller makes the control system more susceptible to hunt the setpoint erratically [31].

If PID controllers are not tuned appropriately the response of the control system will be either sluggish or unstable, thus most of the research done for PID controllers is focused in developing effective calibration methods, these approaches will be explained in the "Advanced Control Methods" section of this document, as these procedures implement contemporary control engineering techniques. In the HVAC industry the most

common approach to tune PID loops is the Ziegler and Nichols (Z-N) method [32]. The Z-N method has been proved to only be adequate under the conditions for which it is tested, this is because the gain values are set only to characteristics of the disturbances that the system experiences during the test period and not over the whole spectrum of broad dynamics a VAV system process experiences [25].

2.3.1.1.3 PID control strengths and weaknesses in VAV applications

PID loops are currently the primary control method used for VAV control applications, due to the fact that they are easy to use, as they do not require deep understanding of the underlying working of the AC system process, all that matters is that some measured process variable can be strongly influenced by some control output variable, HVAC control engineers can achieve this straightforwardly with current control and computer technology, making their implementation also very cost effective. However, PID control is far from being the optimal solution for VAV systems, since each VAV box is throttled at very fast intervals to meet their airflow setpoint, this causes a large pressure drop in the ductwork, which has to be constantly compensated by the supply fan speeding up and then down when a system overshoot occurs, this results in a lot of unnecessary energy consumption. To compensate this issue constant retuning of the gain parameters is required which is often complex, and rarely done in the field, making the PID control robustness weak. PID loops function as single input singe output (SISO) control systems, each loop operates independently of each other, this can create conflicts between zones in the VAV system, as some terminal units can be starved of air while others overfed, and as a consequence no overall optimal operation of the system can be achieved [25].

2.3.2 Advanced/Optimal Control Methods

The following section contains a summary of the state-of-the-art techniques and developments for control of VAV systems, it also includes a discussion on the concept of adaptability and its distinction from robustness regarding control engineering.

2.3.2.1 *Adaptive Control*

Most modern controllers are built with robustness in mind, which is the capability to perform satisfactory within a defined range of uncertainty, for example in VAV systems this would be the ability to meet the setpoint even in shoulder season, where cooling and heating could be requested at the same time in different zones of the building, these are disturbances that are expected by the "nominal" controller design. In real control applications the parameters of a "nominal" controller and the dynamics for which it was tuned are subject to change over time, in a VAV system, heat exchangers and filters get dirty which causes large pressure drops and lowers the heat transfer efficiency; air leakage from ducts can increase; and quick ambient temperature swings can incite poorly tuned controllers to overshoot constantly, conditions like these drop the overall VAV system performance [33]. To avoid these issues advanced control methods, deploy adaptive control which is an approach that furnishes the controller with tools that are able to automatically adjust and tune its parameters in real time as they deviate from their design values during operation, with the goal of accomplishing the best performance out of the controlled system [34, 26].

2.3.2.2 *Model-Free Control*

These control methods do not rely in mathematical models but rather used reinforcement learning approaches to develop the sequence of operations of the controller based in the knowledge of historical working conditions. Control settings are designated by experts on the systems based on the patterns that are identified by testing the VAV system, or by analyzing operational information extracted from a BAS. This technique mimics the actions an expert operator would take to adjust a system, as specified by the logic placed in the knowledge database [3]. Examples of Model-Free Control in VAV systems are the use of Fuzzy Logic Controllers (FLC), for Autotuning and Gain Scheduling techniques of PID Loops [25].

Autotuning for PIDs is an adaptive control technique that automates the procedure of testing and calculating the gain values of the controller, when coupled with expert systems like FLC for VAV equipment it has been shown to reduce overshoot, oscillation and power consumption over a conventional PID scheme [35]. This method employs the expert system to evaluate the performance of the PID loop every time there is a change of setpoint, or under the presence of considerable disturbances. Parameters like damping, period of oscillation and static gain are calculated by the autotuning mechanism called "Relay" (Figure 2.4). The PID loop is disabled during this testing procedure, and switches back inline once the relay has passed on the new calibration values [3].

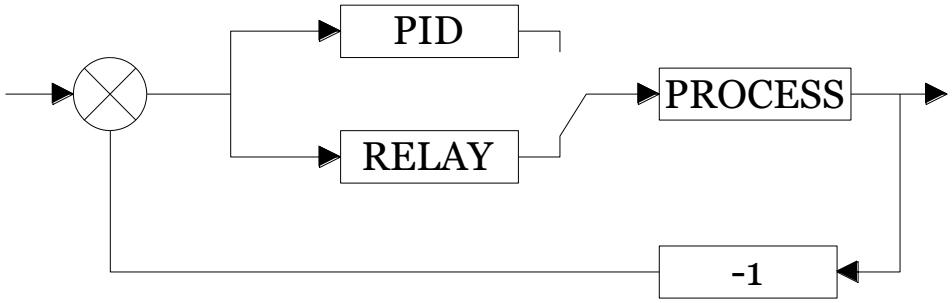

Figure 2.4 Block diagram of a PID relay auto-tuner [3].

Gain scheduling is another adaptive technique that is similar autotuning, but the main difference is that the expert system has a schedule or table with pre-programmed gain values, that modify the operating PID values, each the expert system identifies a different operating condition of the system. The gain values that are contained in the schedule, are established by an expert who carries out detailed simulations of the system or by analyzing historical data (Figure 2.5). This method is well suited when the non-linearities of the system are well known. The gain schedule table can be constantly updated to compensate for unexpected operation conditions, this allows to improve the performance of the control system continuously [3].

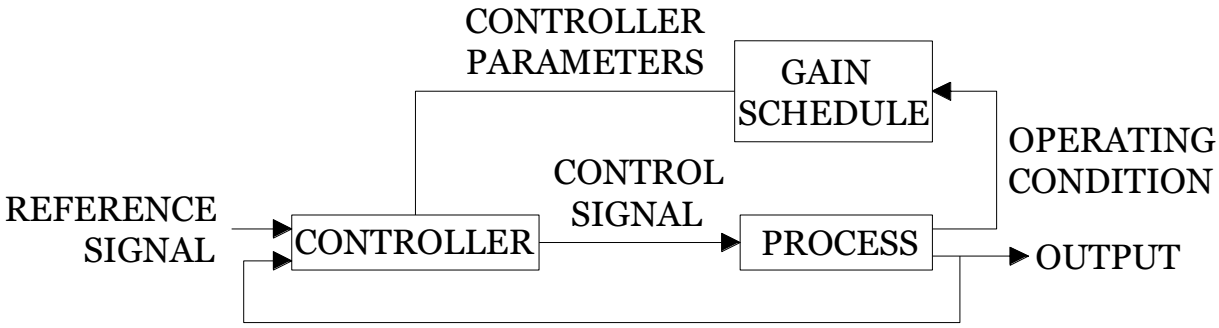

Figure 2.5 Block diagram of a Gain Scheduling controller [3].

The main drawbacks of Model-Free control approaches are that they still rely heavily on PID loops; which makes them prone for the same issues like instability, lag, and their inability to find a holistically optimal solution for the operation of VAV equipment; also the fact that to design them extensive information of the system must be acquired either by simulation or testing which can become time consuming [25].

2.3.2.3 *Model-Based Control*

Model-Based Control often called Model Predictive Control (MPC) as well, is an approach that employs an internal model to predict the behavior of the system over a defined horizon of time, the output results from these simulations, are processed through and optimization solver, which in turn determines from the data what the best control action would be to minimize energy consumption or operational cost of the building system, after theses outputs are executed the cycle restarts. Constrains are also added to the model to guarantee the necessary conditions for comfort, health and safety of the building occupants. The MPC formulation to represent the objective function is the following equation (2-3), the model can be derived from white, black or a combination of both techniques which is the most common approach for HVAC systems [8].

$$minJ = f(u, x, y) \tag{2-3}$$

Where:

$$\dot{x} = f(x, u, w)$$
$$0 = h(x, u)$$

$$x^L \leq x \leq x^U$$
$$y^L \leq y \leq y^U$$
$$u^L \leq u \leq u^U$$

$J =$ *Cost function*
$x =$ *vector of state variables*
$y =$ *vector of system output*
$u =$ *control input*
$w =$ *vector of state disturbances*
$\dot{x} =$ *derivative of state variables*
superscript $L =$ *lower bound*
superscript $U =$ *upper bound*

MPC in buildings has demonstrated the potential to save HVAC systems and equipment around 15 to 20% of energy consumption and it is the most widely applied advanced control solution in the process automation industry. However, in commercial buildings and HVAC equipment applications MPC has not gained popularity due to the lack of standardization and tools to enable the easy development of models, optimization solvers, and moving horizon features that comprised the MPC approach [11]. Moreover, another crucial problem for Model-Based Control is the lack of research for the use "Adaptive Control" techniques which any long-term MPC solution should include, to guarantee robustness and optimal performance over the lifecycle of any controlled AC equipment [9].

2.3.2.4 *Hybrid Control Methods*

This control approach mixes both advanced control techniques of Model-Free and Model-Based methods, in an effort to overcome the possible hurdles any of these could bring forward in the process of designing a controller [8]. In VAV systems a very popular utilization of hybrid control has been for self-tuning for PID loops (Figure 2.6). One example is the self-tuning method called PRAC (pattern recognition adaptive controller), that works by pairing autotuning, with a black box model that detects load and setpoint changes, to classify the characteristics that describe the system response, this method offers the benefit of being able to tune the parameters of the PID controller in real time unlike autotuning which requires deadtime during its testing period, and thus provides a more steady control performance [36]. Hybrid controllers for HVAC systems if poorly designed are subject to both the setbacks of Model-Free and Model-Based techniques, where adaptability also plays a major role in the concern for the wide spread adoption of this approach in building control applications [3].

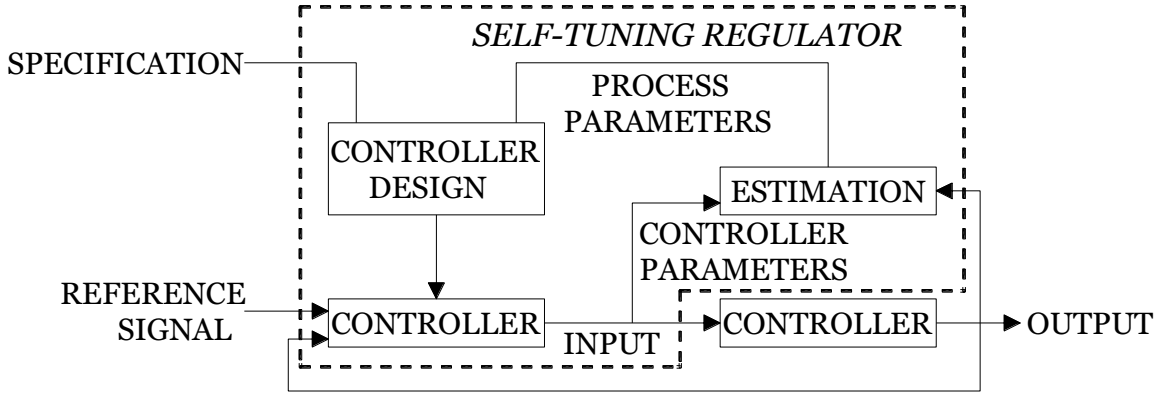

Figure 2.6 Block diagram of a self-tuning controller [3].

2.3.3 Control Strategies for VAV Systems

While variable air volume equipment design and configuration can vary a lot across field applications, the goals and tasks that have to be achieved by a VAV control system can be principally classified in to two groups, local and supervisory control strategies [37, 38]. Local control strategies deal with meeting the setpoints necessary to guarantee a healthy and comfortable indoor environment for the occupants of the building, they are called local because they are measured and regulated by the sensor and actuators respectively located in the VAV equipment itself, these are mainly supply air temperature, supply static pressure control, outdoor airflow rate. Supervisory control strategies on the other hand are placed in to work to optimize the performance of the AC system, these modify the system setpoints, to minimize the cost or energy consumption of the equipment, they are called supervisory because they reset the values of the local setpoints according to needs of the air conditioned zone, primarily they reset the values of supply air temperature, static pressure and outdoor airflow rate [39, 40, 41].

2.3.3.1 *Local Control - AHU Supply Air Temperature*

AHUs provide air at the appropriate temperature needed by a conditioned zone; this is accomplished by regulating its discharge air temperature. The supply air temperature of an AHU is typically set by a thermostat in the zone, or by a supervisory controller. To modulate the cooling and heating elements of the system a sequential split-range strategy is employed (Figure 2.7).

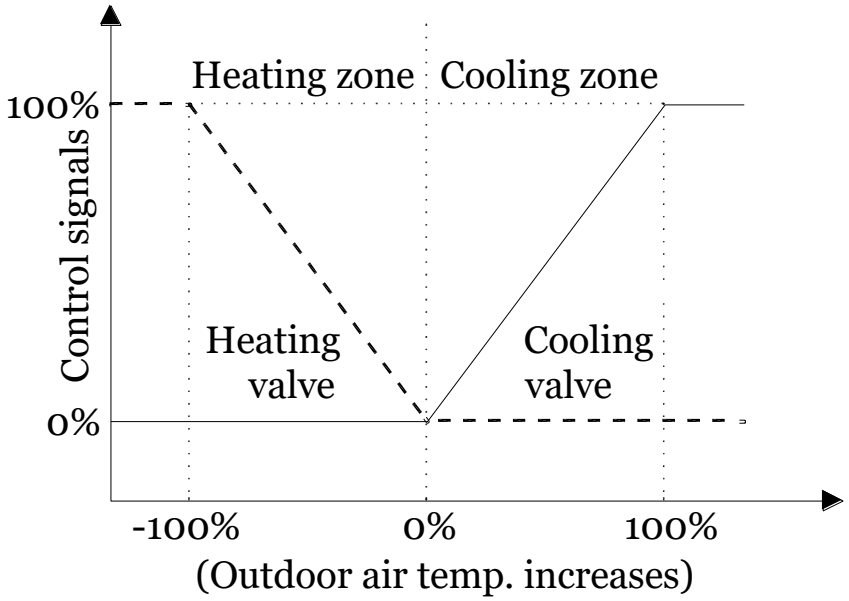

Figure 2.7 Sequential split-range control strategy for SAT control [3].

Sequential split-range control is utilized to avoid simultaneous heating and cooling by the AHU, it works by enabling heating or cooling based on the temperature of outdoor air to reach the setpoint of the supply air temperature. Once the operation mode has been

established be it heating or cooling, the actuator, usually a control valve, will adjust its output based on the measured deviation from the temperature setpoint, where 0% for a control valve means totally closed, and 100% is a fully open position. To evade equipment short cycling this strategy is implemented with a dead zone (dead band) which is a temperature range where no heating or cooling is provided [3].

2.3.3.2 *Local Control - Static Pressure*

Static pressure control is applied to VAV systems for preventing noise generation and energy loss. System resistance varies with the throttling of the terminal units, if the system resistance increases the airflow quantity the central fan supplies decreases, to compensate the system must run the fan at a higher speed to maintain the appropriate system airflow, this is because the speed of the motor is directly proportional to both its airflow and an air static pressure, so at partial load conditions the fan will be operated at lower speeds. The static pressure setpoint is provided by the supervisory control, the quantity of the setpoint is specified to meet the total airflow needed by the VAV boxes even at part load conditions, this setpoint can be fixed or if coupled with an optimal control strategy it can be reset by the supervisory control [3].

2.3.3.3 *Local Control - Zone Airflow*

In VAV systems with pressure independent terminal units, zone airflow control is managed by a cascade arrangement (Figure 2.8), an inner loop temperature controller (FC1) measures the state of the zone through a temperature sensor (T1), the temperature controller compares this input with the supervisory air temperature setpoint and based on the error the inner loop controller outputs the supply airflow setpoint to the outer loop airflow controller (FC2), the airflow controller modulates the damper's (D1) motor (M1) from totally closed to fully open, depending of the amount of the deviation calculated when evaluating the supply airflow through the flow sensor (F1) against the supply airflow setpoint [3].

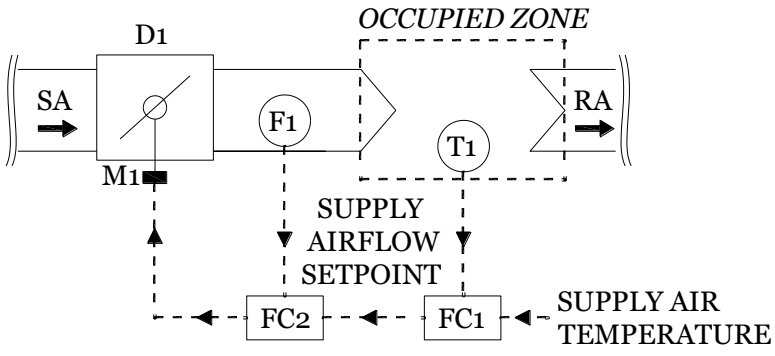

Figure 2.8 Control diagram of a pressure independent VAV box [3].

2.3.3.3.1 VAV Reheat Box Control

Cooling and dehumidification are the dominant modes of operation for AC equipment serving buildings located in warm climate regions, so reheat terminal units are used when the supply air provided by the AHU is to cold to be directly discharged to the conditioned space, where if not treated could cause condensation, comfort and health issues. The two most common control strategies for reheat VAV boxes are the “single maximum” and the “dual maximum” approach. In the “single maximum” approach when cooling is enabled the airflow setpoint is mapped between a maximum flow rate dictated by the nominal cooling load, and a minimum flow rate which is determined based on the nominal heating load requirements, which is in between range of 30 to 50% of the maximum flow rate as recommended by the ASHRAE ventilation standards (Figure 2.9). When reheating is enabled, the VAV box airflow setpoint is fixed at the minimum rate and the heating equipment in the terminal unit is modulated to reach the appropriate air temperature [17].

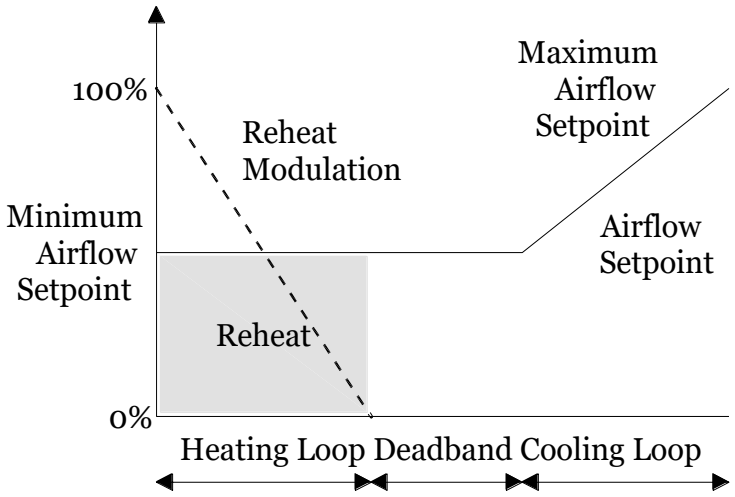

Figure 2.9 "Single maximum" control strategy for VAV Reheat boxes [15].

Under the “dual maximum” control strategy air flow is modulated in both cooling and heating modes, when the supply air temperature is lower than that the limit of the dead band, the heating equipment in the VAV will be engaged, if the air temperature setpoint is not reached with the heating equipment operating at a 100% of its capacity, the airflow will be increased (Figure 2.10). In heating mode, the maximum airflow setpoint is in between the ranges of 50 to 30% of the cooling mode’s maximum airflow setpoint, but the minimum heating and cooling airflow setpoints are both lowered to the smallest value permitted by the ASHRAE ventilation standards [17].

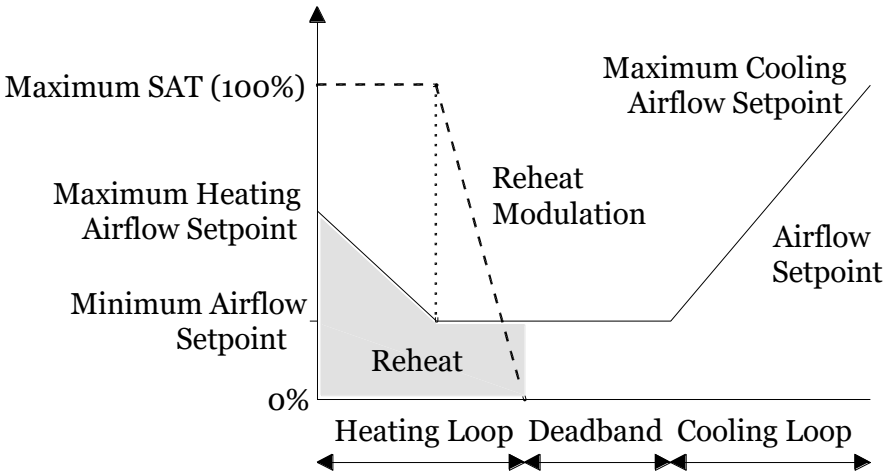

Figure 2.10 "Dual maximum" control strategy for VAV Reheat boxes [15].

The "single maximum" approach guarantees high ventilation rates and heating capacity, but this may come at the expense of higher energy consumption and overcooling of conditioned space due to the minimum airflow limit being too high at part load cooling conditions. The "dual maximum" approach provides better temperature control and lower energy consumption than that of the "single maximum", but because its minimum airflow setpoint just complies to the codes recommendation it may not provide appropriate ventilation in buildings where indoor contaminants concentrations might be of significant concern [17].

2.3.3.3.2 Dual Duct VAV Boxes Control

There are two main strategies used for dual duct VAV boxes, the first is "snap acting" and the second one is "mixing control" [17]. The "snap acting control" is named after the fact that during transitions in between operating modes which ever cold or hot side damper is enabled will be closed completely as the control systems exits the dead band (Figure 2.11).

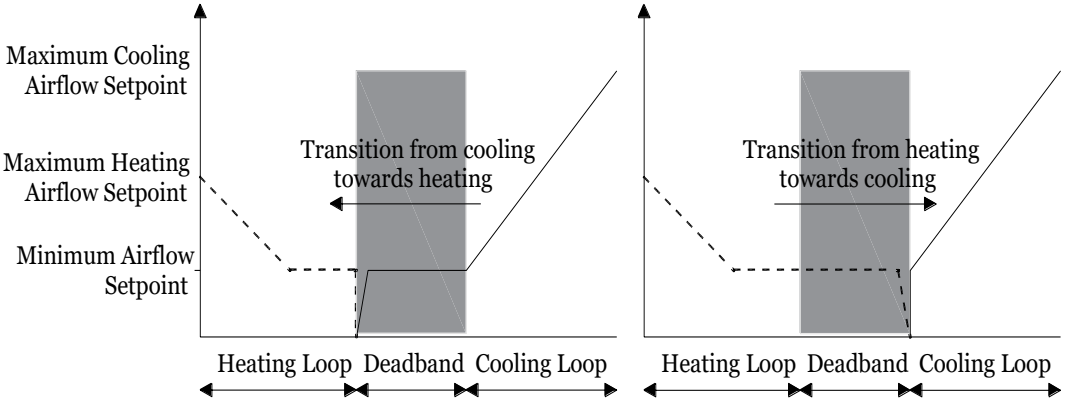

Figure 2.11 "Snap acting" control strategy for dual duct VAV boxes [15].

The “mixing control” strategy aims at maintaining constant ventilation throughout the transition of both its cooling and heating operation modes, to do this the active hot or cold side damper is mapped from its maximum to its minimum airflow setpoint linearly, but as the switchover begins to take place, when the supply air temperature approaches the dead band region, the inactive damper will begin to open at an inverse degree of the active one to preserve the minimum volume control (Figure 2.12). To avoid surpassing the maximum airflow setpoint, the “mixing control” strategy does not allow the active damper to continue opening if the airflow exceeds the setpoint, if the airflow is beyond 10% of the stated maximum limit, the active damper will be totally closed until the airflow falls below setpoint [17].

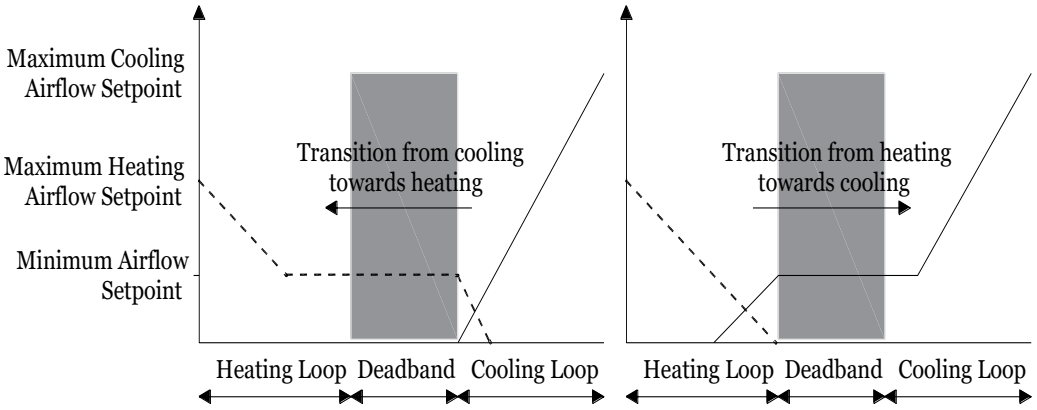

Figure 2.12 "Mixing control" strategy for dual duct VAV boxes [15].

The “snap acting” control strategy does not require reheat energy, so its operational and initial installation cost are lower than those of the “mixing control” approach, but its temperature regulation performance is poor, another shortcoming of “snap acting” control is that it cannot be paired with optimal outdoor air ventilation schemes like Demand Control Ventilation (DCV). On the other hand, “mixing control” provides better thermal comfort and delivers appropriate ventilation rates even at a minimum airflow rate condition [17].

2.3.3.3.3 Fan Powered VAV Boxes Control

Series fan-powered boxes are always started before the central unit fans to ensure them from not running backwards, this configuration provides continuous ventilation but as consequence they have a very low operational efficiency, series fan-powered boxes are only recommended for spaces that require a high minimum flow rate to maintain appropriate air mixing to prevent stratification. Parallel fan-powered boxes are only powered when the system requires heating, they are more efficient than series fan-powered boxes, this is due to the fact that the heat produced by the fan’s operation is harvested and supplied to the conditioned, this can offset or completely eliminate the need for reheating equipment, they are also provided with a backdraft damper located on the outlet of the fan to prevent backward rotation when the unit is off [17].

2.3.3.4 *Local Control - Outdoor Airflow Rate*

The simplest form of outdoor airflow rate control in VAV systems is the coupling of sequential split-range controls with the modulation of outside air intake (this is also called free cooling or economizer control). When the heating mode is enabled the supply air flow setpoint is set to the minimum value, and the heating equipment is modulated from 0% to a 100% to meet the supply air temperature setpoint, as the outdoor temperature rises, the sequential split-range strategy will make the switchover to cooling mode. Once on cooling mode, the first stage will be to control the OA damper and RA damper, this is done by comparing the return air enthalpy with the outdoor air enthalpy, if the enthalpy of the RA is higher than that of OA, both dampers will begin to modulate to mix the return and outdoor airstreams to reach the supply air temperature point. The OA damper will be opened gradually and the RA damper will close at the same exact rate, if the supply air temperate is not achieved even when the OA damper is fully opened and the RA entirely closed, the cooling equipment will be engaged. Finally, if the system remains in cooling mode and the enthalpy value from OA is higher than that of the RA, the OA airflow setpoint will be set to its minimum [3].

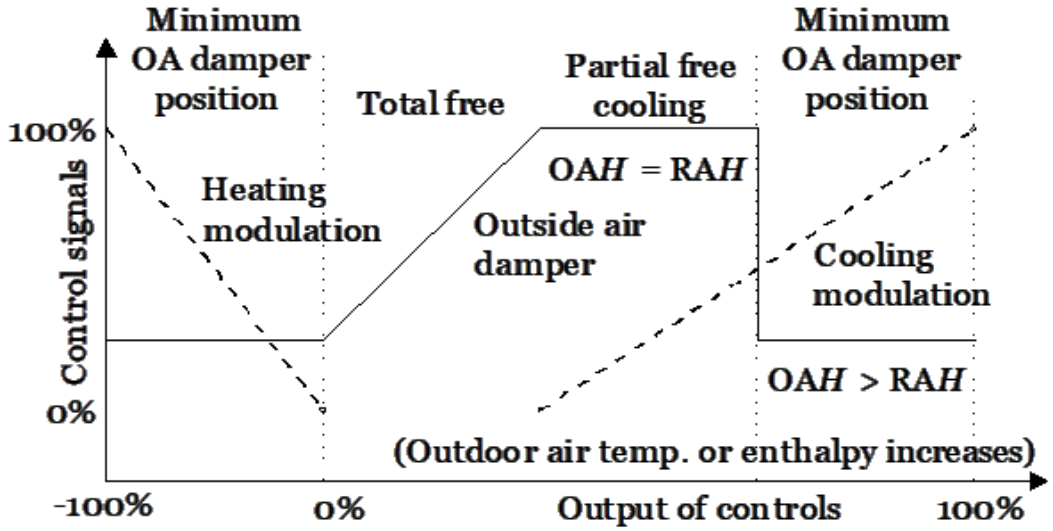

Figure 2.13 Split-range control strategy for outdoor airflow rate regulation [3].

2.3.3.5 *Supervisory Control – Supply Static Pressure or Supply Airflow Setpoint Reset*

The total amount of supply airflow VAV systems can deliver, can be based either on the measurement of duct static pressure or total airflow, as both system properties are interlinked, regulating the speed of the central fan will have a direct effect on the overall total air pressure, airflow and fan power consumption [42, 43]. For this reason, the optimal control strategies for static pressure and supply airflow reset are placed under the same rubric.

For commercial buildings the "Trim and Respond" control strategy for static pressure setpoint reset is the most used. Under this method the duct static pressure is adjusted based on the operating position of the dampers, which are polled at fixed intervals of times, typically every 2 minutes [17]. Dampers that record an opening degree above 95% are said to be in a high position, a maximum threshold for the quantity of dampers that can be in such state is placed on the control system, so if the number of dampers operating in a high position exceeds that of the maximum limit, the static pressure setpoint of the system is increased. Dampers that are located between 80% to less than 95% of their total opening capacity will be considered in a moderate position these actuators will have no effect on the response of the system as they are within the dead band of the control strategy. While dampers that are closed below 80% are said to be in a low position, if the sum of dampers operating in this position surpasses the maximum threshold of the number of dampers that can be in a low position, the control system decreases the static pressure setpoint. The maximum static pressure setpoint is set to satisfy the system full-load condition, while the minimum value is set to maintain appropriate airflow rate at the lowest volume requirement of ventilation, but as a rule thumb in most applications it is just assumed to be one-third of the maximum static pressure setpoint [44].

Another technique is the "PID Control" method in which the maximum and minimum static pressure setpoints are determined in the same way as the "Trim and Response" approach. However, this strategy works by adjusting the static pressure setpoint based on the VAV boxes that require the largest amount of static pressure to be maintained fully open or above a 90% open degree, through a PID loop. The number of boxes that are included in this threshold are the high limit value (N_{max}). If the quantity of dampers that are working at full load capacity exceed the high limit value by one damper ($N_{max} + 1$) the static pressure setpoint is increased [3]. An alternative to this method utilizes the actual additions of the demanded airflow set-points to determine the performance of the system. If the airflow calculated is less than that of the total required by the system the "PID control" raises the static pressure setpoint [45].

"PID control" is not recommended because it has been proven to be harder to tune and control when compared to the "Trim and Respond" method, the later method also offers the advantage of having the capability of "starving" or "ignoring" rogue zones, where faulty design or poor operational conditions may always demand elevated static pressures to operate at their needed capacity. Rogue zones if not discounted can a have high impact on the energy consumption of the system [17].

A promising model-based approach is the Total Air Volume (TAV) Method which dismisses the use of static pressure in favor of the actual fan and system performance [44]. The principle of this approach is to supply the total quantity of air volume quantity based on the predicted interaction of the fan curve and the operating resistance curve of the system; the formulation details of this technique will be discussed in section 3. The drawbacks of the aforementioned method that are also partially the motivations of the present document are; firstly, addressing the issues of developing the model of the ventilation system when there is a lack of documentation concerning the equipment, installation, testing and balancing data, among other necessary details; and secondly, is dealing with coupling the TAV Method with adaptability control techniques to update the model in real time, as ventilation systems in buildings are constantly subjected to modifications and equipment performance problems [33].

2.3.3.6 *Supervisory Control - AHU Supply Air Temperature Setpoint Reset*

It has been proven that the two main parameters in VAV systems to achieve greater energy efficiency are optimizing its Supply Air Temperature (SAT) and supply airflow rate [46]. When the SAT setpoint in a system is too low in cooling, the terminal units will try to close to the minimum degree as possible which will save fan power, but cause poor system performance as the air gets dumped in to conditioned spaced, producing inappropriate air circulation, inadequate air mixing, and overcooling. Just like static pressure reset strategies, there are two main options for SAT reset, the "Trim and Respond" logic and the "PID control". For both strategies the goal is to use the hottest SAT that satisfies all zones in cooling, or the coldest possible SAT for all zones in heating [17, 47].

Under the "Trim and Respond" logic the system reviews the airflow setpoints of all the VAV boxes, and determines the amount of units that operating in high and low conditions (in relationship to their maximum and minimum airflow setpoints), if the number of terminal units operating in low conditions exceeds the high limit for boxes that can operate under low flow, the SAT is increased, if on the contrary the number of terminal unit exceeds the high limit for boxes that can operate under high flow conditions, the SAT is lowered [17].

On the "PID control" the temperature is reset by assigning the output of a PID loop to the zone with the heating or cooling maximum load, if the zone has a request of over 99% or greater of its airflow, the air temperature will be lowered by the PID in cooling mode, and raised by the PID in heating [3].

SAT reset strategies are paired with occupancy detection or occupancy schedules, for temperature setback, to save energy in zones that are not busy. Another common practice is to configure the maximum and minimum SAT setpoint range depending on the temperature of the outdoor air [17].

When comparing both strategies "Trim and Respond" is preferred for the same reasons as stated on the previous static pressure setpoint reset section.

2.3.3.7 *Supervisory Control - Outdoor Airflow Rate Setpoint Reset*

The outdoor ventilation must be managed according to the needs of the conditioned space, a poorly ventilated zone will have Indoor Air Quality (IAQ) problems, due to high concentration of pollutants, like carbon dioxide, and volatile organic compounds (VOCs), whilst and overventilated zone will waste energy as a consequence of the increased effort to condition the excess air being supplied to the building [48, 49]. To combat this problem ASHRAE in its standard 62.1 instituted a method called Demand Control Ventilation (DCV) which has become along with its variants de facto control strategy for outdoor airflow rate setpoint reset [25].

DCV uses the recorded measurement of CO2 concentration as an indication of air quality within the conditioned space, this is because sensors and methods for quantifying other type of common pollutants like VOCs, Ozone (O3), Nitrogen Dioxide (NO2) and Sulfur Dioxide (SO2) are not considered accurate o reliable [50]. But it has been proven that just focusing on regulating CO2 concentration levels alone cannot assure satisfactory levels of ventilation, this is because other factors, like fluctuating occupancy, size of the occupied space, and indoor pollutants from construction materials and furnishings, also play an important role, in the IAQ of a building. A proposed solution to ameliorate the performance of DCV was stablished by Wang and Jin in which the control strategy is founded in the dynamic balance of CO2 in the space, which can accomplish an appropriate response even under oscillatory occupancy conditions, and compensate the shortcoming of just using CO2 concentration as the main IAQ indicator [51]. Furthermore, to make the strategy robust the method was paired with sequential split-range control by to modulate the outdoor airflow rate and is illustrated in Figure 2.14 [52].

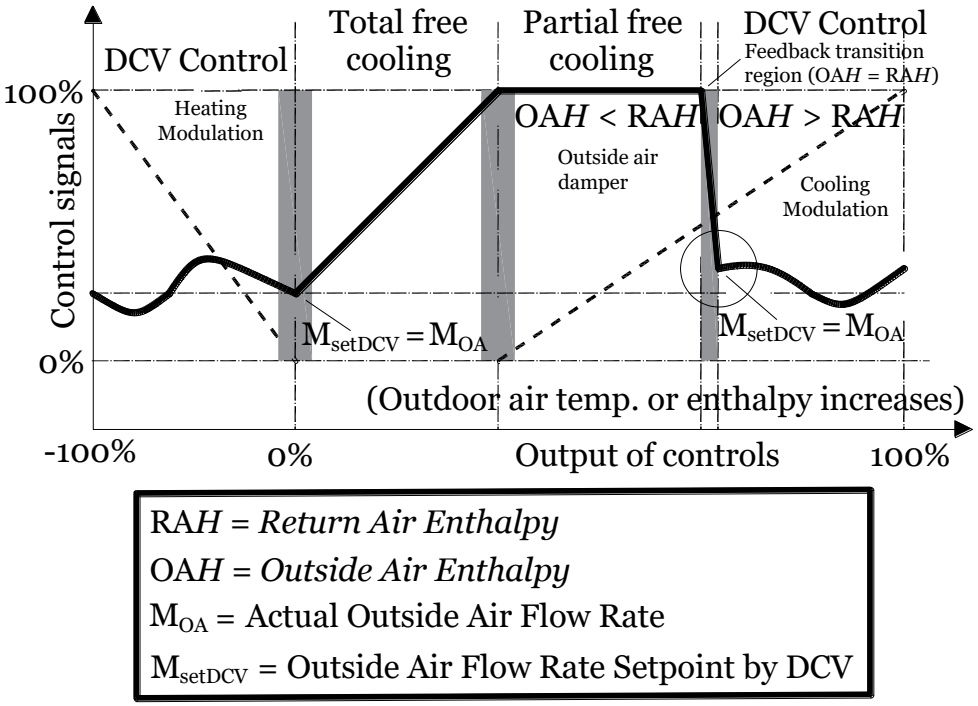

Figure 2.14 Sequential split-range strategy with DCV control [3].

2.3.3.8 *Supervisory Control – Zone Temperature Setpoint Optimization*

Model-based control of zone temperature can enhance occupant comfort by reducing temperature overshoot and achieving a more stable space regulation by decreasing the frequency and damping the response of the actuators of an HVAC system. Zone air temperature mainly responds to weather and internal loads (disturbances), as well as the thermal energy supplied by HVAC systems. The cooling load at any given time for a conditioned zone is determined by the convection from its internal gains and surfaces, and because a large percent of these gains are radiated to the interior surfaces, the state of a building's thermal storage coupled with the effects of the convective heating will also play a major role in the zone's thermal dynamics. A supervisory MPC methodology can provide a comprehensive way to manage a zone's disturbances (like sunshine, outside temperature, occupancy, light and plug loads, etc.) and exploit thermal mass for its conditioning to improve energy efficiency by operating the system at beneficial part-load and weather conditions, which regular PID controls cannot. As an example, pertaining to VAV systems Figure 2.15 illustrates the general relationship of the supervisory temperature control to the local airflow control of a conditioned zone. The supervisory controller can receive hourly data regarding the weather conditions and the status of the internal loads to optimize the required zone airflow setpoints, while the local controller can adjust the damper position and fan speed in a minutely fashion in order to maintain the ideal zone temperature [53, 54, 3].

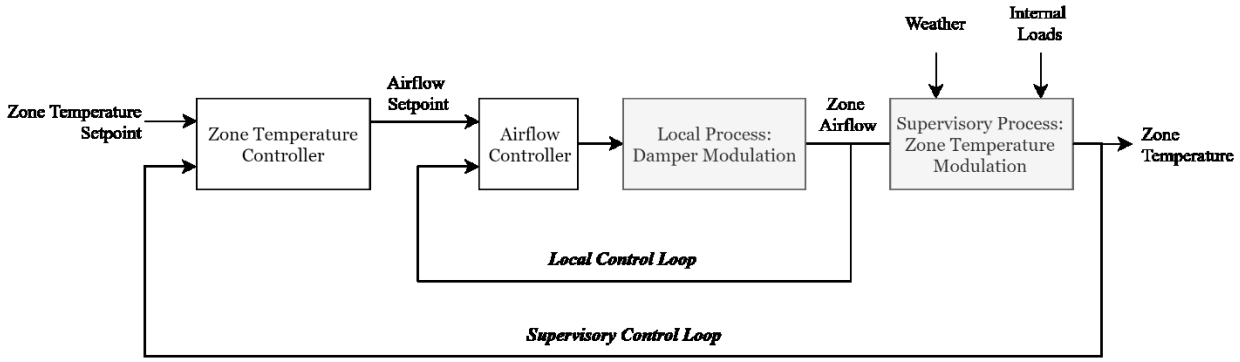

Figure 2.15 Zone temperature control schematic.

3 Introduction to the TAV Control Method & Air Systems Model Design

The TAV control method is a grey box Model-Based Control approach for multizone VAV systems, it is based on the characteristics of the fan-system interaction, where the operation point is determined by the intersection between the fan and system resistance curves. To develop the controller the volumetric flow-pressure fan curve of the central air handling equipment is required to obtain its effective traits. Ductwork, fittings, and other components are represented as fixed resistances or constant pressure drops to the total pressure supplied by the supply fan at any given motor velocity. VAV boxes are portrayed as variable resistances to be able to predict the effect they will have over the total system resistance. The objective of the TAV control method is to achieve the required airflow setpoints for all terminal units in a VAV system by modulating the positions of its dampers to attain the minimum possible system resistance, which in turn allows the fan motor to run at its lowest possible speed to guarantee the least amount of system power consumption [44].

3.1 Air Systems Main Component Models

Air systems in terms of pressure losses and airflow can be divided in to three main categories:

- Ductwork, fittings and HVAC devices which are constant resistance components [55, 56].
- VAV Boxes control dampers are variable resistance components [57].
- Fans provide enough air pressure to overcome the resistance produced by the system, the amount of air they supply is also dependent on the total system resistance [58].

3.1.1 Duct Modeling

Flow resistance for a given duct section can be derived from the total pressure lost at a given specific volumetric flowrate in Cubic Feet per Minute (CFM) [55, 56]. For a straight duct, the total pressure loss (in. WC) between to planes can be stated as:

$$\Delta P_{T_{loss}} = \frac{8 C_v f L \rho}{g_c \pi^2 D^5} Q^2 \tag{3-1}$$

Where:

$f = Friction\ factor$
$\rho = \ Density\ of\ fluid\ (lb/ft^3)$
$g_c = dimensionql\ constant, 32.2\ lb_m \cdot ft\ /\ lb_f\ \cdot\ s^2$

$C_v = Conversion\ constant$
$L = Length\ (ft)$
$D = \ Diamater\ (ft)$
$Q \ = Volumetric\ flow\ rate\ (ft^3/min)$

Since for any straight duct section, the diameter and length are constant, and the difference in the mean values of friction and air density across an air system will be very small, the airflow resistance can be considered as a constant value, thus it can be defined as:

$$R \ = \ \frac{8C_v f L \rho}{g_c \pi^2 D^5} \left[\left(\frac{in.WC}{(ft^3/min)^2} \right) \right] \qquad (3\text{-}2)$$

By substituting the airflow resistance R into equation 3-1 it can be derived that the total pressure loss of a duct sections is:

$$\Delta P_{T_{loss}} = \ RQ^2 \qquad (3\text{-}3)$$

The relation between total pressure loss and airflow rate in a duct section can be plotted as a parabola whose vortex coincides with the origin of the graph (Figure 3.1).

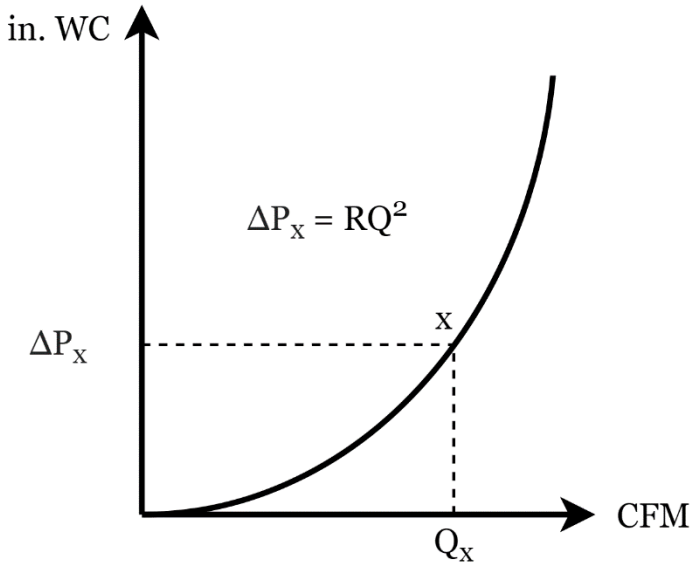

Figure 3.1 Total pressure loss and flow resistance of a duct section [16].

3.1.2 Duct Fittings and Air System Components Modeling

The ductwork of an air system can contain fittings likes elbows, transitions, contractions, filters, heat exchangers, coils, among others. All these components represent additional dynamic pressure losses, since this quantity is also constant it can be denoted as a local loss coefficient (C_{dy}). The flow resistance for duct fittings and air system components can be expressed as:

$$R = \frac{8\rho\left(\frac{C_v f L}{D} + C_{dy}\right)}{g_c \pi^2 D^4}\left[\frac{in.WC}{(ft^3/min)^2}\right] \quad (3\text{-}4)$$

Since R is also a constant value the total pressure loss of a duct fitting or air system component can be calculated using equation 3-3 as well.

A word of caution for modeling elements like filters and coils, as these components tend to increase their dynamic pressure losses, as they typically collect dust and other particulate matter which makes their local loss coefficient larger over time. Coils that are used for both heating and cooling, may have larger local loss coefficients during the summertime as in cooling mode condensation might take place, increasing the resistance of the component to the flow of air [44]. To overcome the aforementioned concerns, the model must be field calibrated and retuned periodically as required, the "Model Calibration and Adaptability" chapter of this document describes techniques to address these issues.

3.1.3 VAV Boxes Modeling

VAV terminal units in air systems utilize dampers as airflow control components. The airflow resistance and local loss coefficient of a damper is determined by several factors like the shape and materials of their blades, frame members, and rotating mechanisms. Airflow regulation is achieved by varying the free face area of the damper as this proportionally increases/decreases their resistance [57]. The total pressure loss of a fully open damper can be stated as:

$$\Delta P_{T_{loss}} = k\frac{\rho}{2}\left(\frac{Q}{A}\right) \quad (3\text{-}5)$$

Where:

$k = Damper\ drag\ coefficient\ (local\ loss\ coeficient)$
$\rho = Density\ of\ fluid\ (lb/ft^3)$
$A = Cross-sectional\ area\ when\ damper\ is\ fully\ open\ (ft^2)$
$Q = Volumetric\ flow\ rate\ (ft^3/min)$

For control modeling purposes the value of the airflow resistance of a damper must be expressed as a function of its angular position, from closed to fully open, so the damper drag coefficient can be fitted to following expression [44]:

$$R_{damper} = \ a \cdot e^{\left(-c\left(\frac{d}{100}\right)\right)} + b \ \left[\left(\frac{in.WC}{(ft^3/min)^2}\right)\right] \tag{3-6}$$

Where:

$a, b \ and \ c \ = Coefficients \ derived \ experimentally$
$d \ = Damper \ opening \ degree \ expressed \ in \ percent \ (0 \ to \ a \ 100)$

3.1.4 Fans Modeling

A fan curve is a mathematical representation of its performance, for system control the most important relationship is that of volume flow versus its static pressure. Under a constant operational speed a fan curve can be modeled as a polynomial equation, the order of which will depend on the specific shape of the fan's performance in question, for this study a fourth order polynomial equation will be used [44, 59]:

$$P_s = \ a_4Q^4 + a_3Q^3 + a_2Q^2 + a_1Q + a_0 \tag{3-7}$$

Where:

$a_0 \ through \ a_4 = Coefficients \ derived \ experimentally$
$P_s \ = Fan \ total \ static \ pressure \ (in.WC)$
$Q \ = Volumetric \ flow \ rate \ (ft^3/min)$

3.1.4.1 *Effects of Air Density Change on Fan Performance*

Manufacturers in North America typically provide fan curves rated at standard air conditions. The Air Movement and Controls Association (AMCA) along with ASHRAE are the main institutions that create the guidelines for rating fans, and they define standard air as air having the following properties a density of 0.075lbm/ft³, a temperature of 68°F, a relative humidity of 50%, and a barometric pressure of 29.92 inches mercury at sea level [60]. With a fan operating at constant speed a change in air density will have the following effect over its performance:

$$Q_c = Q \tag{3-8}$$

$$P_{sc} = \ P_s \ (\rho_c/\rho) \tag{3-9}$$

Where:

$Q = Volumetric\ flow\ rate\ at\ standard\ air\ density\ (ft^3/min)$
$Q_c = Volumetric\ flow\ rate\ at\ operating\ air\ density\ (ft^3/min)$
$P_s = Fan\ total\ static\ pressure\ at\ standard\ air\ density\ (in.WC)$
$P_{sc} = Fan\ total\ static\ pressure\ at\ operating\ air\ density\ (in.WC)$
$\rho = Standard\ air\ density\ (0.075 \text{lbm/ft}^3)$
$\rho_c = Operating\ air\ density\ (in.WC)$

From expressions 3-8 and 3-9 it can be stated that the change of air density has no effect over the airflow a fan can deliver, but it will increase or decrease the amount of total static pressure that a fan will be able provide [58].

3.1.4.2 *Fan Affinity Laws*

Fan affinity laws dictate that if the operational air density and fan size remain constant, the relationship of its characteristics to its operational speed can be expressed as:

$$Q_2 = Q_1 \left(\frac{N_2}{N_1}\right) \tag{3-10}$$

$$P_{s2} = P_{s1} \left(\frac{N_2}{N_1}\right)^2 \tag{3-11}$$

$$H_2 = H_1 \left(\frac{N_2}{N_1}\right)^3 \tag{3-12}$$

Where:

$N_1\ and\ N_2 = Fan\ operational\ speed\ 1\ and\ 2\ (RPM)$
$Q_1\ and\ Q_2 = Volumetric\ flow\ rate\ at\ operational\ speed\ 1\ and\ 2\ (ft^3/min)$
$P_{s1}\ and\ P_{s2} = Fan\ total\ static\ pressure\ at\ operational\ speed\ 1\ and\ 2\ (in.WC)$
$H_1\ and\ H_2 = Fan\ Power\ Input\ (kW)$

These relationships are useful for controlling and predicting the performance of the fan in air system [58].

3.2 Interactions of Air Systems Components

Air systems can be represented as electrical circuits, where components like ducts, fittings, and other devices are airflow resistances that can be placed series or parallel arrays to simplify their analysis [55, 56].

3.2.1 Airflow Resistances Connected in Series

Per the conservation of mass principle or the continuity equation, it can be stated that in a duct section comprised of several elements in series (

Figure 3.2), the flow rate will be constant across of all them, thus the total pressure loss across said array can be calculated using the following relationships:

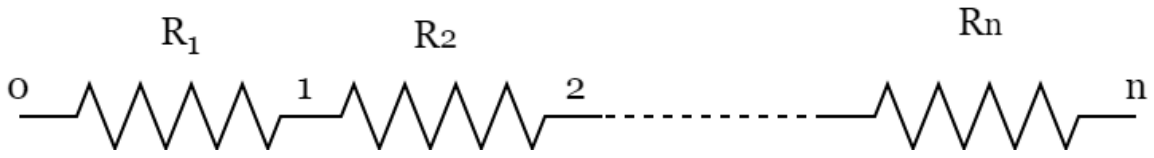

Figure 3.2 Airflow Resistances in Series.

$$\Delta P_{T_{loss}} = \Delta P_{T_{01}} + \Delta P_{T_{12}} + \cdots + \Delta P_{T_n} \quad (3\text{-}13)$$

$$R_T = R_1 + R_2 + \cdots + R_n \quad (3\text{-}14)$$

$$R_T Q^2 = (R_1 + R_2 + \cdots + R_n) Q^2 \quad (3\text{-}15)$$

3.2.2 Airflow Resistances Connected in Parallel

For an air system that has multiple sections in a parallel array (Figure 3.3), the total airflow will be equal to the sum of the flow through each branch (airflow resistance):

$$Q_T = Q_1 + Q_2 + \cdots + Q_n \quad (3\text{-}16)$$

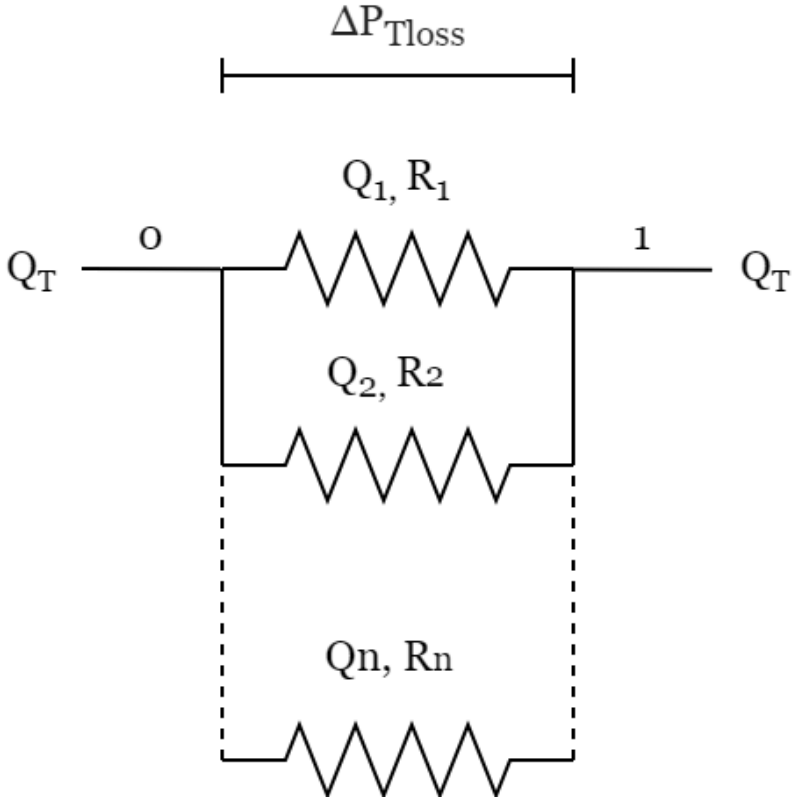

Figure 3.3 Airflow resistances in parallel.

For components in a parallel distribution the total pressure loss will be the same across all its resistance elements ($\Delta P_{T_{loss}} = \Delta P_{01)}$. By substituting equation 3-3 on equation 3-16 it can be stated that:

$$Q_T = \sqrt{\frac{\Delta P_{01}}{R_1}} + \sqrt{\frac{\Delta P_{01}}{R_2}} + \cdots + \sqrt{\frac{\Delta P_{01}}{R_n}} \tag{3-17}$$

$$\frac{1}{\sqrt{R_T}} = \frac{1}{\sqrt{R_1}} + \frac{1}{\sqrt{R_2}} + \cdots + \frac{1}{\sqrt{R_n}} \tag{3-18}$$

3.2.3 Fan and Ductwork System Interaction for the TAV Method

The point where the system resistance curve (or system curve) meets the fan performance curve is called the operation point, this determines the actual airflow the air system will be able to deliver [58].

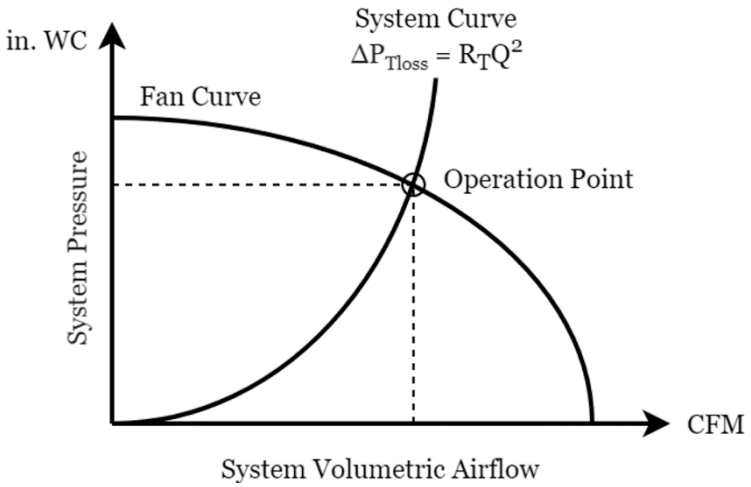

Figure 3.4 Interaction of system curve and fan curve.

For a given (total) airflow resistance, the total pressure loss, as the airflow varies can be calculated using the following equation [58]:

$$\Delta P_{T_{loss2}} = \Delta P_{T_{loss1}} \left(\frac{Q_2}{Q_1}\right)^2 \qquad (3\text{-}19)$$

These interactions are the basis of the TAV method, which aims at achieving the lowest possible total system resistance for any given total airflow demand, this allows the central fan(s) to operate at the lowest possible speed and power input (Figure 3.5).

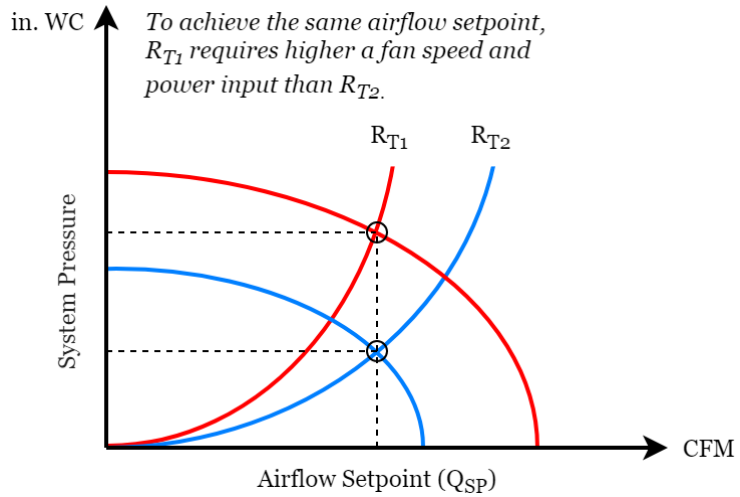

Figure 3.5 Airflow setpoint versus fan-system operation.

4 Testbed Setup & Model Design

The following section is an overview of the experimental setup used to test an actual operating VAV system, technical details can be found on the appendices A and B of this document.

4.1 Testbed Setup Overview

For this study a typical Fan Coil Unit (FCU) that serves a multizone VAV system was employed, the equipment is housed in the 16th level of Concordia University's EV building, a seventeen-floor high rise institutional edifice located on the heart of the downtown area of the city of Montreal, Quebec, Canada.

The system is comprised of 5 perimeter zones, situated on the corner of the building where the south-east and west facades meet. To condition these zones single duct inlet and outlet FCUs are utilized for both return and supply air. Return air is taken from a common false ceiling plenum and mixed with fresh air inside the mechanical room where all the equipment is contained. To provide fresh air the mechanical room is equipped with a fresh air damper, which in turn is supplied air by the AHUs located on the roof of the building.

The employed FCU has a nominal capacity of 3000CFM at 1200RPMs, and houses a filter, a coil for both cooling and heating, the fan is equipped with a variable frequency drive, for speed control (for technical details on the equipment consult appendix A). The central unit feeds five single duct VAV boxes, but due to physical constrains on the number of available inputs and outputs of the control system and lack of open communication protocols, only two zones will be used for the experimental study, the rest of the VAV boxes will be closed off completely.

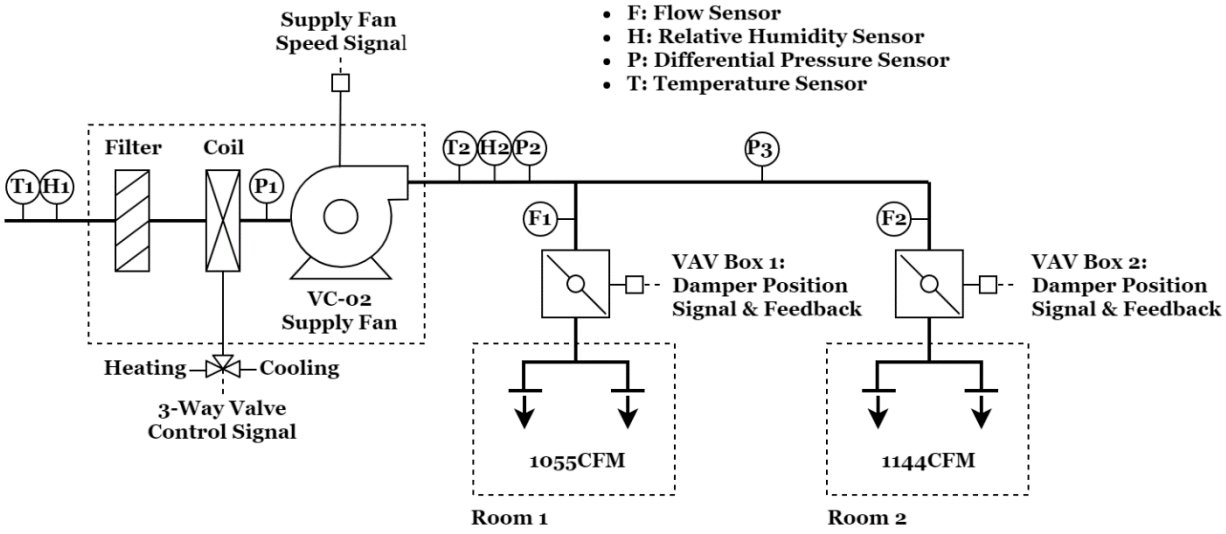

Figure 4.1 Piping and instrumentation drawing of the experimental setup.

Room one requires a total airflow of 1055CFM operating at full capacity, whilst room two requires a total airflow of 1144CFM. Each room has two square air diffusers balanced to deliver the same amount of airflow (50% of the total airflow supplied by its corresponding VAV box). VAV Box 1 and 2, are of the same model and manufacturer thus they have the same nominal capacity (0 to 1400CFM).

Below is a schedule of the sensors utilized for the experimental setup (for technical details on the sensors and instruments used for the study consult appendix B):

Sensor	Measurement	Available from BAS
F1	VAV Box 1 Airflow	Yes
F2	VAV Box 2 Airflow	Yes
H1	Supply Air Relative Humidity	Yes
H2	Return Air Relative Humidity	Yes
P1	Fan Inlet Total Pressure	No
P2	Fan Outlet Static Pressure	No
P3	Duct Static Pressure	Yes
T1	Supply Air Temperature	Yes
T2	Return Air Temperature	Yes

Table 4.1 Experimental setup sensor schedule.

The row labeled "Available from BAS" on Table 4.1 indicates whether the sensor was already installed before the test, sensors P1 and P2 had to be furnished to evaluate the performance of the fan, they where installed according to the AMCA Standard 230-90 for Field Performance Measurement of Fan Systems [61].

Currently all local level control loops are regulated by PIDs, the position of the dampers in each VAV box is throttled to achieve the required airflow setpoints provided by the BAS. The fan is equipped speed is adjusted to maintain a constant duct static pressure; this is done to ensure enough airflow is always available as dampers move to modulate the system.

To implement the TAV controller, a Raspberry Pi 3 b+ single board computer was used as the main controller. Interfaced to the building controller using 3 standard 4-20mA input/output boards. The Python programming language was used to formulate and solve the calibration methods listed in section five for both the fan curve and air system models, by using data collected from the BAS. The TAV controller operation listed on section 6.0 was also executed using a Python script running on the Raspbian operating system of the Raspberry Pi.

4.2 Model Structure & Design

Figure 4.2 illustrates on the left the initial model structure for the experimental setup, the fan serves the role of a power supply, components whose loss coefficients are fixed are bundled up into single resistances, while branches are represented as parallel connections. The two VAV boxes to be controlled are to be considered as variable resistances. The model can be further simplified by collapsing all fixed resistance components of each branch to represent the initial constant resistance value of its variable resistor (VAV box).

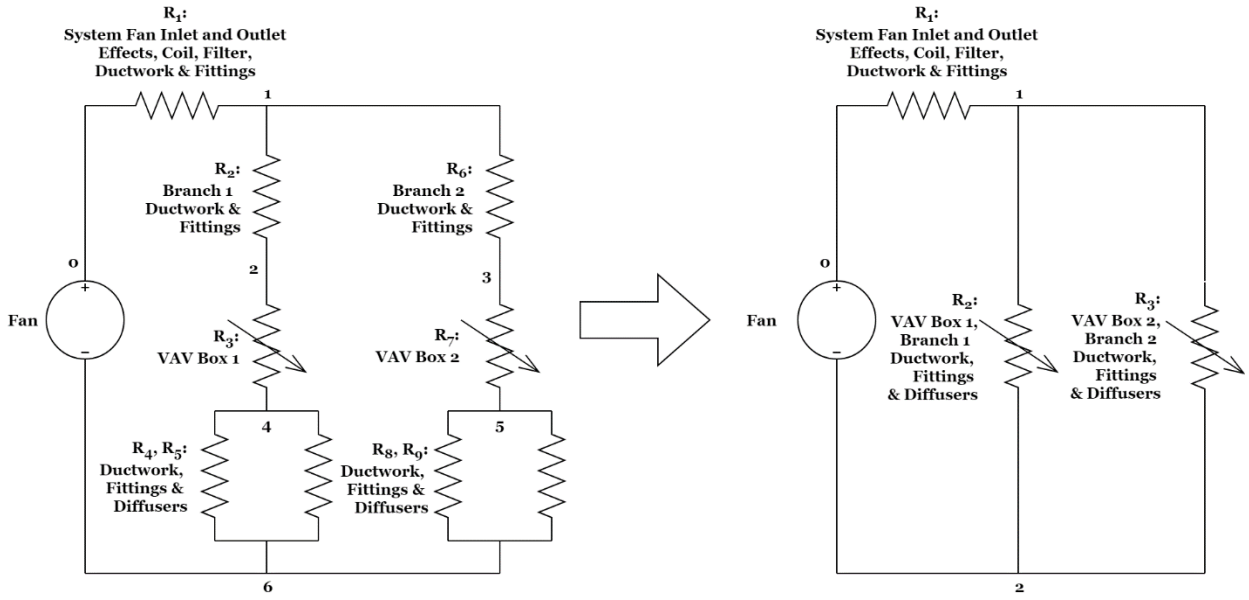

Figure 4.2 Experimental VAV system model structure.

The following equations can be stablished for both branches of the experimental air system:

$$R_{b1} = R_1 + \ R_2 \tag{4-1}$$

$$R_{b2} = R_1 + \ R_3 \tag{4-2}$$

Where:

$R_{b1} = Branch\ 1\ total\ airflow\ resistance$
$R_{b2} = Branch\ 2\ total\ airflow\ resistance$

To obtain the total equivalent resistance at any point of operation with both branches open (at any degree) the following relationship can be used [55]:

$$R_T = R_1 + \frac{R_2 R_3}{R_2 + R_3 + 2\sqrt{R_2 R_3}} \tag{4-3}$$

5 Model Calibration & Adaptability

One of the main goals of the present document is to illustrate a general methodology for model calibration of any air system with field measured and gathered data, as opposed to the original TAV approach which models every single component in the air system by using loss coefficients obtained from the ASHRAE standards for duct design [44]. In addition, the relationship between adaptability and calibration will be described along with a procedure to implement them.

5.1 Fan Performance Curve Model Calibration

In order to be able to determine correctly the characteristics of any VAV system, an accurate fan performance curve must be established, this document will follow the procedure proposed by Guopeng Liu and Mingsheng Liu on the paper title "Development of simplified in-situ fan curve measurement method using the manufacturers fan curve". Optionally, if no information is available from the manufacturer the method set in the AMCA 203-90 publication for "Field Performance Measurement of Fan Systems" can be utilized [61]. Fan performance needs to be validated because the manufacturer's curve is greatly affected not only by the operating air density, but also the by the actual fan installation, this drop in performance cause by subpar inlet and outlet fan configuration can produce a larger than expected pressure loss in the air system, which is commonly called "the system effect" [59]. It has been estimated that by using the nominal fan performance curve the its volumetric airflow could be overrated by 15% of its actual operating airflow [62]. Another reason the fan curve was field evaluated for this study was the lack of total static pressure data available from the manufacture below the 1200CFM airflow mark, these points are well within the range of the operation of the system, extrapolation was required to obtain these total static pressure values.

5.1.1 Manufacturer's Fan Performance Curve

The first step is to obtain the performance of the fan, which is the nominal total static pressure versus its volumetric airflow at standard air conditions as rated by the manufacturer (see Table 5.1).

Airflow (CFM)	Total Static Pressure (in. WC)	Airflow (CFM)	Total Static Pressure (in. WC)	Airflow (CFM)	Total Static Pressure (in. WC)
3200	1.904	2500	2.009	1800	2.042
3100	1.926	2400	2.016	1700	2.047
3000	1.945	2300	2.021	1600	2.053
2900	1.963	2200	2.026	1500	2.060
2800	1.977	2100	2.030	1400	2.070
2700	1.990	2000	2.034	1300	2.083
2600	2.000	1900	2.038	1200	2.100

Table 5.1 Manufacturer's fan performance data at 1200RPM [63].

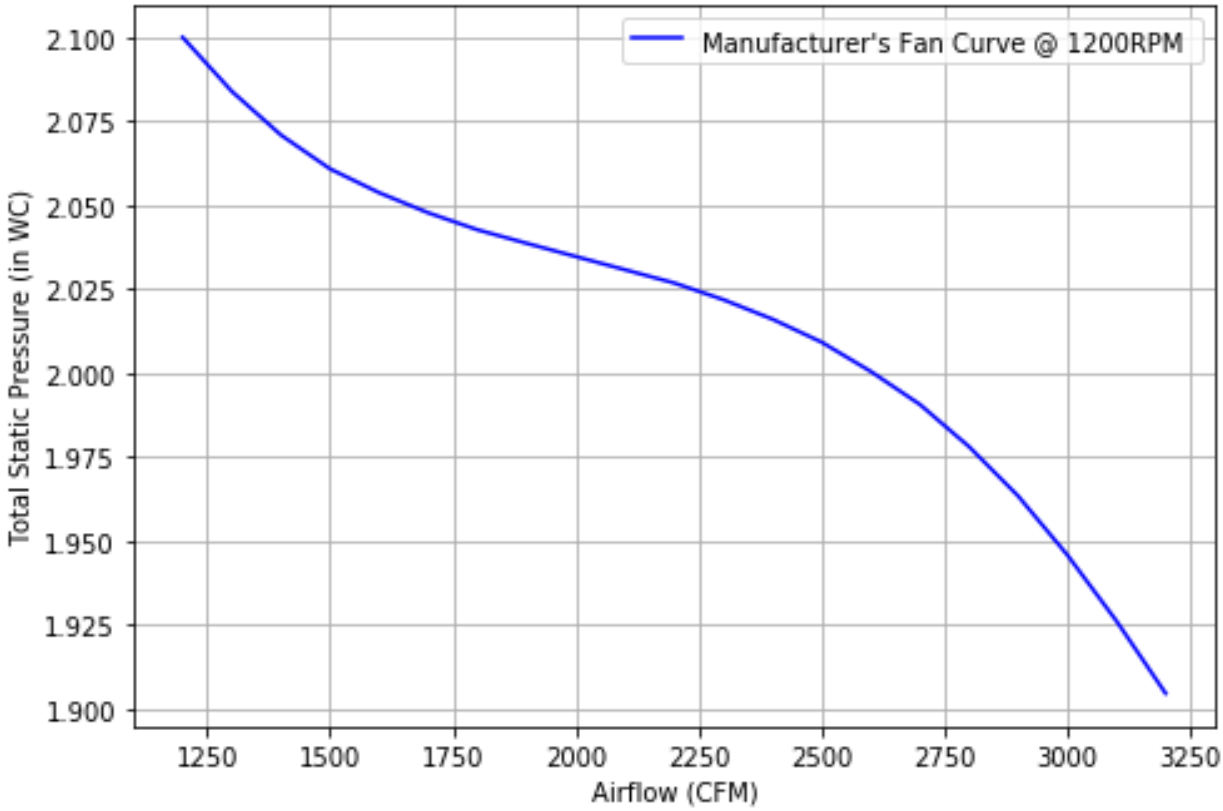

Figure 5.1 Manufacturer's fan curve at standard air conditions [63].

5.1.2 Procedure for Conducting the Field Measurement Test

To verify the performance of fan as installed, the following procedure was employed, as mentioned previously this is based on the AMCA 203-90 publication for Field Performance Measurement of Fan Systems:

1. All the dampers of the system were fully opened (set to a 100%).
2. The speed of the supply fan was set to a 100% for the complete duration of test. The supply fan of the FCU used for the experiment had a belt drive with a ratio of 0.65 from the motor's drive to the fan's shaft, so the total speed when the fan was set to a constant 100% speed signal was approximately 780RPM.
3. The heating and cooling were locked out to have a constant air temperature and density from the inlet of the unit to the inlet of the supply fan.
4. The damper positions where modulated simultaneously to obtain combinations which yielded airflows ranging from approximately 200CFM to 2000CFM, in increments of roughly 50CFM at a time. Each damper-airflow combination was locked and measured for a total time of 5 minutes (consult appendix C for an overview of the trended data of the test).

5. At each damper-airflow combination the measurements in Table 5.2 were taken (consult appendix B for technical details of the sensors and instruments used).
6. To verify the reliability of the field measurements a combination of Electronic Balancing Tools and calibrations instruments were used as benchmarks (for technical details consult appendix D).

Measurement	Sensor(s)	Variable
Fan inlet static pressure	P1	$P_{s,inlet}$
Fan outlet static pressure	P2	$P_{s,outlet}$
Return air relative humidity	H2	H_R
Return air dry bulb temperature	T1	T_R
Supply air relative humidity	H1	H_S
Supply air dry bulb temperature	T2	T_S
Total volumetric airflow	F1 through F5	Q

Table 5.2 Measurements in Figure 4.1 used for calibrating the fan curve.

5.1.3 Calculating Air Density

To be able to compare the field measurements to the manufacturer's fan performance curve the values must be adjusted to be equivalent to those at standard air conditions. To correct the values the absolute air pressures at both the fan's inlet and outlet must be obtained, the following expression was employed:

$$P_{abs} = P_b + \frac{P_s}{13.6} \qquad (5\text{-}1)$$

Where:

$P_{abs} = \ Absolute\ pressure\ of\ air\ at\ plane\ of\ measurement\ (in.HG)$
$P_b = \ Atmospheric\ air\ pressure\ (29.52\ in.HG)^*$
$P_s = \ Static\ pressure\ at\ plane\ of\ measurement\ (in.WC),\ 0\ in.WC\ at\ the\ inlet$

Since no humidification device is available on the FCU, and no dehumidification can take place with the heat exchanger control valve locked out, it can be stated by using the psychrometric properties of air that across the unit there will be only sensible heat gains as the air travels through the system, thus the humidity ratio will be constant, so even with no supply air relative humidity sensor the air density at the outlet can be calculated only using the dry bulb temperature.

*Note: Atmospheric pressure was calculated using an altitude of 367ft, per the recommendation of the building facilities team, and based on the equation given by ASHRAE for Standard Atmosphere $P_b = 29.921(1 - 6.8754 \times 10^{-6} \times altitude)^{5.2559}$ [21].

To obtain the densities at both measuring planes of the fan, the function "GetMoistAirDensity" from the open source PsychroLib python library of psychrometric functions was used to calculate thermodynamic properties of air [64].

$$\rho_{inlet} = GetMoistAirDensity(T_R, HR, 29.52) \quad (5\text{-}2)$$

$$\rho_{outlet} = GetMoistAirDensity(T_S, HR, P_{abs,outlet}) \quad (5\text{-}3)$$

Where:
$\rho_{inlet} = Air\ density\ at\ fan\ inlet\ (lbm/ft^3)$
$\rho_{outlet} = Air\ density\ at\ fan\ outlet\ (lbm/ft^3)$
$HR = Humidity\ ratio\ (lbw/lba)$
$P_{abs,outlet} = Absolute\ pressure\ at\ fan\ outlet\ (in.HG)$
$T_R = Return\ air\ dry\ bulb\ temperature\ (F)$
$T_S = Supply\ air\ dry\ bulb\ temperature\ (F)$

5.1.4 Airflow Rates

To find the total airflow at the outlet of the fan, the airflows of all the VAV boxes where summed, it was assumed that the dry bulb temperature across all of the branches of the air system was the same as the supply air temperature, thus the following equation was applied:

$$Q_{outlet} = Q_{b1} + Q_{b2} + Q_{b3} + Q_{b4} + Q_{b5} \quad (5\text{-}4)$$

Where:

$Q_{outlet} = Volumetric\ flow\ rate\ at\ fan\ outlet\ (ft^3/min)$

$Q_{b1}\ through\ Q_{b5} = Volumetric\ flow\ rate\ for\ branches\ 1\ through\ 5\ (ft^3/min)$

The airflow at standard condition for the fan's inlet was found by using an air density and speed adjustment factors:

$$Q_{inlet} = Q_{outlet}(\rho_{outlet}/\rho_{inlet})(1200RPM/780RPM) \quad (5\text{-}5)$$

Where:

$Q_{inlet} = Volumetric\ flow\ rate\ at\ fan\ inlet\ (ft^3/min)$

5.1.5 Fan System Effect Factor (SEF)

To calculate the fan system effect factor, it was necessary to obtain the operating velocity pressure at the fan's inlet, the ensuing equation was utilized:

$$P_{v,inlet} = (Q_{inlet}/\ 1096A_{inlet})^2 \rho_{inlet} \quad (5\text{-}6)$$

Where:

$P_{v,inlet} = Fan\ inlet\ velocity\ pressure\ (in.WC)$
$A_{inlet} = Fan\ inlet\ area\ (13.4ft^2)$

With the velocity pressure available, the operating total static pressure of the fan without the fan system effect can be calculated per the following equation [65, 58]:

$$P_s' = P_{s,outlet} - P_{s,inlet} - P_{v,inlet} \quad (5\text{-}7)$$

Where:

$P_s' = Total\ static\ pressure\ without\ the\ fan's\ system\ effect\ (in.WC)$
$P_{s,outlet} = Static\ pressure\ at\ the\ fan's\ outlet\ (in.WC)$
$P_{s,inlet} = Static\ pressure\ at\ the\ fan's\ inlet\ (in.WC)$
$P_{v,inlet} = Velocity\ pressure\ at\ the\ fan's\ inlet\ (in.WC)$

To adjust the total static pressure obtained from the test to standard air conditions air density and speed correction factors were applied:

$$P_{sc}' = P_s'(1200RPM/780RPM)(0.075lbm/ft^2/\rho_{inlet}) \quad (5\text{-}8)$$

Where:

$P_{sc}' = Total\ static\ pressure\ without\ the\ fan's\ system\ effect\ at\ standard\ air\ conditions\ (in.WC)$

Finally, to estimate the fan's SEF as proposed by the method of Guopeng Liu and Mingsheng Liu, equation 5-9 is used with the five data points where the least system resistance (largest airflows) were recorded in order to minimize the error of the airflow measuring instruments. The airflows used in the equation have to be equal for both the total fan static pressure of the manufacture's curve and the test fan static pressure measured values, these values are averaged to attain the SEF [59].

$$R_{SEF} = (P_s - P'_{sc})/Q^2_{inlet} \quad (5\text{-}9)$$

Where:

$R_{SEF} = Airflow\ resistance\ of\ the\ fan's\ system\ effect\ factor\ (in.WC/[ft^3/min]^2)$
$P_s = Total\ fan\ static\ pressure\ as\ rated\ by\ the\ manufacturer\ (in.WC)$
$P'_{sc} = Total\ fan\ static\ pressure\ from\ as\ field\ measured\ adjusted\ to\ standard\ air\ conditions\ (in.WC)$
$Q_{inlet} = Volumetric\ flow\ rate\ at\ fan\ inlet\ (ft^3/min)$

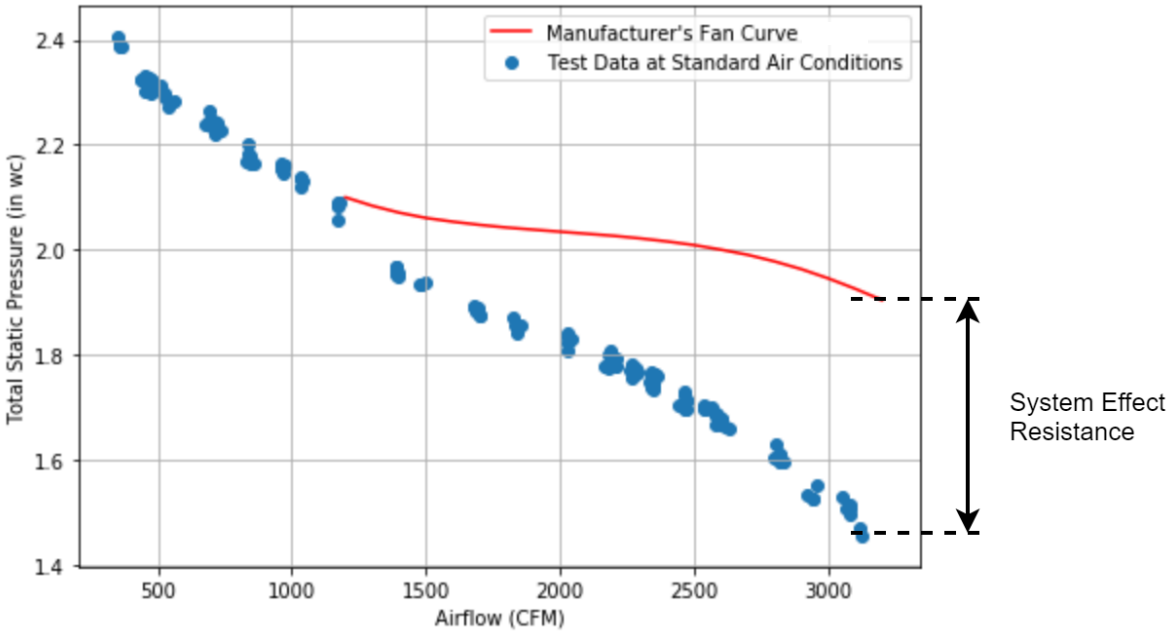

Figure 5.2 Field measured airflow resistance of the fan's system effect.

5.1.6 In-Situ Fan Curve Model

The test yielded a value of $4.5314x10^{-8}$ for the fan's system effect resistance. By substituting the SEF on equation 5-9, the missing fan total static pressure values can be extrapolated using the airflow points recorded from the fan calibration experiment (Figure 5.3).

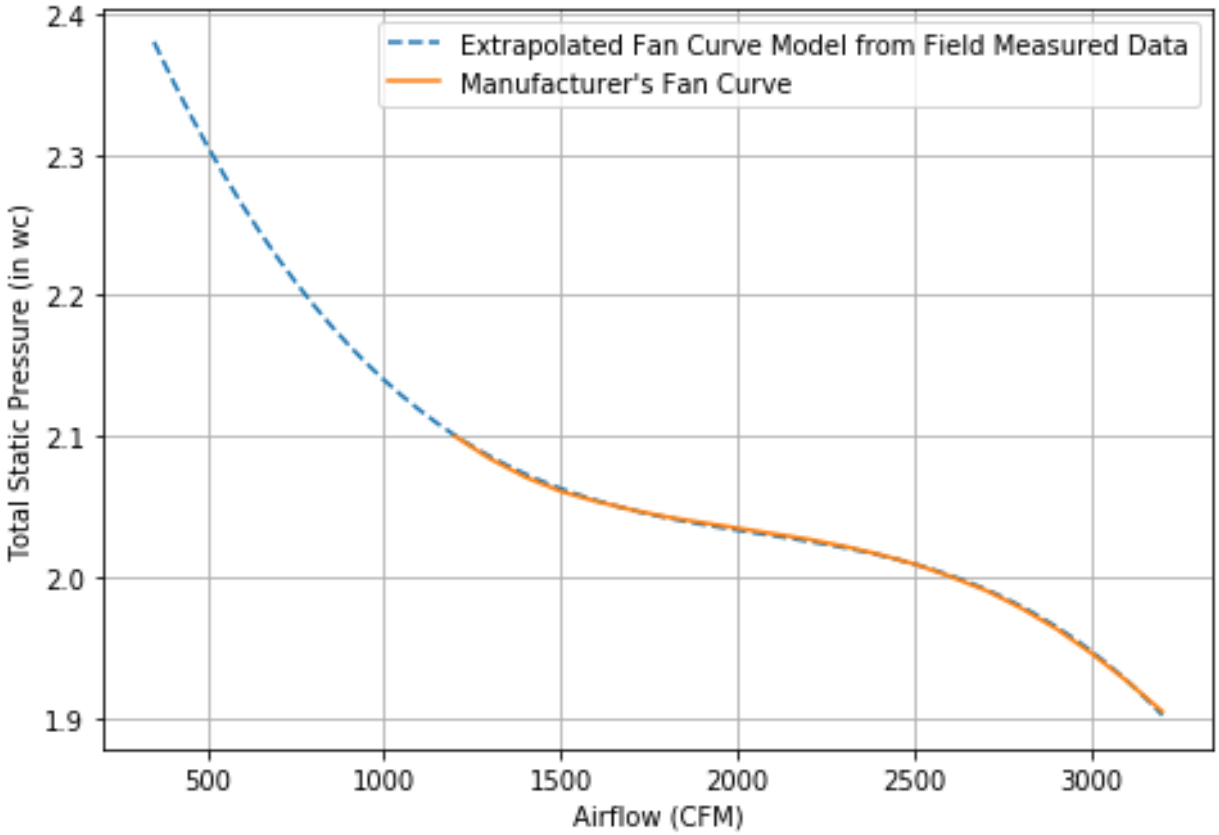

Figure 5.3 Extrapolated fan curve model obtained from the field test data.

By fitting the extrapolated fan curve obtained from the field test onto equation 3-7 the following model was obtained for the in-situ fan performance curve:

$$P_s = -5.405 \times 10^{-16}Q^4 - 5.274 \times 10^{-11}Q^3 + 3.402 \times 10^{-7}Q^2 - 7.502 \times 10^{-4}Q + 2.603 \quad (5\text{-}10)$$

Where:

$P_s = Fan\ total\ static\ pressure\ (in.WC)$
$Q = Volumetric\ flow\ rate\ (ft^3/min)$

5.2 Air System Model Calibration & Adaptability

One of the main motivations for pursuing this topic, was to create a practical procedure for applying model-based control into any type of VAV system. The novel TAV approach although great in concept, has some serious shortcomings that make it unfeasible to deploy in to a real-time VAV control system. A model for any air system based only on fix loss coefficients and the manufacturer's fan performance curve would not be able to provide proper, reliable and safe control to any ventilation system for following reasons [56]:

- Differences from the installed system to the designed system, such as longer or shorter duct sections, additional or missing duct fittings, or change of relative location from the air system elements in regard to each other. Which can greatly modify the overall airflow resistance of the system.
- Fan performance characteristics that are affected by operational changes in the system like temperature, humidity, and pressure (which modify the air density).
- The effects of changes in the system whether it be deliberate or accidental, like dirty ducts, coils and filters, broken or locked dampers, which over time increase the airflow resistance of the system.
- Excessive leakage or increased resistance due to poor quality workmanship at the installation.

To be able to overcome these hurdles the consecutive section provides a continuous calibration (self adaptive) procedure for models to be used for control of any VAV system.

5.2.1 General Structure of VAV Systems

Before diving in to the calibration of the air system model, it must stated that generally most VAV systems have the same basic structure, which is a main supply air duct fed from a central air handling equipment, that divides off in to branches for each VAV box of the ventilation system (see Figure 2.1 for reference) [14]. This can be translated into an airflow resistance model where per each new node added to the system (a T branch) two new airflow resistances are appended. The constant resistances represent the continuation of the main duct, while the variable resistances depict the total airflow resistance of each new branch, whose initial value would be equal to the VAV box fully open plus the constant airflow resistance of that bifurcation. The general structure is depicted on Figure 5.4.

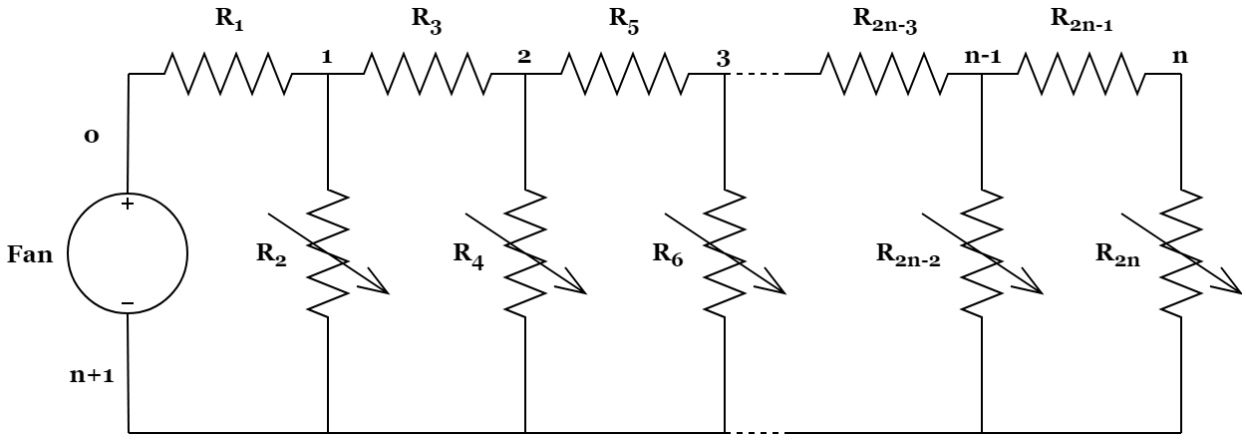

Figure 5.4 Generalized air system model structure for VAV Systems.

5.2.2 Procedure for Conducting the Initial Air System Calibration Test

To attain the airflow resistance characteristics of a VAV system when no historical data or previous trend logs are available the following procedure can be applied:

1. Leave only one branch open and close the rest, modulate the position of its VAV box from a fully open position to 30%* opening (for this study 5% steps in at 3-minute intervals where employed).
2. Set the speed of the supply fan at the highest allowable speed, to minimize the uncertainty of measuring low airflows, for this test the fan speed was set to a 100% for the entirety of the test.
3. For every damper position record the total airflow, fan outlet static pressure, supply air temperature and relative humidity.
4. Repeat step one for the rest of the branches of the VAV system.
5. Finally, fully open all the dampers in the system and record the airflow at each VAV box, fan outlet static pressure, supply air temperature and relative humidity (consult appendix E for an overview of the trended data of the air system calibration test).

Measurement	Sensor(s)	Variable
Fan outlet static pressure	P2	$P_{s,outlet}$
Return air relative humidity	H2	H_R
Return air dry bulb temperature	T1	T_R
Supply air relative humidity	H1	H_S
Supply air dry bulb temperature	T2	T_S
Total volumetric airflow	F1 and F4	Q

Table 5.3 Measurements in Figure 4.1 used for calibrating the air system.

*Note: The minimum damper position of this system was based on the mechanical specifications of this particular building, a 30% open degree was stated to maintain the minimum airflow rate of all zones in the air system.

5.2.3 Air System General Calibration Formulation

Using the general model depicted on Table 5.3 Measurements in Figure 4.1 used for calibrating the air system. a comprehensive method for calibration can de developed. Starting by testing with only branch 1 open (and the rest closed) the total airflow resistance of branch 1 can be obtained for different damper positions:

$$P_s = (R_1 + R_2)Q^2 = R_{b1}Q^2 \Rightarrow R_{b1} = \frac{P_s}{Q^2} \tag{5-11}$$

Testing with only branch 2 open, the total airflow resistance for branch 2 for different damper positions can be obtained:

$$P_s = (R_1 + R_3 + R_4)Q^2 = R_{b2}Q^2 \Rightarrow R_{b2} = \frac{P_s}{Q^2} \tag{5-12}$$

Testing with only branch 3 open, the total airflow resistance for branch 3 for different damper positions can be obtained:

$$P_s = (R_1 + R_3 + R_5 + R_6)Q^2 = R_{b3}Q^2 \Rightarrow R_{b3} = \frac{P_s}{Q^2} \tag{5-13}$$

Testing with only branch n-1 open, the total airflow resistance for branch n-1 for different damper positions can be obtained:

$$P_s = \left(R_1 + R_3 + R_5 + \cdots + R_{2(n-1)-1} + R_{2(n-1)}\right)Q^2$$

$$= \left(\sum_{m=1}^{n-1} R_{2m-1} + R_{2(n-1)}\right)Q^2 \Rightarrow R_{b(n-1)} = \frac{P_s}{Q^2} \tag{5-14}$$

Testing with only branch n open, the total airflow resistance for branch n for different damper positions can be obtained:

$$P_s = \left(R_1 + R_3 + R_5 + \cdots + R_{2(n-1)} + R_{2(n)}\right)Q^2$$

$$= \left(\sum_{m=1}^{n} R_{2m-1} + R_{2n}\right)Q^2 \Rightarrow R_{bn} = \frac{P_s}{Q^2} \tag{5-15}$$

Each branch total resistance can be fit in to equation 3-6, by representing its initial value as the addition of the fixed total airflow resistance of the ductwork and the damper at a fully open position:

$$R_b = a \cdot e^{\left(-c\left(\frac{d}{100}\right)\right)} + b \tag{5-16}$$

Where:

$a, b \text{ and } c = Coefficients\ derived\ experimentally$
$d = Damper\ opening\ degree\ expressed\ in\ percent\ (0\ to\ a\ 100)$
$R_b = Branch\ total\ airflow\ resistance$

With all the branches open the airflow resistances of R_1, R_3, etc. can be derived. For branch 1:

$$P_s = R_1 Q^2 + R_2 Q_{b1}^2 = R_1 Q^2 + (R_{b1} - R_1) Q_{b1}^2 \Rightarrow (Q^2 - Q_{b1}^2) R_1 + R_{b1} Q_{b1}^2$$

For branch 2:

$$P_s = R_1 Q^2 + R_3 (Q - Q_{b1})^2 + R_4 Q_{b2}^2$$

$$= R_1 Q^2 + R_3 (Q - Q_{b1})^2 + (R_{b2} - R_1 - R_3) Q_{b2}^2$$

$$= (Q^2 - Q_{b2}^2) R_1 + ((Q - Q_{b1})^2 - Q_{b2}^2) R_3 + R_{b2} Q_{b2}^2$$

For branch 3:

$$P_s = R_1 Q^2 + R_3 (Q - Q_{b1})^2 + R_5 (Q - Q_{b1} - Q_{b2})^2 + R_6 Q_{b3}^2$$

$$= R_1 Q^2 + R_3 (Q - Q_{b1})^2 + R_5 (Q - Q_{b1} - Q_{b2})^2 + (R_{b3} - R_1 - R_3 - R_5) Q_{b3}^2$$

$$= (Q^2 - Q_{b3}^2) R_1 + ((Q - Q_{b1})^2 - Q_{b3}^2) R_3 + ((Q - Q_{b1} - Q_{b2})^2 - Q_{b3}^2) R_5 + R_{b3} Q_{b3}^2$$

For branch n-1:

$$P_s = \sum_{m=1}^{n-1} R_{2m-1} \left(\left(Q - \sum_{k=1}^{m-1} Q_{bk} \right)^2 - Q_{bn-1}^2 \right) + R_{bn-1} Q_{bn-1}^2$$

To simplify the procedure the system's equations can be written in matrix form:

$$\boldsymbol{Q} \cdot \boldsymbol{r} = \boldsymbol{p} \tag{5-17}$$

Where **Q** is the (n-1)-by-(n-1) coefficient matrix, **r** is the (n-1)-size unknows vector and **p** is the (n-1)-size constant vector:

$$\boldsymbol{Q} = \begin{bmatrix} Q_2 - Q_{b1}^2 & 0 & 0 & \cdots & 0 & 0 \\ Q_2 - Q_2^2 & ((Q - Q_{b1})^2 - Q_{b2}^2) & 0 & \cdots & 0 & 0 \\ \vdots & \vdots & \vdots & \ddots & \vdots & \vdots \\ Q_2 - Q_{n-2}^2 & ((Q - Q_{b1})^2 - Q_{bn-2}^2) & ((Q - Q_{b1} - Q_{b2})^2 - Q_{bn-2}^2) & \vdots & \left(\left(Q - \sum_{k-1}^{n-3} Q_{bk}\right)^2 - Q_{bn-2}^2\right) & 0 \\ Q_2 - Q_{n-1}^2 & ((Q - Q_{b1})^2 - Q_{bn-1}^2) & ((Q - Q_{b1} - Q_{b2})^2 - Q_{bn-2}^2) & \vdots & \left(\left(Q - \sum_{k=1}^{n-3} Q_{bk}\right)^2 - Q_{bn-1}^2\right) & \left(\left(Q - \sum_{k=1}^{n-2} Q_{bk}\right)^2 - Q_{bn-1}^2\right) \end{bmatrix}$$

$$\boldsymbol{r} = \begin{bmatrix} R_1 \\ R_3 \\ \vdots \\ R_{2n-5} \\ R_{2n-3} \end{bmatrix}$$

$$\boldsymbol{p} = \begin{bmatrix} P_s - R_{b1} Q_{b1}^2 \\ P_s - R_{b2} Q_{b2}^2 \\ \vdots \\ P_s - R_{bn-2} Q_{bn-2}^2 \\ P_s - R_{bn-1} Q_{bn-1}^2 \end{bmatrix}$$

By solving the linear equation 5-17 all the airflow resistances of the air system can be obtained.

5.2.4 Airflow Resistances of the Experimental Setup

From the data gathered and using the air system calibration the following value was obtained for airflow resistance 1:

$$R_1 = 1.492 \times 10^{-7}\ in.WC/(ft^3/min)^2$$

For branches 1 and 2, by fitting the experimental data unto equation 5-16, the following expressions were obtained:

$$R_2 = (7.674 \times 10^{-5})\, e^{\left(-8.126\left(\frac{d}{100}\right)\right)} + (4.805 \times 10^{-7})\ \text{in. WC}/(\text{ft}^3/\text{min})^2$$

$$R_3 = (1.673 \times 10^{-4})\, e^{\left(-10.073\left(\frac{d}{100}\right)\right)} + (6.943 \times 10^{-7})\ \text{in. WC}/(\text{ft}^3/\text{min})^2$$

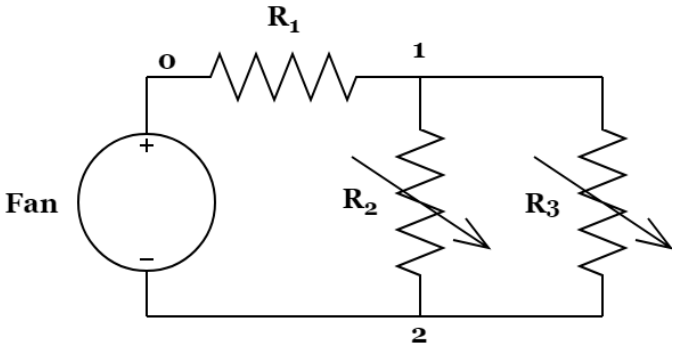

Figure 5.5 Simplified experimental air system model.

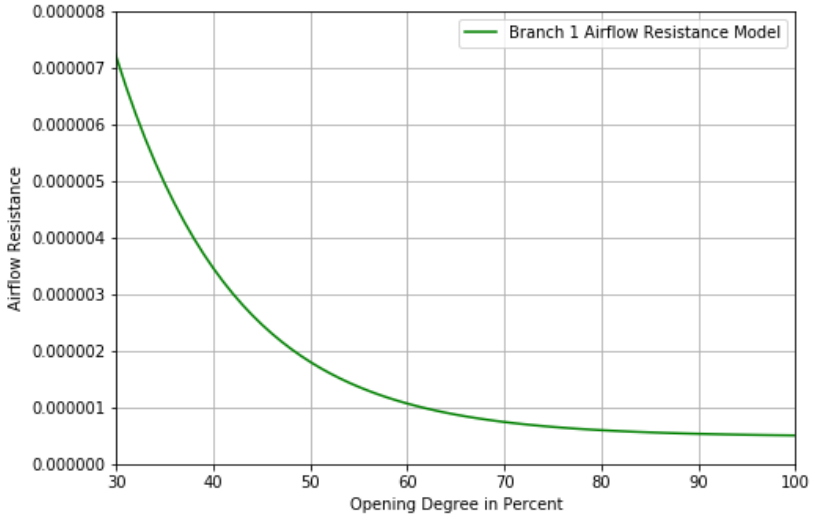

Figure 5.6 Branch 1 airflow resistance model (in. WC/ CFM²).

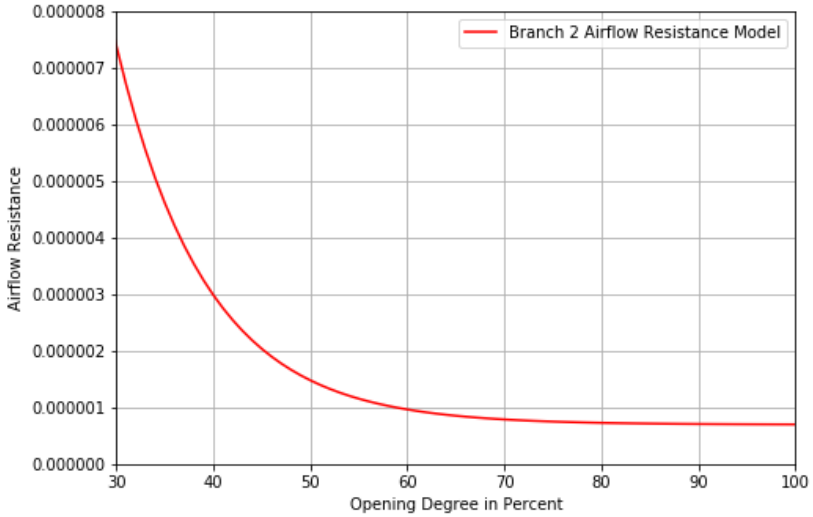

Figure 5.7 Branch 2 airflow resistance model (in. WC/CFM²).

5.2.5 Adaptability (Continuous Calibration)

Once the initial values for the air system model have been attained, a criterion for acceptability of model performance must be instated, for this study the guidelines of the AMCA 203-90 and AMCA 200-95 are used. The AMCA states that due to the uncertainty of airflow rate determinations which can range from 2 to 10%, as well as field effects on the actual system, a calculated resistance can vary as much as ±10% to the actual air system resistance [56, 61]. Thus, the accepted threshold that was used for this study was ±10% of the airflow setpoints required.

After the preliminary testing is done and the field calibration has taken place, inevitably the model will start to drift from the actual system performance, to avoid faults, trend logs of all the measurements of the system must be kept in a database, whenever the model steps out of the acceptance threshold the BAS must run the methodology stated in the "Air System General Calibration Formulation" online to recalibrate the system (adapt the model), this will guarantee to continuously get the most efficient performance out of the VAV system, even as it decays over time. If the model recalibration were to continuously fail, that would be an indication of a persistent fault like excessive air leakage, a damaged or stuck damper, excessively dirty coils and/or filters, etc.

6 TAV Control

The following section details the modified sequence of operation for the TAV control method, as well as the formulation of the controller.

6.1 TAV Control Strategy

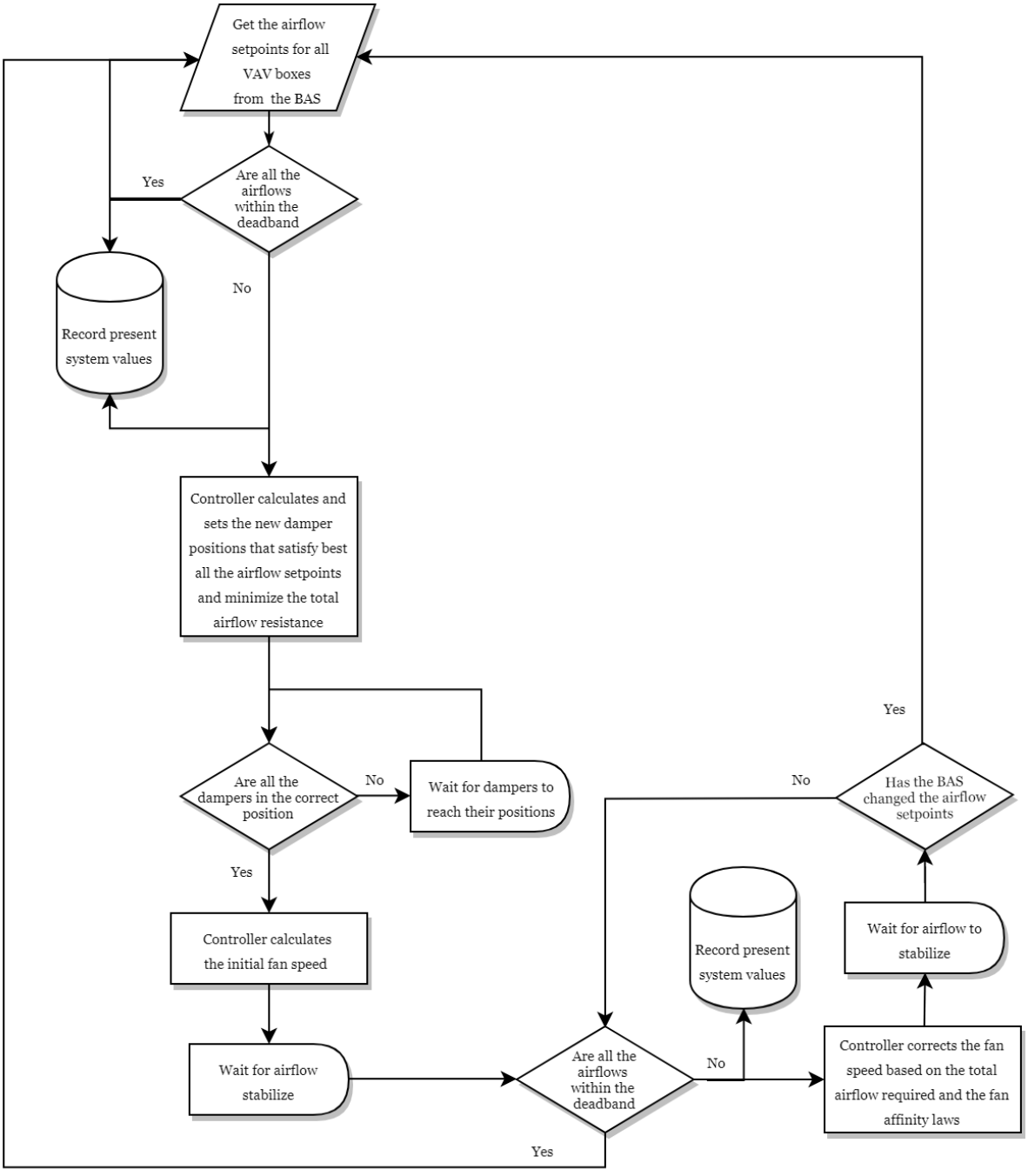

Figure 6.1 Flowchart for the TAV control strategy.

6.2 TAV General Controller Operation

Initially the BAS hands over the TAV controller airflow setpoints for all the VAV boxes on the air system, to calculate the optimal position for all the dampers, first all of the airflow ratios must be found based on the total supply air flow setpoint. By defining q_m as Q_{bm}/Q for any branch, and using the general model depicted on Table 5.3 Measurements in Figure 4.1 used for calibrating the air system. for branch n:

$$\sum_{m=1}^{n-1} R_{2m-1}\left(\left(Q-\sum_{k=1}^{m-1} Q_{bk}\right)^2 - Q_{bn-1}^2\right) + R_{bn-1}Q_{bn-1}^2 =$$

$$= \sum_{m=1}^{n} R_{2m-1}\left(\left(Q-\sum_{k=1}^{m-1} Q_{bk}\right)^2 - Q_{bkn}^2\right) + R_{bn}Q_{bn}^2 \Rightarrow$$

$$\sum_{m=1}^{n-1} R_{2m-1}\left(Q-\sum_{k=1}^{m-1} Q_{bk}\right)^2 - \sum_{m=1}^{n-1} R_{2m-1}Q_{bn-1}^2 + R_{bn-1}Q_{bn-1}^2 =$$

$$= \sum_{m=1}^{n} R_{2m-1}\left(Q-\sum_{k=1}^{m-1} Q_{bk}\right)^2 - \sum_{m=1}^{n} R_{2m-1}Q_{bn}^2 + R_{bn}Q_{bn}^2$$

$$\cancel{\sum_{m=1}^{n-1} R_{2m-1}\left(Q-\sum_{k=1}^{m-1} Q_{bk}\right)^2} - \sum_{m=1}^{n-1} R_{2m-1}Q_{bn-1}^2 + R_{bn-1}Q_{bn-1}^2 =$$

$$= \cancel{\sum_{m=1}^{n-1} R_{2m-1}\left(Q-\sum_{k=1}^{m-1} Q_{bk}\right)^2} + R_{2n-1}\left(Q-\sum_{k=1}^{n-1} Q_{bk}\right)^2 + \sum_{m=1}^{n} R_{2m-1}Q_{bn}^2 + R_{bn}Q_{bn}^2 \Rightarrow$$

$$- \sum_{m=1}^{n-1} R_{2m-1}Q_{bn-1}^2 + R_{bn-1}Q_{bn-1}^2 =$$

$$= R_{2n-1}\left(Q - \sum_{k=1}^{n-1} Q_{bk}\right)^2 - \sum_{m=1}^{n} R_{2m-1}Q_{bn}^2 + R_{bn}Q_{bn}^2 \Rightarrow$$

$$\left(R_{bn-1} - \sum_{m=1}^{n-1} R_{2m-1}\right)Q_{bn-1}^2 = R_{2n-1}Q_{bn}^2 + \left(R_{bn} - \sum_{m=1}^{n} R_{2m-1}\right)Q_{bn}^2 \Longrightarrow$$

$$\left(R_{bn-1} - \sum_{m=1}^{n-1} R_{2m-1}\right)Q_{bn-1}^2 = \left(R_{bn} + R_{2n-1} - \sum_{m=1}^{n} R_{2m-1}\right)Q_{bn}^2 \Longrightarrow$$

$$\left(R_{bn-1} - \sum_{m=1}^{n-1} R_{2m-1}\right)Q_{bn-1}^2 = \left(R_{bn} - \sum_{m=1}^{n-1} R_{2m-1}\right)Q_{bn}^2 \Longrightarrow$$

$$\left(R_{bn-1} - \sum_{m=1}^{n-1} R_{2m-1}\right)\left(\frac{Q_{bn-1}}{Q}\right)^2 = \left(R_{bn} - \sum_{m=1}^{n-1} R_{2m-1}\right)\left(\frac{Q_{bn}}{Q}\right)^2 \Longrightarrow$$

$$\left(R_{bn-1} - \sum_{m=1}^{n-1} R_{2m-1}\right)q_{n-1}^2 = \left(R_{bn} - \sum_{m=1}^{n-1} R_{2m-1}\right)q_n^2 \Longrightarrow$$

$$\left(\frac{q_n}{q_{n-1}}\right)^2 = \left(R_{bn-1} - \sum_{m=1}^{n-1} R_{2m-1}\right) \div \left(R_{bn} - \sum_{m=1}^{n-1} R_{2m-1}\right) \Rightarrow$$

$$\frac{q_n}{q_{n-1}} = \sqrt{\left(R_{bn-1} - \sum_{m=1}^{n-1} R_{2m-1}\right)} \div \sqrt{\left(R_{bn} - \sum_{m=1}^{n-1} R_{2m-1}\right)} = \lambda_{n-1}$$

Following the same procedure, for branch n-1:

$$\left(R_{bn-2} - \sum_{m=1}^{n-2} R_{2m-1}\right)Q_{bn-2}^2 = R_{2n-3}(Q_n + Q_{n-1})^2 + \left(R_{bn-1} - \sum_{m=1}^{n-1} R_{2m-1}\right)Q_{bn-1}^2 \Rightarrow$$

$$\left(R_{bn-2} - \sum_{m=1}^{n-2} R_{2m-1}\right)q_{n-2}^2 = R_{2n-3}(q_n + q_{n-1})^2 + \left(R_{bn-1} - \sum_{m=1}^{n-1} R_{2m-1}\right)q_{n-1}^2 \Rightarrow$$

$$\left(R_{bn-2}-\sum_{m=1}^{n-2}R_{2m-1}\right)q_{n-2}^2=R_{2n-3}(\lambda_{n-1}q_{n-1}+q_{n-1})^2+\left(R_{bn-1}-\sum_{m=1}^{n-1}R_{2m-1}\right)q_{n-1}^2\Rightarrow$$

$$\left(R_{bn-2}-\sum_{m=1}^{n-2}R_{2m-1}\right)q_{n-2}^2=R_{2n-3}(\lambda_{n-1}+1)^2q_{n-1}^2+\left(R_{bn-1}-\sum_{m=1}^{n-1}R_{2m-1}\right)q_{n-1}^2\Rightarrow$$

$$\left(R_{bn-2}-\sum_{m=1}^{n-2}R_{2m-1}\right)q_{n-2}^2=\left(R_{2n-3}(\lambda_{n-1}+1)^2+\left(R_{bn-1}-\sum_{m=1}^{n-1}R_{2m-1}\right)\right)q_{n-1}^2\Rightarrow$$

$$\left(R_{bn-2}-\sum_{m=1}^{n-2}R_{2m-1}\right)q_{n-2}^2=\left(R_{2n-3}(\lambda_{n-1}^2+2\lambda_{n-1})^2+\left(R_{bn-1}-\sum_{m=1}^{n-2}R_{2m-1}\right)\right)q_{n-1}^2\Rightarrow$$

$$\frac{q_{n-1}}{q_{n-2}}=\sqrt{\left(R_{bn-2}-\sum_{m=1}^{n-2}R_{2m-1}\right)}\div\sqrt{R_{2n-3}(\lambda_{n-1}^2+2\lambda_{n-1})+R_{bn-1}-\sum_{m=1}^{n-2}R_{2m-1}}=\lambda_{n-2}$$

For branch 3:

$$\frac{q_3}{q_2}=\sqrt{R_{b2}-\sum_{m=1}^{2}R_{2m-1}}\div\sqrt{R_5(\lambda_3^2+2\lambda_3)+R_{b3}-\sum_{m=1}^{2}R_{2m-1}}$$

$$=\sqrt{\frac{R_{b2}-R_1-R_3}{R_5(\lambda_3^2+2\lambda_3)+R_{b3}-R_1-R_3}}=\lambda_2$$

For the branch 2:

$$\frac{q_2}{q_1}=\sqrt{R_{b1}-\sum_{m=1}^{1}R_{2m-1}}\div\sqrt{R_3(\lambda_2^2+2\lambda_2)+R_{b2}-\sum_{m=1}^{1}R_{2m-1}}$$

$$=\sqrt{\frac{R_{b1}-R_1}{R_3(\lambda_2^2+2\lambda_2)+R_{b2}-R_1}}=\lambda_1$$

After calculating all the λ coefficients, the airflow ratios can be obtained:

$$Q = Q_{b1} + Q_{b2} + Q_{b3} + \cdots + Q_{bn-2} + Q_{bn-1} + Q_{bn} \Rightarrow$$

$$1 = q_1 + q_2 + q_3 + \cdots + q_{n-2} + q_{n-1} + q_n$$

This creates a system of n equations, which can be expressed in the form of $\boldsymbol{\lambda} \cdot \boldsymbol{q} = \boldsymbol{s}$, where **λ** is the (n)-by-(n) coefficient matrix, **q** is the (n)-size unknown vector and **s** is the n-size constant vector:

$$\boldsymbol{Q} = \begin{bmatrix} -\lambda_1 & 1 & 0 & \cdots & 0 & 0 & 0 \\ 0 & -\lambda_2 & 1 & \cdots & 0 & 0 & 0 \\ \vdots & \vdots & \ddots & \vdots & \vdots & \vdots & \vdots \\ 0 & 0 & 0 & \cdots & 0 & -\lambda_{n-1} & 1 \\ 1 & 1 & 1 & \cdots & 1 & 1 & 1 \end{bmatrix}$$

$$\boldsymbol{q} = \begin{bmatrix} q_1 \\ q_2 \\ \vdots \\ q_{n-1} \\ q_n \end{bmatrix}$$

$$\boldsymbol{s} = \begin{bmatrix} 0 \\ 0 \\ \vdots \\ 0 \\ 1 \end{bmatrix}$$

Solving for **q**, we can obtain all the ratios for the branches. Then, solving (for example) for branch 1 we can obtain the total equivalent airflow resistance:

$$P_s = R_1 Q^2 + R_2 Q^2 = R_1 Q^2 + (R_{b1} - R_1) Q_{b1}^2 = R_1 Q^2 + (R_{b1} - R_1) q_1^2 Q^2$$

$$= (R_1 + (R_{b1} - R_1) q_1^2) Q^2 = R_T Q^2$$

The optimization problem that is solved is:

$$minimize\ f(dp_1, dp_2, \cdots, dp_n, fs) = \sum_{m=1}^{n} \left(Q_{bm}(dp_1, dp_2, \cdots, dp_n, fs) - Q_{bm,sp}\right)^2 + fs^2$$

Where dp_m is the damper position of branch m, Q_{bm} is the airflow for branch m and $Q_{bm,sp}$ is the airflow setpoint for branch m and fs is the fan speed.

6.3 TAV Control Method Implementation

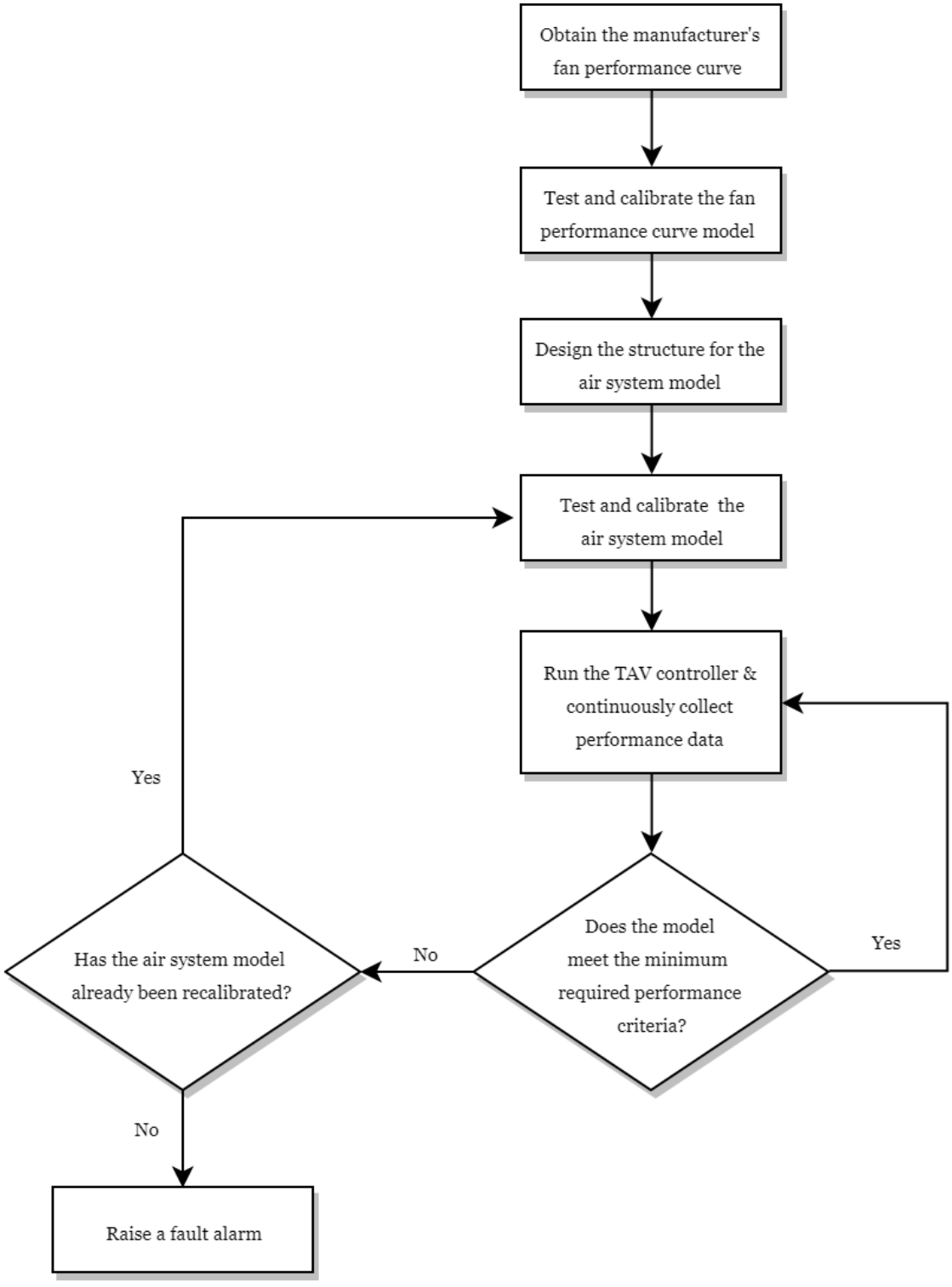

Figure 6.2 Flowchart for the implementation of the TAV control method.

7 Test Results

The following section provides a performance overview for both the TAV and PID control methods on the same VAV System, using identical conditions of airflow setpoints (Table 7.1). The setpoints were chosen from typical operation conditions gathered from historical data collected from the BAS.

Condition	Duration Time (Seconds)	VAV Box 1 Airflow Setpoint (L/S)	VAV Box 2 Airflow Setpoint (L/S)
1	90	370	370
2	270	340	310
3	60	280	350
4	180	400	150
5	60	360	355
6	230	180	230
7	100	315	190
8	420	225	240
9	90	390	320

Table 7.1 Airflow setpoints schedule for the test.

7.1 Results Overview

The following plots illustrate the performance of both the TAV and PID controllers, for VAV boxes 1 and 2.

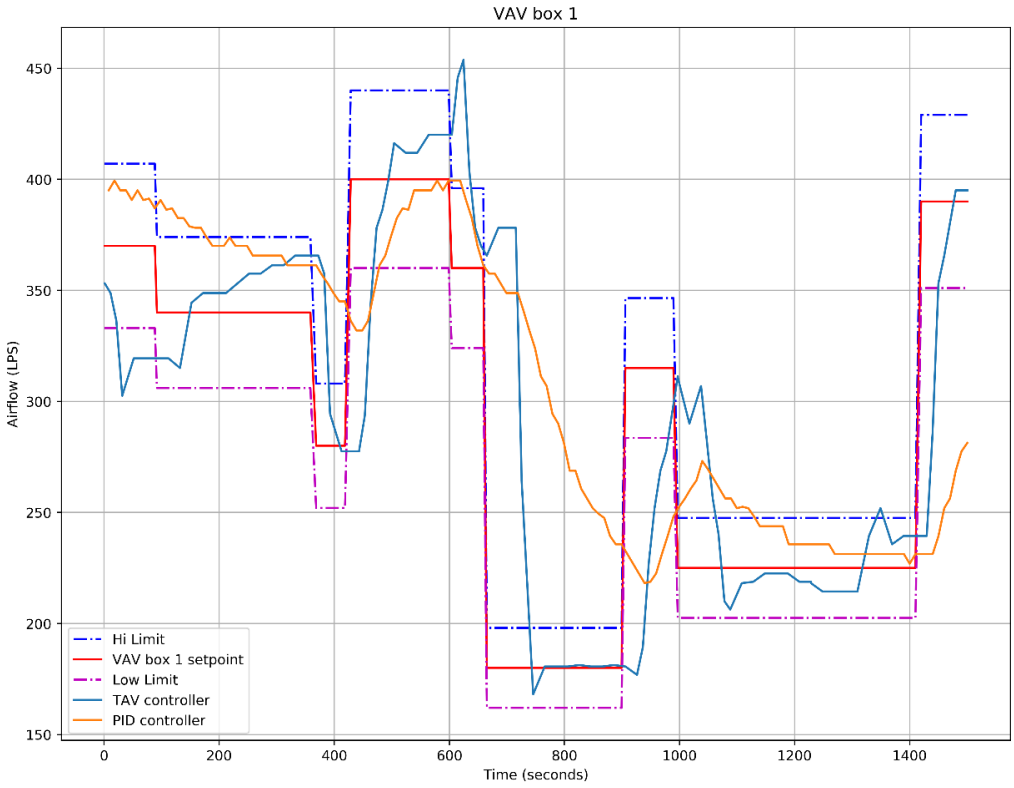

Figure 7.1 VAV box 1 TAV vs. PID performance overview.

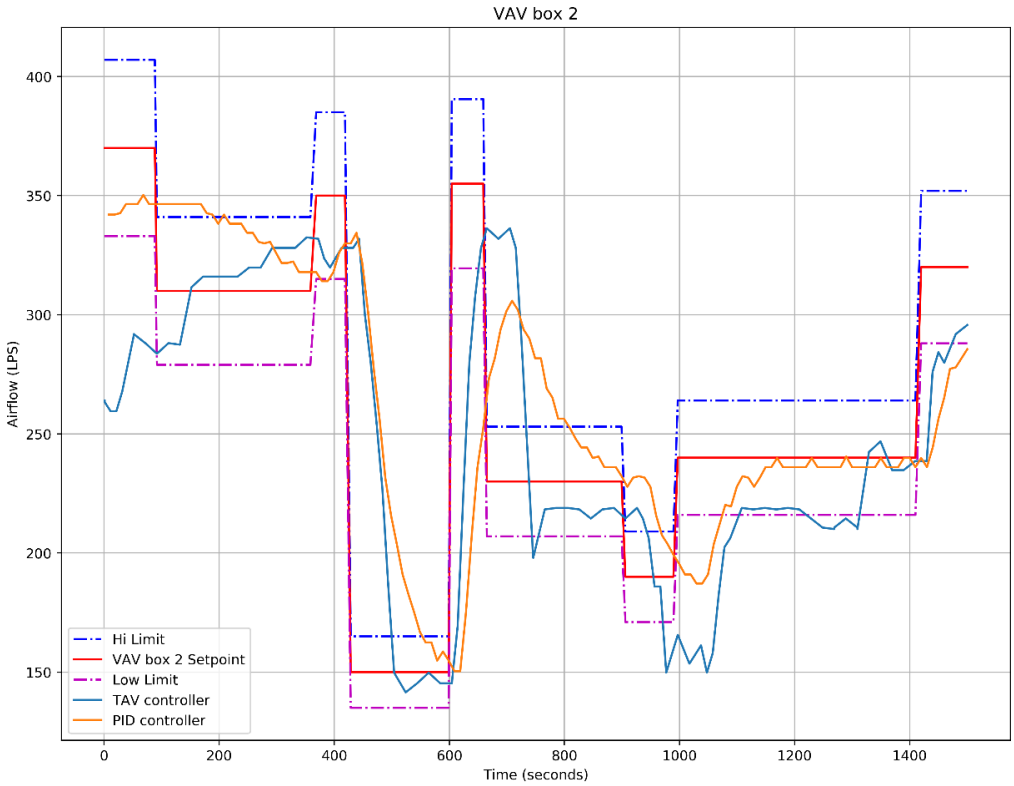

Figure 7.2 VAV box 2 TAV vs. PID performance overview.

7.2 Evaluation Criteria

Both control methods will be compared using a deadband of ±10% based on the following metrics [66, 67]:

- Response time: The amount of time required for the airflow to reach its setpoint (within its deadband threshold), when there is a change of operating conditions (change of setpoint).
- Overshoot: The maximum registered difference between the airflow and its setpoint after the airflow has reached the setpoint.
- Offset: This is the average constant error that prevails between the airflow and its setpoint once a steady state has been reached.

Additionally, energy efficiency will be compared by the registered the operational fan speed at each condition.

7.2.1 Response Time

Table 7.2 details the response time performance of both control strategies. VAV box 1 under PID control did not reach its setpoint 6 times, while VAV box failed twice. Under TAV control VAV Box 1 successfully reached its setpoint every time, and VAV box failed only on the start to reach its setpoint. PID control performed better under discrete changes but did not adapt well to large airflow setpoints like those of conditions 6 and 9.

Condition	Duration Time (seconds)	VAV Box 1 TAV Control Response Time (seconds)	VAV Box 1 PID Control Response Time (seconds)	VAV Box 2 TAV Control Response Time (seconds)	VAV Box 2 PID Control Response Time (seconds)
1	90	0	0	Did not reach the setpoint	0
2	270	0	87	0	100
3	60	30	Did not reach the setpoint	0	0
4	180	48	57	79	133
5	60	37	22	50	Did not reach the setpoint
6	230	79	Did not reach the setpoint	73	147
7	100	90	Did not reach the setpoint	52	77
8	420	73	140	113	84
9	90	39	Did not reach the setpoint	63	Did not reach the setpoint

Table 7.2 Response time performance of both control methods.

From the samples taken, the average response time of the TAV control method was 61s while the average response time for the PID control method was 94s, for the valid sample points which are the conditions that were met by controller.

It should be noted that the full time for the damper to travel from its closed to its fully open position is 90 seconds according to its datasheet (Siemens GDE series actuator). The use of timesteps shorter than the complete runtime of the damper actuator should be avoided in real life VAV system applications, as the response time for any control method applied to ventilation systems will be constrained by the travel time of its actuators, this is illustrated in Figure 7.3 and Figure 7.4.

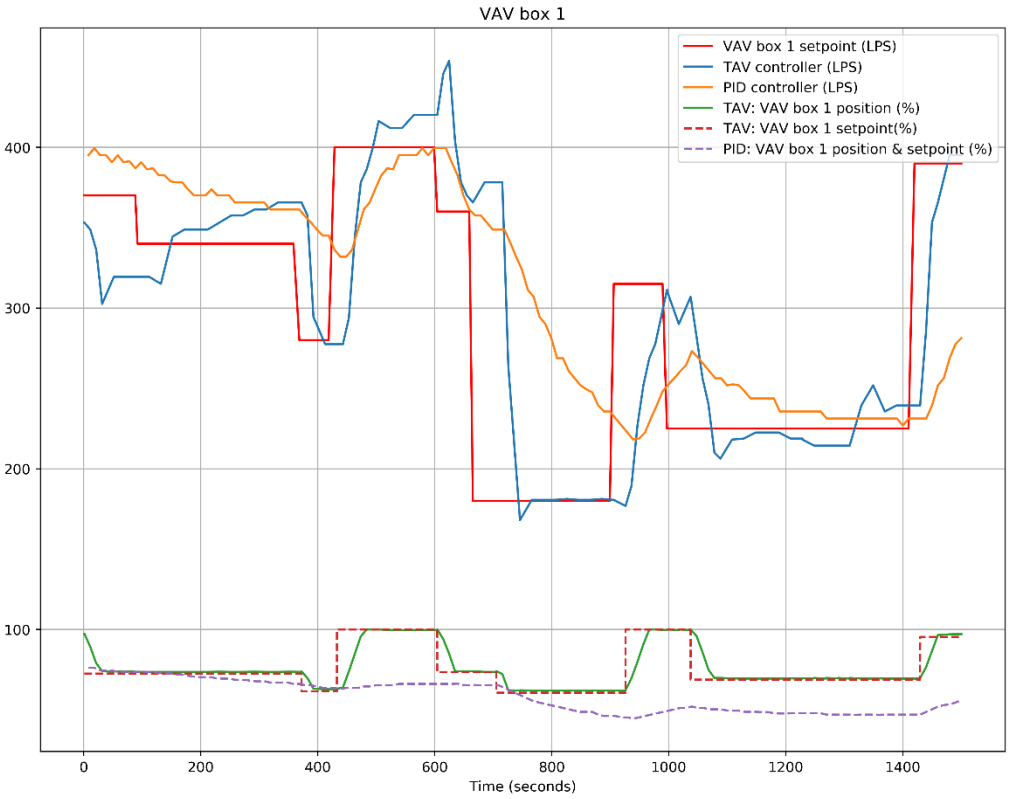

Figure 7.3 VAV box 1 damper control overview for both control methods.

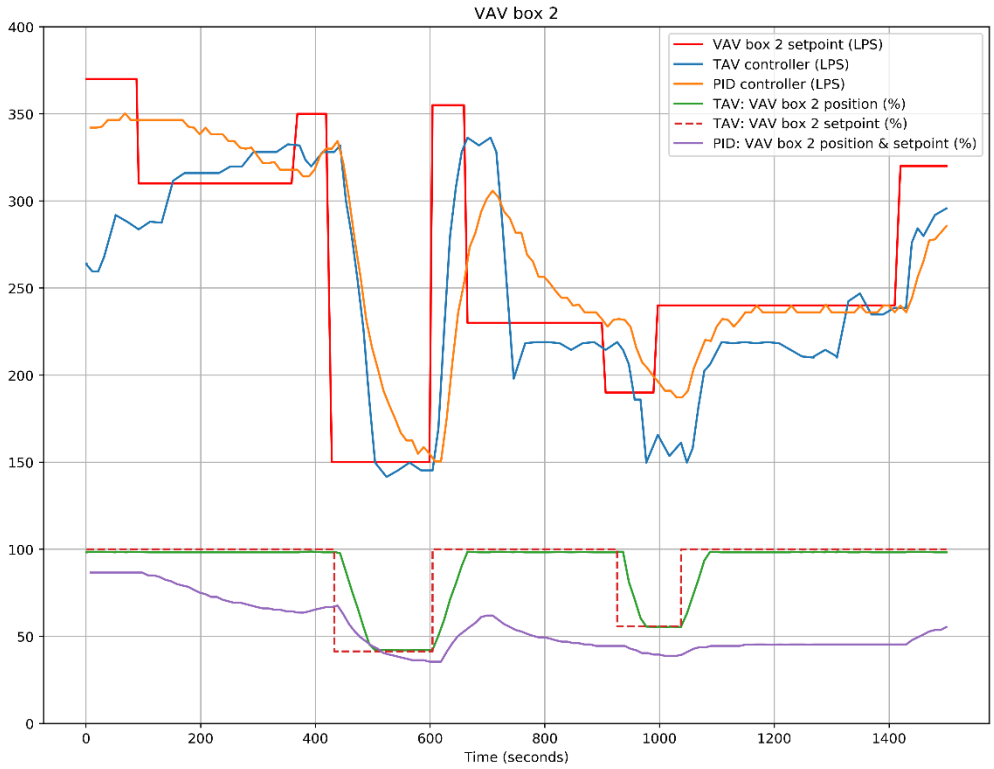

Figure 7.4 VAV box 2 damper control overview for both control methods.

7.2.2 Overshoot

Table 7.3 details the overshoot performance of both control strategies. PID control once reached its setpoint, tends to have little to no overshoot. TAV control in general presented more overshoot on VAV box 2 during the test on conditions 6 through 8 (Figure 7.5). This happened because the TAV controller was trying to correct the airflow by throttling the fan speed while the damper of VAV box 2 was locked. The programmed sampling rate of 10 seconds was not able to catch the change of airflow setpoints.

Condition	VAV Box 1 Airflow Setpoint (L/S)	VAV Box 1 TAV Overshoot (L/S)	VAV Box 1 PID Overshoot (L/S)	VAV Box 2 Airflow Setpoint (L/S)	VAV Box 2 TAV Overshoot (L/S)	VAV Box 2 PID Overshoot (L/S)
1	**370**	31	0	**370**	Did not reach the setpoint	0
2	**340**	0	0	**310**	0	1
3	**280**	0	Did not reach the setpoint	**350**	0	1
4	**400**	0	0	**150**	0	0
5	**360**	0	0	**355**	0	Did not reach the setpoint
6	**180**	0	Did not reach the setpoint	**230**	9	0
7	**315**	0	Did not reach the setpoint	**190**	22	0
8	**225**	4	0	**240**	6	0
9	**390**	0	Did not reach the setpoint	**320**	0	Did not reach the setpoint

Table 7.3 Overshoot performance of both control methods.

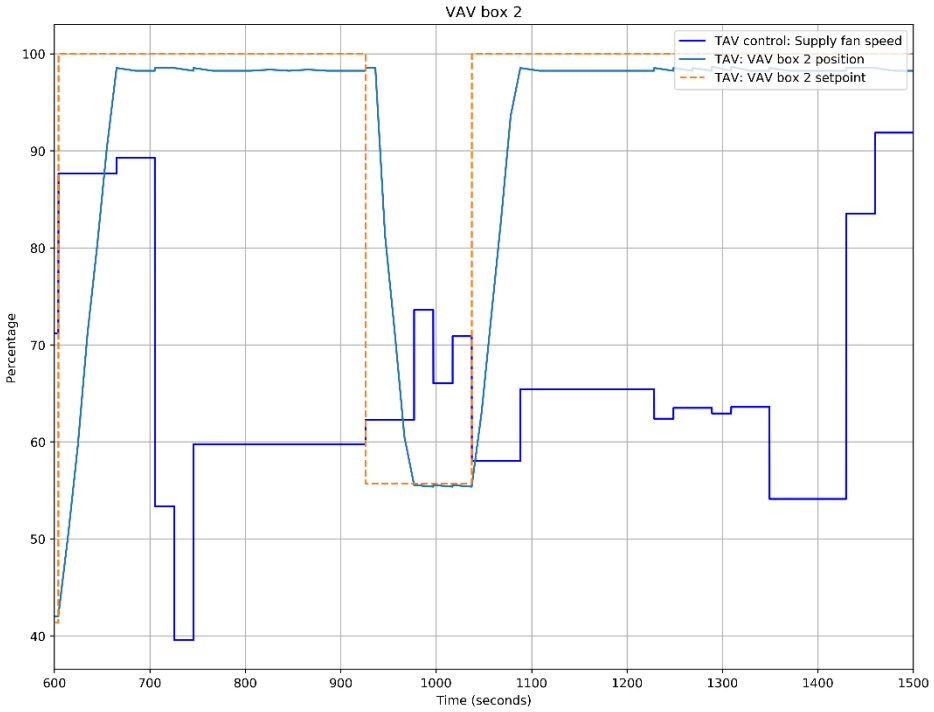

Figure 7.5 TAV controller output for VAV box 2 during conditions 6 to 8.

7.2.3 Offset

Condition	VAV Box 1 Airflow Setpoint (L/S)	VAV Box 1 TAV Average Airflow/Offset (L/S)	VAV Box 1 PID Average Airflow/Offset (L/S)	VAV Box 2 Airflow Setpoint (L/S)	VAV Box 2 TAV Average Airflow/ Offset (L/S)	VAV Box 2 PID Average Airflow/ Offset (L/S)
1	**370**	324.7/45.3	393.2/23.2	**370**	Did not reach the setpoint	345.6/24.4
2	**340**	348.4/8.4	370.0/30.0	**310**	314.5/4.5	329.7/19.7
3	**280**	285.6/5.6	Did not reach the setpoint	**350**	325.9/24.1	318.8/31.5
4	**400**	407.3/7.3	385.5/14.5	**150**	146.2/3.8	158.9/8.9
5	**360**	376.9/16.9	378.0/18	**355**	329.6/25.4	Did not reach the setpoint
6	**180**	179.5/0.5	Did not reach the setpoint	**230**	215.1/14.9	240.7/10.7
7	**315**	298.6/16.4	Did not reach the setpoint	**190**	175.1/14.9	203.9/13.9
8	**225**	223.4/1.6	234.1/9.1	**240**	221.9/18.1	235.1/4.9
9	**390**	376.3/13.7	Did not reach the setpoint	**320**	293.3/26.7	Did not reach the setpoint

Table 7.4 Offset performance of both control methods.

Form the data presented on Table 7.4 the average offset for both control methods can be obtained, the TAV method had an average offset of 4.7% while the PID control method yielded an average offset of 5.8%. Overall, both control strategy performed very similarly once the airflow reached the deadband, and both stayed within the accepted threshold of 10% of the airflow setpoint.

7.2.4 Energy Efficiency

By using the third affinity law stated on equation 3-12, a comparison as to how much energy could be saved on average by using TAV control in respect to the output speed of the PID control can be stated:

$$H_{TAV} = 100\left(\frac{N_{TAV}}{N_{PID}}\right)^3$$

Condition	Duration Time (seconds)	TAV Average Supply Fan Speed (%)	PID Average Supply Fan Speed (%)	TAV Average Energy Savings H_{TAV} (%)
1	90	96.5	100	89.8
2	270	100	100	100
3	60	85.5	100	62.5
4	180	72.9	100	38.7
5	60	86.3	100	64.2
6	230	62.4	100	24.2
7	100	63.5	100	25.6
8	420	62.5	100	24.4
9	90	82.9	100	56.9

Table 7.5 Average fan speed for both control methods.

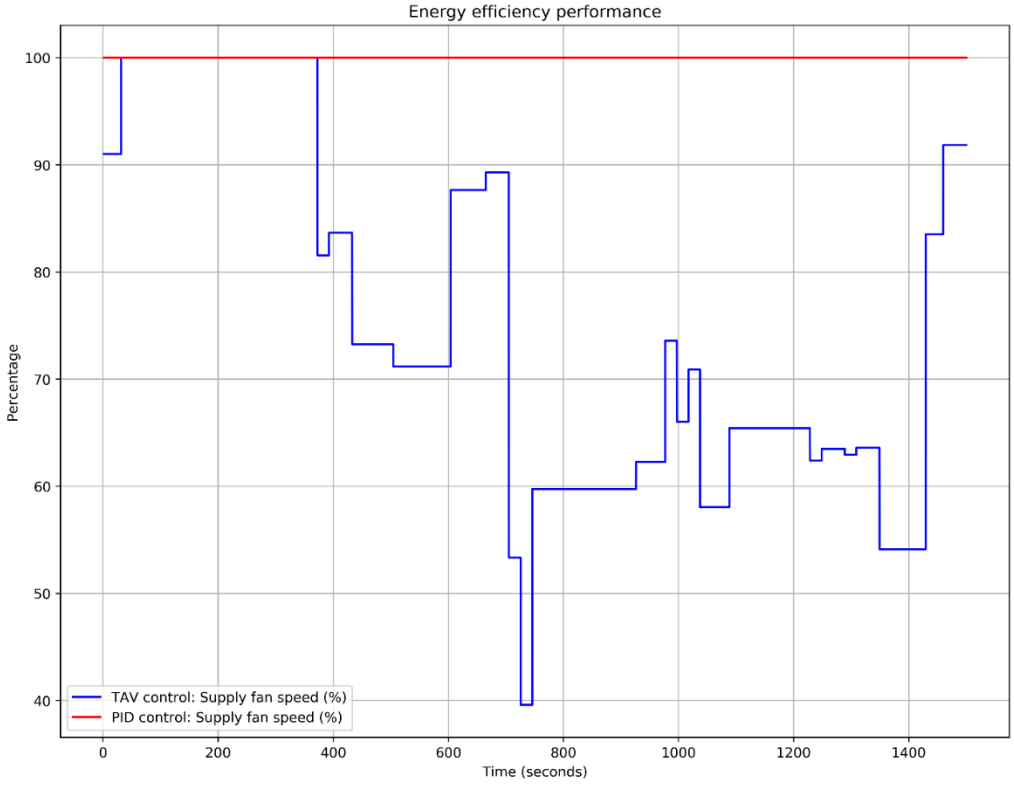

Figure 7.6 Fan speed performance for both control methods.

8 Conclusions

To improve the energy performance of commercial and institutional buildings the use of an advanced control method was proposed to enhance the regulation of VAV systems. The TAV control method was presented as an alternative to the conventional PID control strategy which dominates building systems local control applications. However, to implement the TAV control method, its modeling methodology was modified to be able to use only field gathered data instead of theoretical dynamic loss coefficients. A general fan field performance and self-adaptive (continuous calibration) procedure was proposed based on a threshold of acceptability for the air system to ensure that the model would be reliable, by making it capable of overcoming the challenges of adapting to an as built system, as well as equipment decay and failure, which PID control does naturally. And finally, the control strategy was modified to calculate in real time the optimal total airflow resistance of the air system and deliver both the damper positions and supply fan speed control commands. All these changes and additions were summarized in a generalized packaged methodology that can be applied across any type of VAV system.

To prove that this methodology could be implemented outside laboratory conditions, a regular VAV system with of the shelf commercial sensors and a conventional FCU was used for testing, only using calibration instruments to verify the measurements of the BAS.

From the test results in comparison to the PID control method, the self-adaptive TAV control method improved response time by an average of 36%, where the average response time for PID control was 91 seconds, and for the TAV control was an average 64s, in addition to just failing once to meet the airflow setpoints, while PID failed six times to reach the required airflows on time. On the overshoot criterion PID control was marginally better having little overshoot across the test, while TAV control exhibited some overshoot that could be improved by modifying the airflow correction step of the control strategy. The average offset was roughly the same with 4.7% for the TAV controller and 5.8% for the PID control. Both methods can go toe to toe in terms of control performance, which means the TAV control method exhibits no significant risk of breaching comfort, safety, or reliability on VAV systems.

Finally, on the energy efficiency metric TAV control outdid PID control by matching its control performance and consuming on average 56% of the power that the PID controller would have required during the test. The reason why TAV control can use less energy and still satisfy the same requirements, can be simply be explained by looking at the damper positions for both control strategies during the test (Figure 8.1). TAV control maintained the dampers at a higher opening degree during the test, which lowered the pressure drop across the air system, which in turn allowed the fan to run at lower speeds. PID control can achieve a high degree of performance for local level control, but will always sacrifice energy, since different damper positions can be able to satisfy the same required airflow ratios, but only a certain combination of damper positions will represent the minimum total airflow resistance, which the TAV control method always aims to accomplish.

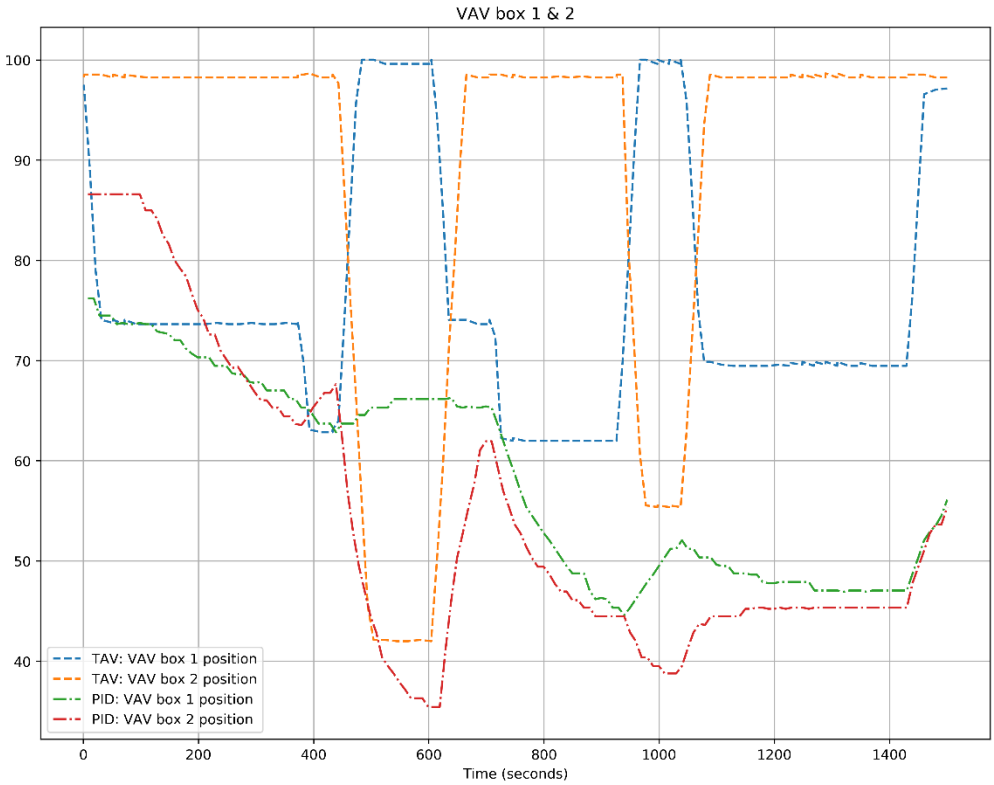

Figure 8.1 Damper positions for both control methods.

8.1 Limitations & Future Work

The comparison test between controllers had a total running time of 25 minutes and was limited to two conditioned zones, which was enough to demonstrate a proof of concept for the self-adaptive TAV control method, but deeper research is required to validate the long term effects of using this controller, over PID controls in VAV systems, under normal building operations, test should be carried out during for the complete duration of occupied and unoccupied periods, as well as during heating, cooling and shoulder seasons, to completely validate the robustness of the proposed control methodology. Additionally, the behaviour of the TAV controller should be evaluated when coupled with advanced supervisory control strategies like building and zone thermal MPC, or demand control ventilation to asses its compatibility. Another limitation is the fact the calibration procedure for both the fan performance curve and air system model is time consuming and requires for the system to go offline while it is being carried out.

Some aspects that were also not covered in the present study and need deeper investigation is the use and benefits of the air system model to provide fault detection and diagnosis mechanisms for conditions like excessive air leakage in ducts, dirty and damaged HVAC components.

Finally, another great field of application where the present research could be applied with further development is the automation of balancing and commissioning air systems.

9 Bibliography

[1] Natural Resources Canada, in *Energy Fact Book 2018 - 2019*, 2018, pp. 35, 40.

[2] U.S. Energy Information Administration, "Energy Use in Commercial Buildings," 28 September 2018. [Online]. Available: https://www.eia.gov/energyexplained/index.php?page=us_energy_commercial.

[3] S. Wang, Intelligent Buildings and Building Automation, London and New York: Spon Press, 2010.

[4] N. Fernandez, S. Katipamula, W. Wang, Y. Xie, M. Zhao and C. Corbin, "Impacts of Commercial Building Controls on Energy Savings and Peak Load Reduction," U.S. Department of Energy, Richland, 2017.

[5] N. Fernandez, S. Katipamula, W. Wang, Y. Huang and G. Liu, "Energy savings modelling of re-tuning energy conservation measures in large office buildings," *Journal of Building Performance Simulation,* pp. 391-407, 2014.

[6] M. Maasoumy and A. Sangiovanni-Vincentelli, "Smart Connected Buildings Design Automation: Foundations and Trends," *Foundations and Trends in Electronic Design,* p. 42, 2015.

[7] S. Kozák, "State-of-the-art in control engineering," *Journal of Electrical Systems and Information Technology,* pp. 1-9, 2014.

[8] Y. Yeo and Y. Yu, "Control Design Based on State-Space Model," in *Modeling and Control in Air-conditioning Systems*, Shanghai, Springer, 2017, pp. 221-222.

[9] T. Hilliard, M. Kavgic and L. Swan, "Model predictive control for commercial buildings: trends and opportunities," *Advances in Building Energy Research,* pp. 172-190, 2015.

[10] A. Afram and F. Janabi-Sharifi, "Theory and applications of HVAC control systems - A review of model predictive control (MPC)," *Building and Environment,* pp. 343-355, 2014.

[11] G. Serale, M. Fiorentini, A. Capozzoli, D. Bernardini and A. Bemporad, "Model Predictive Control (MPC) for Enhancing Building and HVAC System Eergy Efficiency: Problem Formulatio, Applications and Opportunities," *Energies,* p. 631, 2018.

[12] D. Callan, "Evolution of VAV Systems, and Dedicated Outdoor Air Systems as Alternative HVAC Strategy," facilitiesnet, 2015.

[13] ASHRAE, 2015 ASHRAE Handbook - HVAC Applications, Atlanta: American Society of Heating, Refrigeration and Air-Conditioning Engineers., 2015.

[14] E. G. Pita, Air Conditioning Principles and Systems, New York City: Pearson Education, Inc., 2012.

[15] ASHRAE, 2012 ASHRAE Handbook - HVAC Systems And Equipment (SI), Atlanta: American Society of Heating, Refrigeration and Air-Conditioning Engineers, 2012.

[16] S. K. Wang, "Air Systems: Variable-Air-Volume Systems," in *Handbook of Air Conditioning and Refrigeration*, MCGraw-Hill, 2001, p. 21.1.

[17] Pacific Gas and Electric Company, Advanced Variable Air Volume VAV System Design Guide, California: Energy Design Resources, 2009.

[18] R. Z. Homod, "Review on the HVAC System Modeling Types and the Shortcomings of Their Application," *Journal of Energy,* 2013.

[19] A. Afram and F. Janabi-Sharifi, "Review of modeling methods for HVAC Systems," *Applied Thermal Engineering,* pp. 507 - 519, 2014.

[20] Z. Afroz, G. Shafiullah, T. Urmee and G. Higgins, "Modeling techniques used in building HVAC control systems: A Review," *Renewable and Sustainable Energy Reviews,* 2018.

[21] ASHRAE, 2013 ASHRAE Handbook - Fundamentals, Atlanta: American Society of Heating, Refrigeration and Air-Conditioning Engineers, 2013.

[22] F. Calvino, M. L. Gennusa, G. Rizzo and G. Scaccianoce, "The control of indoor thermal comfort conditions: introducing a fuzzy apative controller," *Energy and Buildings,* pp. 97-102, 2004.

[23] B. Dong, Z. O'Neil, D. Luo and B. Trevor, "Development and calibration of a reduced-order energy performance model for a mixed-use building," in *Proceedings of the 13th conference on internation building performance simulation association BS2013*, Chambéry, 2013.

[24] A. Andriamamonjy, R. Klein and D. Saelens, "Automated grey box model implementation using BIM and Modelica," *Energy & Buildings,* vol. 188, no. 189, pp. 209-225, 2019.

[25] G. S. Okochi and Y. Yao, "A review of recent developments and technological advancements of variable-air-volume (VAV) air-conditioning systems," *Renewable and Sustainable Energy Reviews,* pp. 784-817, 2016.

[26] A. I. Dounis, "Advanced control systems engineering for energy and comfort management in a building environmental review," *Renewable & Sustainable Energy Reviews,* vol. 13, pp. 1246-1261, 2009.

[27] B. Whitman, B. Johnson, J. Tomczyk and E. Silberstein, "Automatic Control Components and Applications," in *Refrigeration & Air Conditioning Technology*, Clifton Park, DELMAR CENGACE Learning, 2008, pp. 261-289.

[28] G. J. Levermore, Building energy management systems, United Kingdom, 1992.

[29] R. Rogers, "Building a Benchtop PID Controller," Keithley Instruments, Inc., Cleveland, 2013.

[30] C. Sloup, M. Bunker, M. Riesberg, T. Coleman and J. Simpson, Building Automation Control Devices and Applications, Illinois: American Technical Publishers, Inc., 2008.

[31] J. Bai and X. Zhang, "A new adaptive PI controller and its application in HVAC systems," *Energy Conversion and Management,* pp. 1043-1054, 2007.

[32] D. S. Rieger and C. G., "Advanced control strategies for heating, ventilation, air-conditioning, and refrigeration systems - An overview: Part I: Hard control," *HVAC&R Research,* pp. 2-21, 2011.

[33] K. W. Roth, D. Westphalen, M. Y. Feng, P. Llana and L. Quartararo, "Energy Impact of Commercial Building Controls and Performance Diagnostics: Market Characterization, Energy Impact of Buildings Faults and Energy Savings Potential," U.S. Department Of Energy, Cambridge, MA, 2005.

[34] I. D. Landau, R. Lozano, M. M'Saad and A. Karimi, Adaptive Control Algorithms, Analysis and Applications, London: Springer, 2011.

[35] M. Phil, T. T. Chow, W. Chan and W. Tse, "Fuzzy air handling system controller," *Building Serv. Eng. Res. Technol.,* pp. 95-105, 1994.

[36] J. E. Seem, "A New Pattern Recognition Adaptive Controller with Application to HVAC Systems," *Automatica,* pp. 969-982, 1998.

[37] S. Wang and X. Jin, "Model-based optimal control of VAV air-conditioning system using genetic algorithm," *Building and Environment,* pp. 471-487, 2000.

[38] S. Wang, "Dynamic simulation of building VAV air-conditioning system and evaluation of EMCS on-line control strategies," *Building and Environment,* vol. 34, pp. 681-705, 1999.

[39] S. Wang and Z. Ma, "Supervisory and Optimal Control of Building HVAC Systems: A Review," *HVAC&R Research,* vol. 14, no. 1, pp. 3-32, 2008.

[40] N. Nassif, S. Kajl and R. Sabourin, "Simplified Model-Based Optimal Control of VAV Air-Conditioning System," in *Ninth International IBPSA Conference*, Montreal, 2005.

[41] S. Yuan and R. Perez, "Multiple-zone ventilation and temperature control of a single-duct VAV system using model predictive strategy," *Energy and Buildings,* vol. 38, pp. 1248-1261, 2006.

[42] ASHRAE, "Supervisory Control Strategies and Optimization," in *2015 ASHRAE Handbook - HVAC Applications*, Atlanta, American Society of Heating, Refrigeration and Air-Conditioning Engineers, 2015, pp. 42.2-42.43.

[43] J. Walaszczyk and A. Cichon, "Impact of the duct static pressure reset control strategy on the energy consumption by the HVAC system," in *E3S Web of Conferences*, Wroclaw, Poland, 2017.

[44] Y. Yeo and Y. Yu, "Modeling and Control Strategies for VAV Systems," in *Modeling and Control in Air-Conditioning Systems*, Shanghai, Springer, 2017, pp. 423-476.

[45] T. Hartman, "Terminal Regulated Air Volume (TRAV) Systems," *ASHRAE Trans. ,* vol. 99, no. 1, pp. 791-800, 1993.

[46] Y.-P. Ke and S. A. Mumma, "Optimized supply-air temperature (SAT) in variable-air-volume (VAV) systems.," *Energy,* vol. 22, no. 6, pp. 601-614, 1997.

[47] I.-S. Joo, L. Song, M. Liu and M. Carico, "Demand-based Optimal Control to Save Energy: A Case-Study in a Medical Center," in *Proceedings of the Sixteenth*

Symposium of Improving Building Systems in Hot and Humid Climates, Plano, Texas, 2008.

[48] K. F. Woldekidan, *Indoor Enviromental Quality (IEQ) and Building Energy Optimization through Model Predictive Control (MPC). Dissertations,* Syracuse: Surface, 2015.

[49] B. Rismanchi, J. M. Zambrano, B. Saxby, R. Tuck and M. Stenning, "Control Strategies in Multi-Zone Air Conditioning Systems," *Energies,* vol. 12, p. 347, 2019.

[50] W. D. and Y. W., "The State-of-the-Art in Sensor Technology for Demand-Controlled Ventilation," NRC Publications Archive, Ottawa, 2005.

[51] S. Wang and X. Jin, "CO2 based occupancy detection for online outdoor air flow control," *Indoor and Built Environment,* no. 7, pp. 165-181, 1998.

[52] S. Wang and X. Xu, "A robust control strategy for combining DCV conrol with economizer control," *Energy Conversion and Management,* vol. 43, no. 18, pp. 2569-2588, 2002.

[53] A. Peter R, S. B. Leeb and L. K. Norford, "Control with Building Mass - Part 1: Thermal Response Model," *ASHRAE Transactions,* vol. 112, no. 1, 2006.

[54] J. E. Braun, "Load Control Using Building Thermal Mass," *Journal of Solar Energy Engineering,* vol. 125, pp. 292-301, 2003.

[55] S. K. Wang, "Air Systems: Air Duct Design," in *Handbook of Air Conditioning and Refrigeration*, MCGraw-Hill, 2001, p. 17.39.

[56] Air Movement And Control Association International, Inc., AMCA Publication 200-95 (R2011) Air Systems, Arlington Heights, IL: AMCA International, 2011.

[57] R. V. Becelaere, H. J. Sauer and F. Finaish, "Flow Resistance Characteristics of Airflow Control Dampers (RP-1157)," *HVAC&R Research,* vol. 11, no. 1, pp. 119-131, 2005.

[58] Air Movement And Control Association International Inc., AMCA Publication 201-02 (R2011) Fans and Systems, Arlington Heights, IL: AMCA International, 2011.

[59] G. Liu and M. Liu, "Development of simplified in-situ fan curve measurement method using the manufacturers fan curve," *Building and Environment,* vol. 48, pp. 77-83, 2012.

[60] ANSI/AMCA, AMCA Publication 210-16 Laboratory Methods of Testing Fans for Certified Aerodynamic Performance Rating, Arlington Heights, IL: Air Movement And Control Association International, Inc., 2016.

[61] Air Movement And Control Association Internation Inc., AMCA Publication 203-90 (R2011) Field Measurement if Fan Systems, Arlington Heights, IL: AMCA International, 2011.

[62] J. Stein and M. M. Hydeman, "Development and Testing of the Characteristic Curve Fan Model," *ASHRAE Transactions,* vol. 110, pp. 347-356, 2004.

[63] International Environmental Corporation, *Belt Drive Series Fan Coil Technical Catalog,* Oklahoma City: IEC International Environmental, 2016.

[64] D. Meyer and D. Thevenard, "PsychroLib: a library of psychrometric functons to calculate thermodynamic properties of air," *The Journal of Open Source Software,* vol. 4, p. 33, 2019.

[65] S. C. Sugarman, Testing and Balancing HVAC Air and Water Systems, Lilburn, GA: The Fairmont Press, Inc., 2014.

[66] S. K. Wang, "Energy Management and Control Systems," in *Handbook of Air Conditioning and Refrigeration*, MCGraw-Hill, 2001, p. 5.57.

[67] Honeywell, Engineering Manual of Automatic Control for Commercial Buildings, Minneapolis, Minnesota: Honeywell, 1997.

[68] G. Huang, S. Wang and X. Xu, "Robust Model Predictive Control of VAV Air-Handling Units Concerning Uncertainties and Constraints," *HVAC & Research,* pp. 15-33, 2010.

Appendix A. Equipment Schedule

Device Tag	Equipment	Part Number	Manufacturer	Specifications
VC-02-016-116	Fan Coil Unit	VBC30KYY-RIGHT	IEC, International Environmental	– Vertical Belt Drive – 3000CFM – 575V – 1 1/2HP – 1.56 Amps – 60Hz – 1800 RPM – 2-pipe Cooling and Heating with 6 Rows
BV07-01-106-117	VAV Box 1	DESV10	Titus	– Single Duct Terminal Unit – 1100 CFM – 10” Inlet Size – 0.01 in. WC pressure loss damper totally open
BV06-01-016-401	VAV Box 2	DESV10	Titus	– Single Duct Terminal Unit – 1100 CFM – 10” Inlet Size – 0.01 in. WC pressure loss damper totally open

Table 9.1 Equipment schedule.

Appendix B. Sensor & Instruments Schedule

Device/ Instrument	Type	Part Number	Mfr.	Specifications
F1, F2, F3, F4, F5	Airflow Station & Differential Pressure Transducer	"Aero-Cross" DESV & C264-2.5	Titus & Setra	– Operating Range 0 to 2.5 in. WC – 12 Bit Resolution – Accuracy ±1.0% (0.025 in. WC) – Supply Voltage 9 to 30Vdc – Output Signal 4-20mA
H1, H2	Duct Mounted Relative Humidity Probe	538-893	Siemens	– Operating Range 0 to 100 RH – 12 Bit Resolution – Accuracy ±5% – Output signal 4-20mA
P1, P2	Differential Pressure Transducer	DHLR-L05D	ALL Sensors	– Operating Range ± 5 in. WC – 16 Bit Resolution – Supply Voltage 1.68 to 3.6Vdc – 0.25% Accuracy (0.0125 in. WC) – I2C Interface
P3	Duct Static Pressure Transducer	C264-2.5	Setra	– Operating Range 0 to 2.5 in. WC – 12 Bit Resolution – Accuracy ±1.0% (0.025 in. WC) – Supply Voltage 9 to 30Vdc – Output Signal 4-20mA
T1, T2	Duct Mounted Temperature Probe	544-339	Siemens	– Operating Range: -40 to 240°F – 12 Bit Resolution – Accuracy ±0.54°F (±0.3°C) at 32°F(0°C) – 1kΩ Pt RTD
Controller	Single Board Computer	Raspberry Pi 3b+	The Raspberry Pi foundation	– GB LPDDR2 SDRAM – 2.4 GHz and 5 GHz IEEE 802.11.b/g/n/ac wireless LAN, Bluetooth 4.2, BLE – Extended 40-pin GPIO header
N/A	I/O Boards 1, 2 and 3	Pi-SPi-2Ao (2) Pi-SPi-8AI (1)	Widgetlords Electronics	– (2) 4-20mA with 2 outputs board, 12 Bit Resolution – (1) 4-20ma with 8 inputs, 12 Bit Resolution

Table 9.2 Sensors and instruments schedule.

Appendix C. Fan Test Data Overview

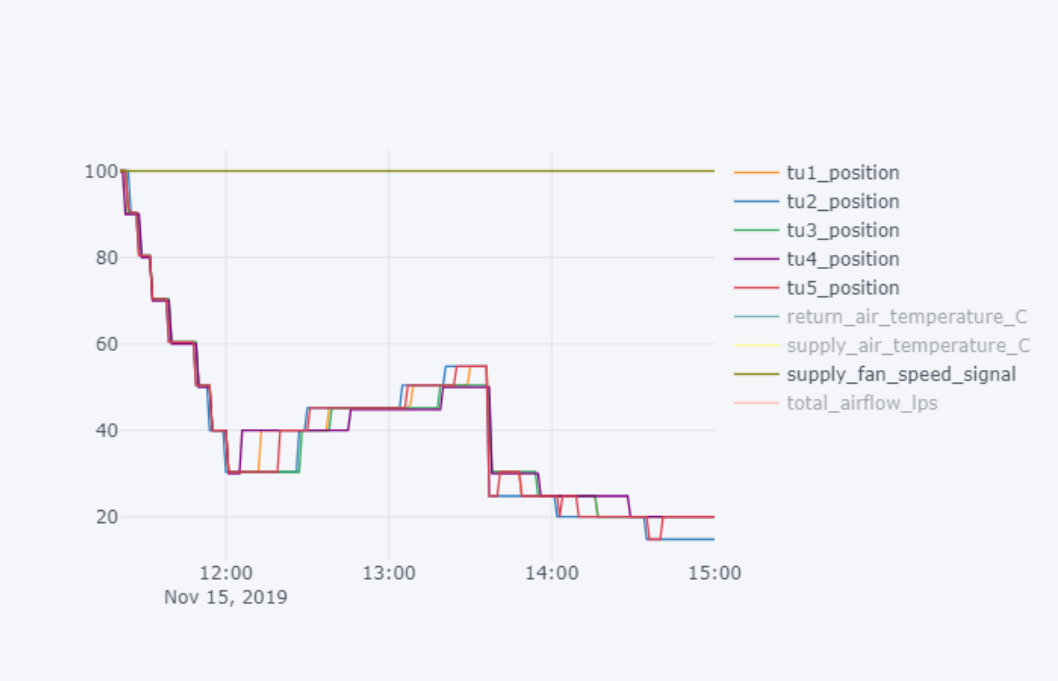

Figure 9.1 Trend log for damper positions versus supply fan speed.

Figure 9.2 Trend log for the fan total airflow (liters per second).

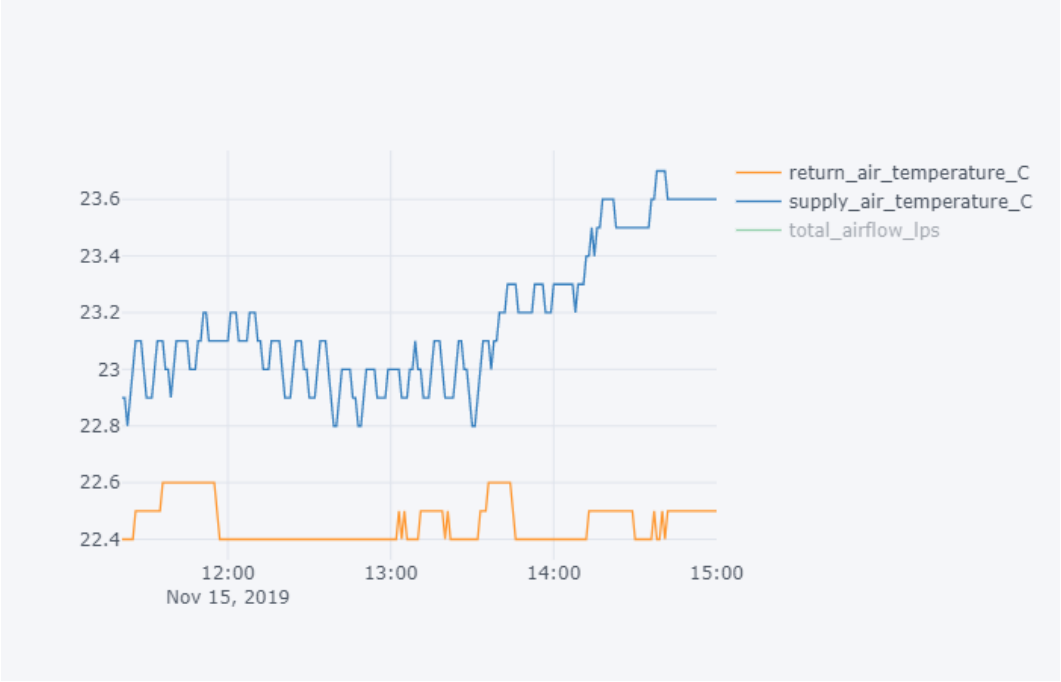

Figure 9.3 Trend log for the return and supply air temperature (Celsius).

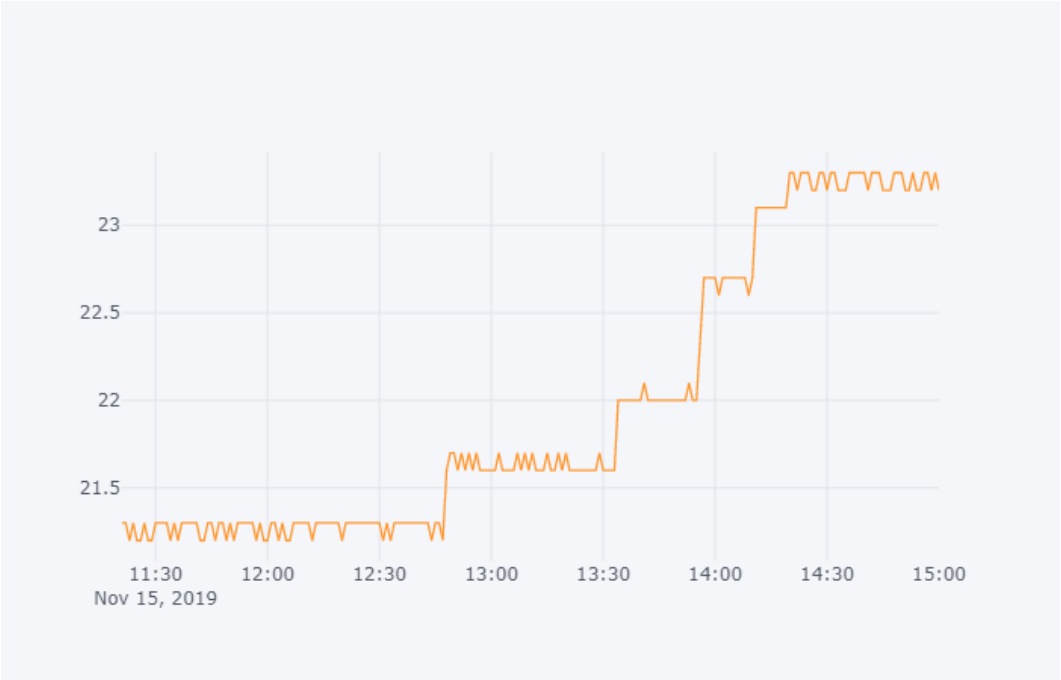

Figure 9.4 Trend log for the relative humidity.

Figure 9.5 Trend log for the fan's inlet static pressure (in. WC).

Figure 9.6 Trend log for the fan's outlet static pressure (in. WC).

Appendix D. Balancing Tools Schedule

Instrument	Part Number	Manufacturer	Specifications
Micrometer	EBT721	Alnor	- Range: Differential pressure... ±15 in. H2O (3735 pa); 150 in. H2O maximum safe operating pressure - Resolution: Pressure 0.00001 in. H2O (0.001 pa) static and differential - Accuracy: Pressure ±2% of reading ±0.001 in. H2O (0.25 pa) static and differential; ±2% of reading absolute
Pitot Tube	EBT721	Alnor	- To obtain air velocity, total and velocity pressure - 18 in length - 1/8 in diameter
Static Pressure Probe	EBT721	Alnor	- To measure static pressure - 1/8 in diameter
Capture Hood	PH721	Alnor	- To obtain air velocity at the diffusers - 2ft x 2ft - Fabric hood with a frame
Temperature/ Humidity Probe	800189	Alnor	- Range: 40 to 140°F (4.4 to 60°C), 0 to 95% RH temperature - Resolution: 0.1% RH Temperature. 0.1°F (0.1°C) - Accuracy: ±3% RH, Temperature ±0.5 °F (0.3°C) from 32 to 160°F (0 to 71°C); max ±2.0 °F (1.2°C) from -40 to 32°F (-40 to 0°C) and from 160 to 250°F (71 to 121°C)

Table 9.3 Balancing tools schedule.

Appendix E. Air System Test Data Overview

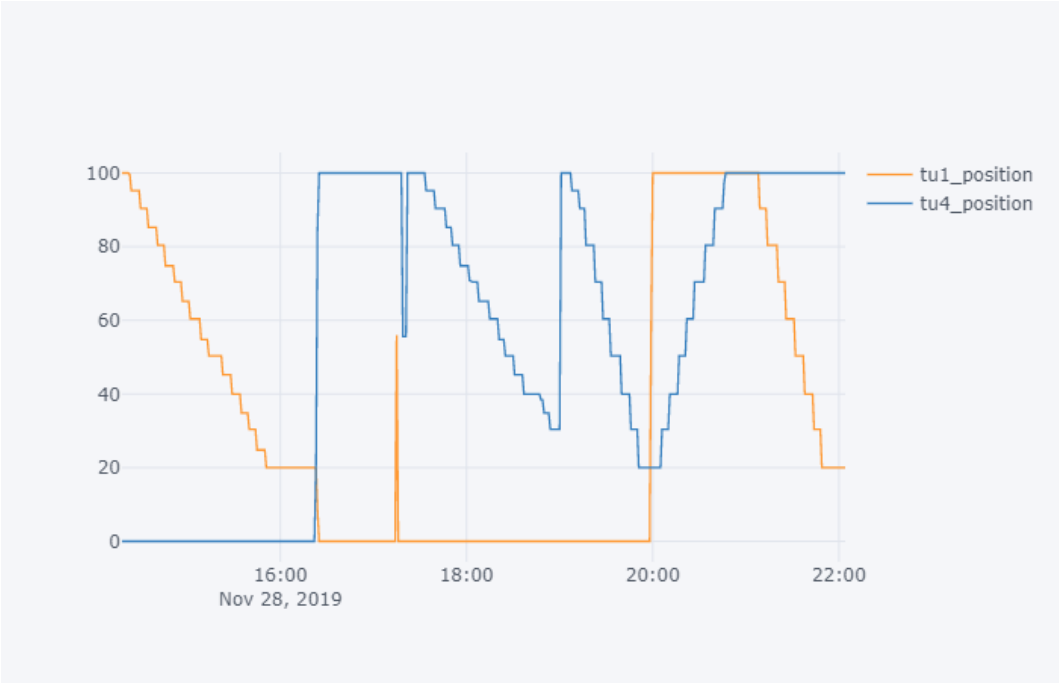

Figure 9.7 Trend log for damper positions of VAV box 1 (tu1) and box 2 (tu4).

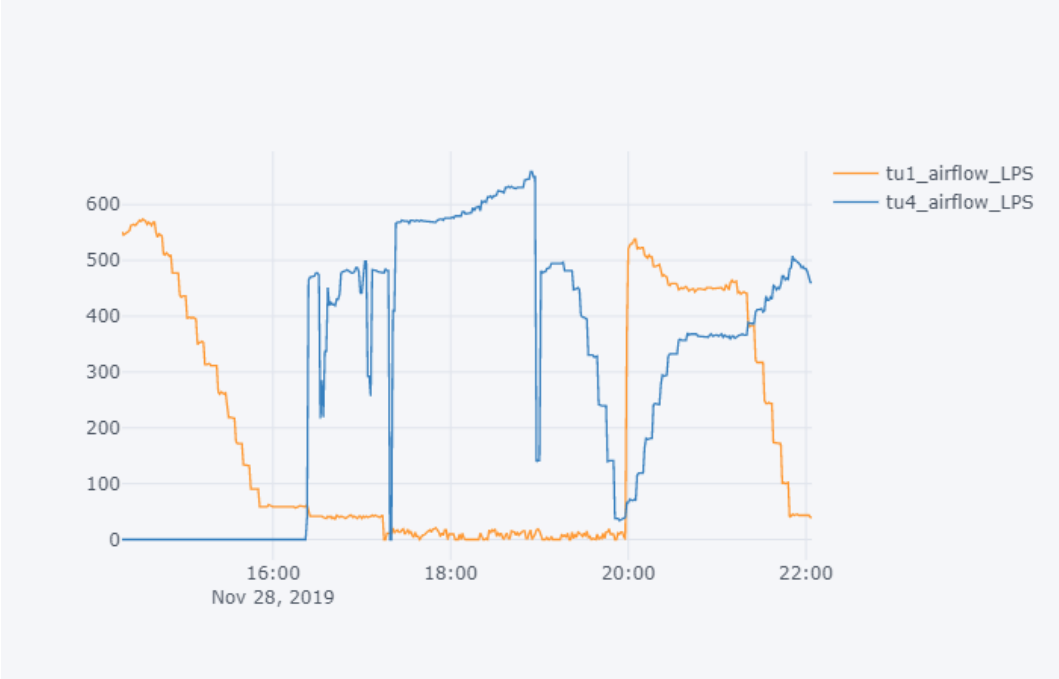

Figure 9.8 Trend log for airflows of VAV box 1 and box 2 (liters per second).

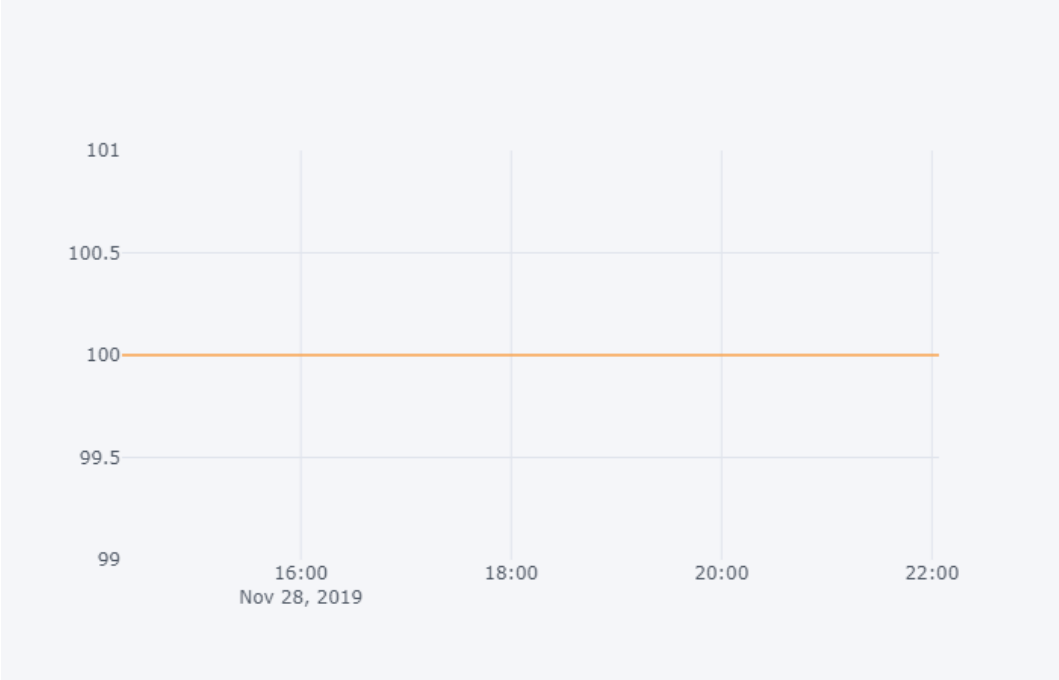

Figure 9.9 Trend log for the supply fan speed.

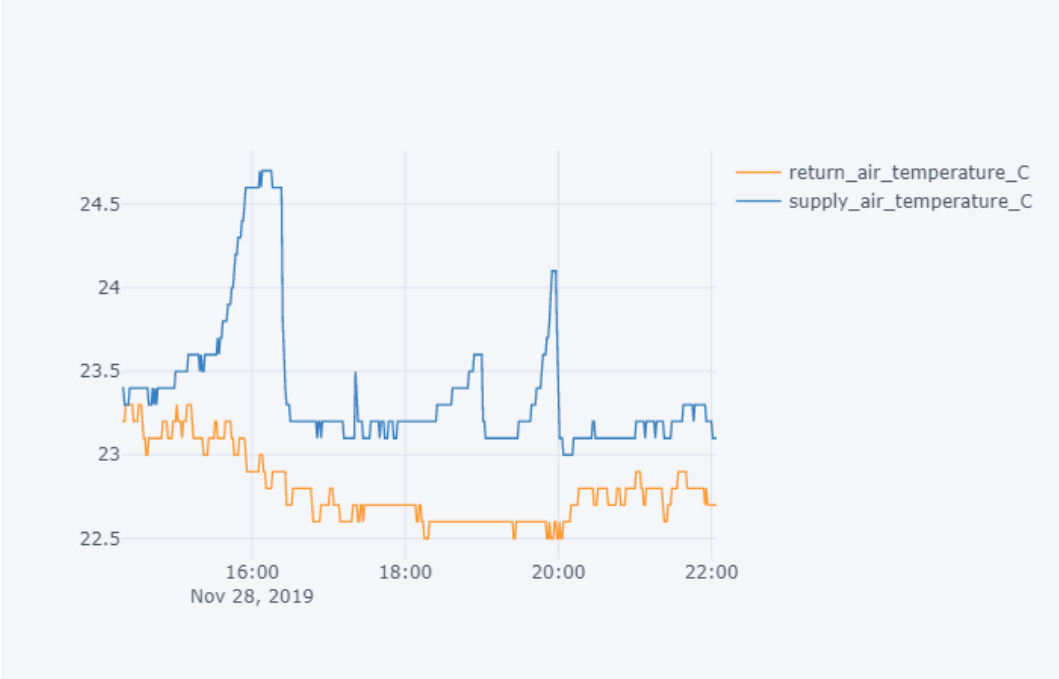

Figure 9.10 Trend log for the return and supply air temperature (Celsius).

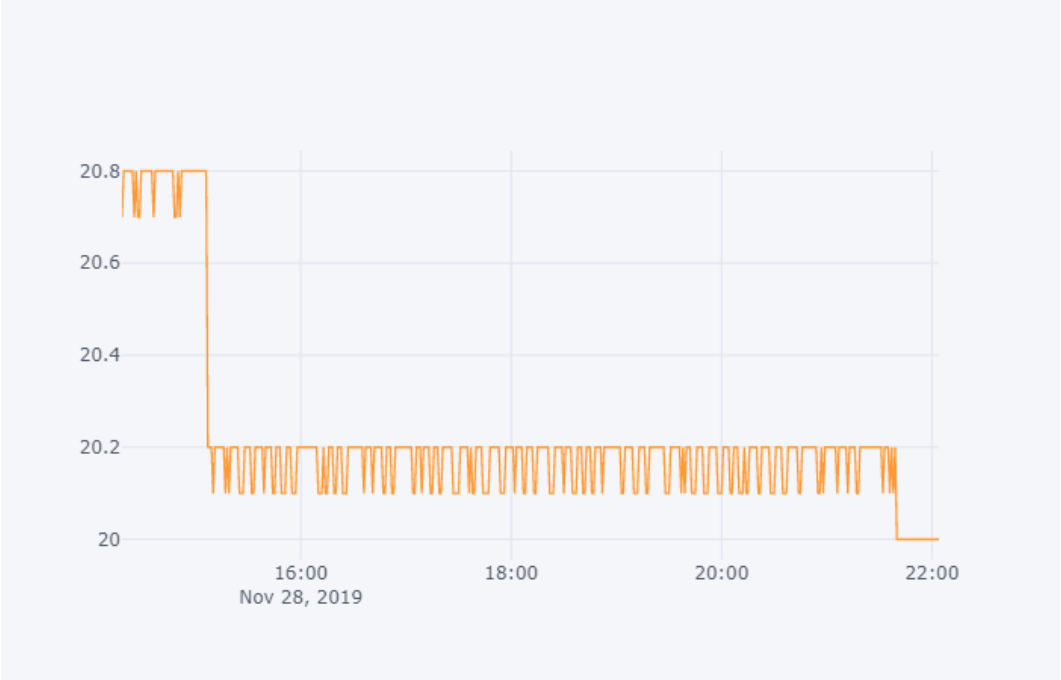

Figure 9.11 Trend log for the relative humidity.

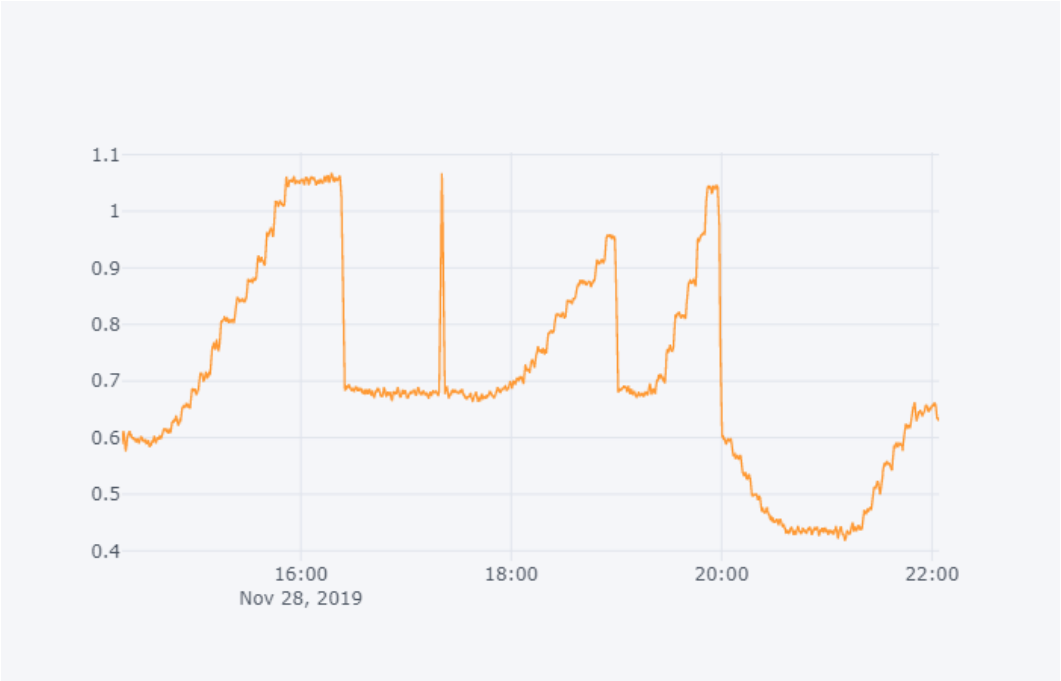

Figure 9.12 Trend log for the fan's outlet static pressure (in. WC).